NIGERIAN MINING JOURNAL

ISSN 1117 - 4307

Volume 19 Number 1 November 2021

A Publication of

NIGERIAN SOCIETY OF MINING ENGINEERS

NIGERIAN MINING JOURNAL

Volume 19 Number 1 November 2021

Table of Contents

NIGERIAN MINING JOURNAL

ISSN 1117-4307

Volume 19 | Number 1 | November 2021

A PUBLICATION OF THE NIGERIAN SOCIETY OF MINING ENGINEERS

Publisher
Nigerian Society of Mining Engineers (NSME)
NSME Secretariat, Bukuru,
P.M.B. 2036,Jos, Plateau State, Nigeria

Editorial Address
Department of Mineral and Petroleum Resources
College of Engineering,
Kaduna Polytechnic, Kaduna.
Tel: 08030495371, 08023636689
Email: nigerianminingjournal@gmail.com
Website: www.nsme.org.ng

NIGERIAN
MINING JOURNAL
ISSN 11774307
A Publication of
Nigerian Society of Mining Engineers

INFORMATION FOR AUTHORS

Scope: NIGERIAN MINING JOURNAL is the technical publication of Nigerian Society of Mining Engineers. The Journal publishes peer-reviewed papers covering various fields of mining, mineral processing and extractive metallurgy. The papers provide in-depth information on research findings from various aspects of actual exploitation of minerals and related engineering practice. Researches based on local technology are particularly welcome.

Manuscripts: Manuscripts submitted for publication must represent original contributions and should not have been proposed for publication elsewhere. The papers should be based on original research, innovations and field experience in mineral exploration, mining, mineral processing, extractive metallurgy and equipment maintenance, relevant to the minerals industry. The manuscript must be prepared preferably in Microsoft Word environment, and should be submitted by email to *nigerianminingjournal@gmail.com*

Abstract: The manuscript must include an abstract summarizing the main aspects of the paper in not more than 200 words. The main results/findings must be stated clearly.

Keywords: A minimum of 5 and maximum of 7 keywords should be included.

Text: Papers should be typewritten with double-line spacing and margins of 25 mm on all sides. Each page should be numbered. The first page should include a concise title of the paper and the author(s) full name(s), affiliation(s) and address(es). In order to maintain consistency, titles such as Mr, Mall, Mrs, Miss, Engr, Dr, Prof, etc., should be avoided, as they frequently change. The author(s) should secure the right of reproduction of any material that has already been published elsewhere.

Units: The S.I. unit is mandatory. However, in isolated accepted cases, authors should insert conversion factors or nomographs for units other than S.I.

Mathematical symbols and formulae: All characters available on a normal typewriter must be typewritten in the text as well as in the equations. Subscripts and superscripts should all be clear. Equations referred to in the text should be placed between parentheses at the right hand margin.

Figures: All illustrations should be drawn using black ink, or suitable computer software, on good quality paper. The originals or good quality photographic prints (maximum 210 x 297mm) should be submitted together with the manuscript. Each figure should carry a brief title *under* it. Figures must be referred to in the text with the number clearly written on the back of the photograph or drawing. Lettering of figures should be large enough to ensure clarity of reproduction after reduction.

Tables: Each table should be typed on a separate sheet as the authors expect it to appear in print. Tables should carry a brief title on top, and should be numbered and referred to in the text.

References: References should be in APA system and must be listed at the end of the article, in alphabetical order of the first author's surname. Citation of papers in the reference list should be as follows:

Books:
Hartman, H.L. & Mutmansky, J.M. (2002). *Introductory Mining Engineering* (2nd Ed.). New Jersey: John Wiley & Sons.

Journals:
Zimbovsky, I.G., Ivanova, T.A., & Chanturia, V.A. (2015). Complexing collecting agent for selective flotation of chalcopyrite. *Journal of Mining Science*. 51(3), 562-567.

Unpublished work:
Arubisan, A.P. (2013). *Amelioration of grain size and its effect on iron ore concentrate in Itakpe, West Central Nigeria*. Unpublished M.Tech. Thesis, Federal University of Technology, Minna.

Proceedings:
Oyeladun, O.A.W, Abubakar, S. & Adewuyi, E.A.A. (2012). Application of Igoli mercury-free gold extraction for recovery of Wamba gold. *Proceedings of Nigerian Society of Mining Engineers,* Ilorin, 2012, 67-70.

Assignment of Copyright Ownership: Submission of a manuscript for possible publication in the Nigerian Mining Journal carries with it the understanding that the manuscript has not been published nor is being simultaneously considered for publication elsewhere. On submission of a manuscript, the author(s) agree that the copyright to their articles is assigned to the Nigerian Society of Mining Engineers (NSME) if and when the articles are accepted for publication.

Hassan, *et al* (2021) Nigerian Mining Journal, (19) 1 - 6

Characterization of Ngaski Gold Resource by Fire Assay, Cyanidation and Carbon Adsorption

Hassan, U. A.[1], Yaro, S. A.[2], Thomas, D. G.[2] , Maina, N. S.[3], Asuke, F.[2] and Akindele, U. M.[4]

[1]*National Steel Raw Materials Exploration Agency, Kaduna*
[2]*Department of Metallurgical and Materials Engineering, ABU Zaria*
[3]*Department of Chemical Engineering, ABU Zaria*
[4]*Department of Mineral and Petroleum Resources Engineering, Kaduna Polytechnic, Kaduna*

Abstract

Ngaski gold resource was characterized by cyanidation and carbon adsorption to establish the type of gold ore resource as well as its economic mesh grind. Chemical composition of Ngaski gold resource was determined using fire assay and leachwell test. Susceptibility of the gold ore to cyanidation was carried out using bottle roll simulated heap leaching and carbon adsorption tests. The simulated heap leach tests were conducted on 100% passing 1.7 mm and 100%-75µm. The head assay results established Ngaski gold ore to contain 3.89g/t Au, 0.007ppm Pt, 0.49ppm Ag, <0.02ppm Rh, <0.02 ppm Pd, and <10 ppm U. The cyanide leaching tests showed gold recoveries of 96.7% and 97.8% for 100% passing 1.7mm and 75µm sized fractions respectively with corresponding recoveries of 67.1% and 71.5% recovered for Ag. The simulated heap leaching data were evaluated using the Freundlich isotherm for the equilibrium test data and Classical Film Diffusion Rate Equation for kinetic test data. Tests data showed Freundlich 'a' value of 6234, 'b' value of 0.77 and a mass transfer rate of 0.03m/h with SSQ of 0.27 with an overall 94.5% of leached gold adsorbed onto the activated carbon. This work established Ngaski gold ore to be free milling and amenable to cyanidation and carbon adsorption extraction with 1.7mm size as its economic mesh of grind.

Keywords: Ngaski Gold ore, cyanidation leaching, fire assay and carbon adsorption, free milling

INTRODUCTION

Gold metal extraction process routes used in exploiting gold deposits depend on the ease with which the gold can be extracted using the established extraction methods of gravity, amalgamation, cyanidation leaching, carbon adsorption, and gold precipitation using zinc dust with lead nitrate. This refers to whether the gold resource is free milling, refractory and complex gold ores (Zhou, Jago and Martin, 2004); (Lunt and Weeks, 2005) and Mardsen and House. (2006). Characterization of gold deposits to establish the ease of extracting the gold from the gold deposit are carried out by various tests including cyanidation leaching, gravity separation, carbon adsorption, gold particle size determination ((Mardsen and House. 2006), (Ulsen et al, 2015), (Beyou et al, 2016), (Richmond et al, 2016), (Bailey, 1985, 1988)). Chemical composition of gold deposits is usually determined by either fire assay; acid digestion and atomic adsorption spectroscopy (AAS) or inductively coupled plasma (ICP); cyanide leaching and AAS with fire assay of the residue; and physical methods comprising panning and amalgamation while the mineralogical composition can be determined using Xray Diffraction (XRD) analysis (SGS Rocks to Results,, 2014).

Processes required to recover fine gold from crushed ore are determined by the free-milling or refractory nature of the ore. This generally involves removal of coarse gold grains by gravity concentration either with or without comminution while fine gold is recovered after size reduction using a combination of cyanidation, carbon adsorption/desorption followed by either electrowinning or zinc precipitation (Lunt and Weeks, 2005).

Cyanidation is a gold extraction process that entails dissolving (leaching) gold from its ores using dilute cyanide solutions (0.2% - 0.5% NaCN) and pH of +9.5 (Adams, 2005). The dissolved gold is then recovered by precipitation with zinc metal or adsorbing the gold onto activated carbon followed by elution and electro winning process. Cyanidation is the

most used gold extraction method including the extraction of gold from refractory ores after pre-treatment using pressure oxidation at 180 – 22-0^{0}C and pressures in excess of 2000KPa (Habashi, 2005), bacterial oxidation, ultra-fine milling to liberate -20µm gold grains and roasting amongst others. The cyanidation process requires that the gold be oxidized in the presence of a complexing agent (a ligand) that can complex with the gold and stabilize it in solution. It is, therefore, necessary that both an oxidant and a ligand be present otherwise gold will not dissolve (Marsden and House, 2006). A pH modifier (acid or alkaline) is usually added to maintain an optimum pH of 9.0 to 9.5 (Perry et al. 1999). Cyanide is universally used because of its relatively low cost, its great effectiveness for gold (and silver) dissolution, and its selectivity for gold and silver over other metals. Despite some concern over the toxicity of cyanide, it can be applied with little risk to health and the environment (Mineral Council of Australia, 2012, Eisler and Wiemeyer, 2004, Ophardt, 2012). The oxidant most commonly used in cyanide leaching is oxygen, supplied from air, which contributes to the attractiveness of the process. The different processes developed for leaching gold with cyanide include agitation leaching, heap leaching, vat leaching, intensive cyanidation and in-situ leaching. The overall dissolution of gold in aerated, alkaline cyanide solutions can be described by the following reaction equation (Ruhmer, 1996):

$$4Au + 8CN^- + O_2 + 2H_2O \leftrightarrow 4Au(CN)_2^- + 4OH^-$$

In the reaction above, oxygen is the oxidant and cyanide ion the complexing agent or ligand. The gold in the aurocyanide ion is present as gold (I). Silver can be substituted for gold. Sodium cyanide is usually selected for leaching because it is the least expensive cyanide. Major factors that generally affect the dissolution rate of gold include cyanide and oxygen concentrations, temperature (<85^{0}C), surface area of gold exposed, degree of agitation and mass transport, gold purity and the presence of other ions in solution (Adams, 2005).

Generally, ground ore or treated concentrate is treated with weak solution of sodium cyanide, which dissolves the gold and forms slurry of gold-bearing solution and barren solids. Some ores can be treated by heap-leaching which involves sprinkling a weak cyanide solution over an open pile of ore stacked on an impervious base. The solution percolates through the ore, leaching gold as it goes, and is drawn off at the base before being treated to recover the gold (Gupta, 2003).

MATERIALS AND METHODS

Materials

Samples, Equipment, Chemicals and Reagents

300kg of Ngaski gold resource Run of Mine made up of 150kg each of produced from Libata and Masamale gold vein resources that make up Ngaski gold resource. The samples were crushed to -2mm and blended to produce test material used in the studies. The equipment used comprise laboratory jaw crusher, cone crusher, ball mill, sieves, sieve shaker, electronic weighing scale (0.01g), stop watch, Digital pH Meter, rotary splitter, fire clay crucible, bone ash cupel, wire type mixer, carbonite furnace (1800°C), Inductively Coupled Plasma, Spatula, scorifying dishes, mixer, rolling-botlles, Bottle Roller, glass wares and charging fork.

Reagents and chemicals used for the test works carried out comprise Tetrabromoethane, sodium cyanide, sodium borate, flour, lime, sulphuric acid, Hydrochloric Acid, Hydrogen Peroxide, Lead Oxide, Sodium Carbonate and Calcium Fluoride.

Experiments

Test works were carried out at SGS Laboratory, Jourhanesburg, South Africa. Representative samples of Ngaski gold resource were produced using coning and quartering sampling techniques and rotary sample splitting. The various test carried out are as follows.

Chemical compositions of the Ngaski gold ore

The chemical composition of Ngaski gold resource was determined using Fire Assay (Lead Fusion finished with AAS and ICP-OES as well as Leachwell Methods.

Fire Assay

The fire assay involves mixing lead (as litharge, PbO) and glass-forming fluxes with finely ground 30g sample (80% to 90% passing 75µm). The crucible containing the flux charge is then placed in a muffle furncace at 850^{0}C followed by raising the temperature to 1,000^{0}C over a period of 30 to 40 min or until complete fusion has occurred (Geological Survey Bulletin 1445,1977). The lead collects the precious metals, forming a gold-silver-lead alloy which is recorvered as a button, separated from the glasss slag (containing base metal and other impurities). The lead is then removed by cupellation. Lead removal involves preheating the cupel at 1,000^{0}C after which the button is placed on the hot cupel. Following the initial melting, the temoperature is quickly reduced, and the cupelling operation is finished at about 830^{0}C. This produces a precious metal prill, which was dissloved entirely in aqua regia [a mixture of nitric (HNO_3) and hydrochloric (HCL) acids] and analyzed for gold, silver and PGM by AAS techniques (SGS Rocks to Results, 2014, Simpson and MacDonald, 2010).

Adsorbent Loading at equilibrium,

$$C_e = a(S_e)^b$$

Where

S_e = Solution Concentration at equilibrium and a, b = Freundich Constant

RESULTS AND DISCUSSION

Chemical Analysis of Ngaski Gold Ore

Results of Ngaski Gold Ore Head Assay
The chemical analysis of the head assay of Ngaski gold ore are tabulated in and 3.

Table 1: Ngaski Gold Ore Head Assay Results - A

Sample Id	Au (g/t)				
	Assay A	Assay B	leachwell A	leachwell B	Average
Head	2.56	3.83	4.26	4.91	3.89

Table 2: Ngaski Gold Ore Head Assay Results - B

Sample Id	Head Assays				
	Pd ppm	Pt ppm	Rh ppm	U ppm	Ag ppm
Head	<0.02	0.007	<0.02	<10	0.49

The results established that Ngaski gold ore contains an average gold content of 3.89 g/t of Au (2.56g/t – 4.91g/t) with < 0.02 ppm Pd, 0.007 ppm Pt, < 0.02 ppm Rh, < 10 ppm U and 0.49 ppm Ag. Assay A and Assay B in Table 1 were obtained from conventional Fire Assay tests while Leachwell A and Leachwell B were from assays obtained from intensive leaching tests with Leachwell tablets. The variation in the Au assay results obtained for the ore sample can be attributed to sample inhomogeneity caused by nugget effect. The Leachwell Test was carried out to facilitate resolving the variance in gold head assays.

The average gold head grade of 3.89g/t shown in which includes the calculated grades from the Leachwell tests tallies with the calculated Au grade from the simulated heap leach test work shown in Table 3. In line with the findings of Marsden and House, (2006), which reported that the search for gold has made it possible for gold deposits as low as 0.1g/t of Au to be mined and processed for its content, makes Ngaski gold ore deposit a potential source of gold that can be exploited for its Au content.

Results of Seven Day Simulated Heap Leaching Tests

Results of seven day simulated heap leach tests carried out on Ngaski gold ore at two different grinds (100% -75µm and 100% -1.7mm are presented graphically in and and summarized in Table

Table 3: Simulated Heap Leach results

	Simulated Heap Leach			
Sample ID	**Head Au (g/t)**	**% Au Dissolution based on calculated head**	**Head Ag (g/t)**	**% Ag Dissolution based on calculated head**
100% -1.7 mm	3.89	96.7	0.49	67.1
100%-75 µm		97.8		71.5

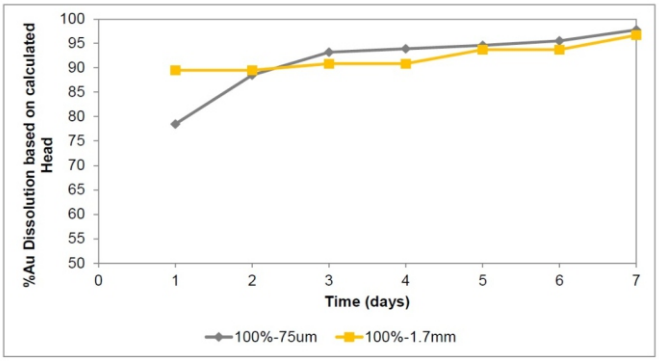

Figure 1: Simulated heap leach kinetics (gold)

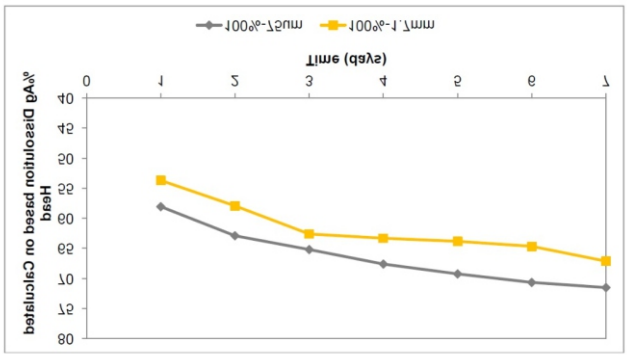

Figure 2: Simulated heap leach kinetics (silver)

Figures 1 and 2 and the summarized result of the simulated heap leach presented in Table 3 show that after the leach period of seven days, the gold dissolution based on the calculated head grade was 97.8% at a grind of 100% passing 75 µm and 96.7% at 100% passing 1.7mm respectively while corresponding silver dissolutions based on calculated head grade were 71.5% and 67.1% respectively. This established Ngaski gold ore to have positively responded to heap leaching and is free milling in line with Marsden and House, 2006 classification of gold ores that classifies gold ores from which cyanidation extracts approximately 95% gold or more as free milling. It also established 1.7mm size as the economic mesh of grind since further milling to 100% passing 75 µm did not appreciably improve gold recovery (1.1%). It was only the silver recovery that increased by 4.4% which cannot justify further milling due to its much lower tenor in the ore.

The insignificant increase in gold recovery with finer grind could be attributable to non-significant increase in the liberation of gold with finer grinding from 1.7mm to 75 µm. The increase in silver could be as a result of increased liberation of silver with finer grind. Presence of pyrite (FeS_2) in the ore, which was established by quantitative XRD to fairly abundant, could have also retarded the dissolution of Au while the presence of galena (PbS), iron (Fe), and pyrite (FeS_2) could have increased the dissolution of Ag significantly. Weiss, (1985) and Davies, (1987) had reported similar observations where they stated that, galvanic interaction between gold and other minerals especially chalcopyrite and pyrite present in gold ores cause reduction in the rate of dissolution of gold. Other reason advanced for reduction in the rate of the gold dissolution is passivation which leads to film formation on the gold grains in cyanide solution.

Results of Gold Adsorption Appraisal using Carbon-in-Pulp (CIP)

Parameters (Freundlich Isotherms) determined for gold adsorption appraisal in CIP are tabulated as table 4, the plots of kinetics results of 100% passing 1.7 mm and 100% passing 75 µm are shown as Figures 5 while the plots of results of the equilibrium isotherms of 100% passing 1.7 mm and 100% passing 75 µm are tabulated as Figure 6.

Table 5: Summary of Parameters (Freundlich Isotherm)

Sample	Freundlich Constants		Mass Transfer	Diffusion Parameter	SSQ Residual	
	A	*b*	(m/h)		Equilibriums	Kinetics
100%1.7 mm	6217	0.91	0.03	20.0	0.10	**0.32**
100%-75 µm	**6251**	**0.63**	**0.03**	**20.0**	**0.06**	**0.22**

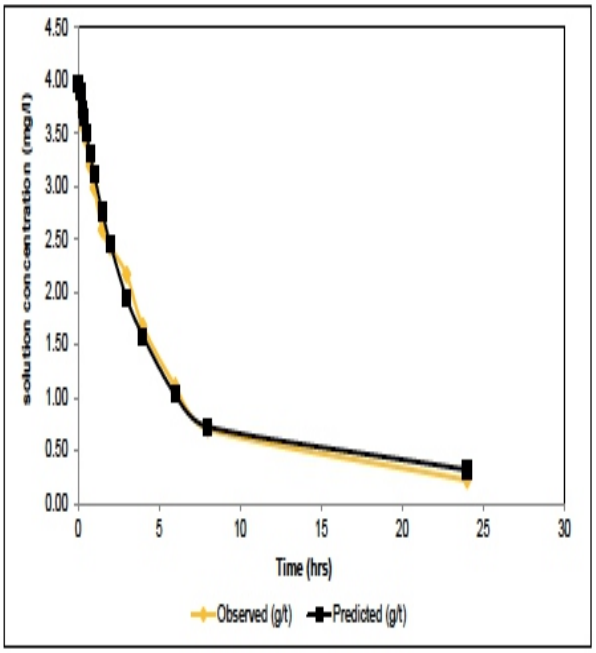

Figure 3: Graph of Solution Concentration Vs Time for - 75µm Ngaski Gold Ore

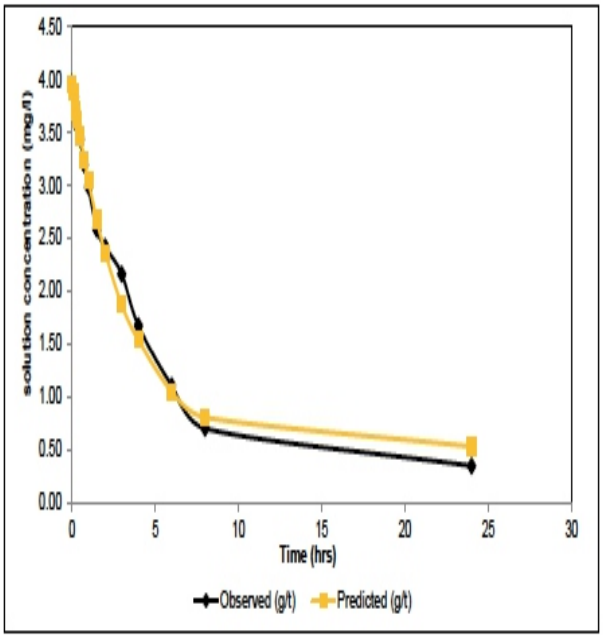

Figure 4: Kinetics results for 100% - 1.7mm Ngaski gold ore sample

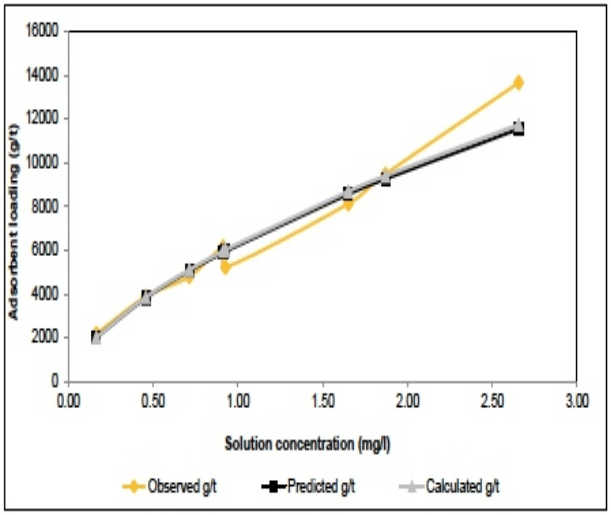

Figure 5: Equilibrium results for the 100% - 1.7mm sample

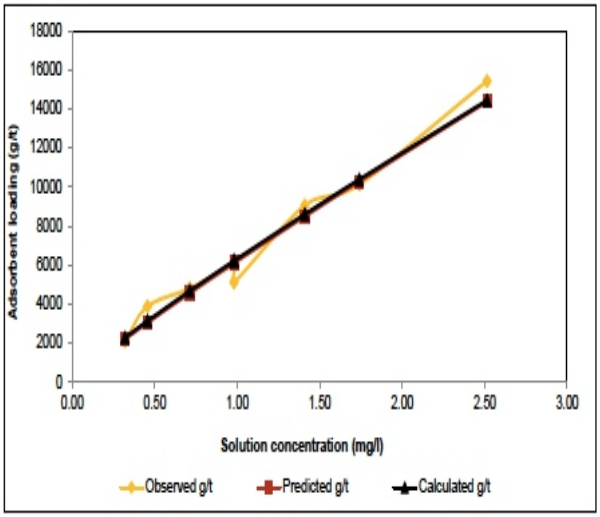

Figure 6: Equilibrium results for 100% -75µm sample

The kinetics and isotherm test work resulted in an average Freundlich value of 6234, b value of 0.77, mass transfer value of 0.03 m/h and an average SSQ value of 0.27.

CONCLUSION

From the research carried out the following conclusions were drawn:

i. That Ngaski gold ore contains an average of 3.89g/t Au, 0.49g/t Ag, <0.02ppm Pd, 0.007ppm

Pt, <0.02ppm Rh, and <10 ppm U.

ii. That Ngaski gold ore is a free milling type which had a leaching recovery of 97.8% for a grind of 100% passing 75 µm and 96.7% for 100% passing 1.7 mm. This conforms with Marsden & House, 2009 classification that categorizes gold ores from which cyanidation extracts approximately 95% gold or more as free milling.

iii. That additional silver recoveries of 71.5% and 67.1% could also be recorded along with gold recoveries when respectively leached at mesh grinds of 100% passing 75 µm and 100% passing 1.7mm.

iv. That Ngaski gold ore is highly amenable to cyanide leaching and carbon adsorption process in view of +95% gold recovery for cyanide leaching and 94.46% recovery of leached gold adsorbed on the carbon.

References

Adams, M. D., (2005): Advances in Gold OreProcessing, Published by Elsevier.

Avraamides J. (1989). CIP carbons—selection, testing and plant monitoring. pp288 –292 in Proceedings of World Gold '89 Symposium. Littleton, CO: SME

Bailey, P. (1988) 'Application of activated carbon to gold recovery'. The extractive metallurgy of gold in South Africa. Stanley, G.G. (ed.), Johannesburg, South African Institute of Mining and Metallurgy, 1987. Chap. 9. DAVIDSON, R. Anglo American Research Laboratories.

Bailey, P.R. (1985). Ancilliary operations: Acid treatment, elutriation, carbon sizing, breakage, Lecture No 24 in South African Institute of Mining and Metallurgy School on Use of Activated African Institute of Mining and Metallurgy

Beyuo, M., Agorhom, E. A., Owusu, C., Diaby, A. L., and Quaicoe, I., (2016). "Gold deportment and Mineralization Characterization Studies for Improved Recovery: A Vase Study at Goldfields Ghana Limited", *4th UMaT Biennial International Conference on Mining and Mineral Processing*. Pp. MR 180-188

BGS International, (2012). Solid mineral occurrences and mineral potential of Nigeria

Davies, G. A., (1987): Separation Processes in Hydrometallurgy, Ellis Horwood Limited England.

Gupta C. K. (2003): Chemical metallurgy, principles and practice, willey-VCH Verlag Gmbh & Co, KGaA, ISBN 3-572-30376-6, pp 479 – 484, 500 - 516

Habashi, F., (2005). Gold- An historical introduction in Adams M. D. (Ed.) Advances in Gold Ore Processing, Amsterdam, Elsevier B.V.

Lunt, D and Weeks, T, (2005), "Refractory gold ores case studies", Adams, M.D. (Ed.), Developments in Mineral Processing, Elsevier, pp 73-96

Marsden, J.O. and House, C.I., (2006). The chemistry of gold extraction, second edition, published by the society of Mining, Metallurgy and Exploration, Inc.

Perry, R., R.E. Browner, R. Dunne, and N. Stoitis. 1999. Low pH cyanidation of gold. Minerals Engineering 12(12):1431–1440

Richmond, K., Asamoah, J. A., (2016). "Influence of Cyanide Concentration on Gold Leachability from Selected Refractory Bio-oxidised Flotation Concentrates". *4th UMaT Biennial International Conference on Mining and Mineral Processing*. Pp. MR81-92

Ruhmer, W. T., (1996). Handbook on the estimation of metallurgical process costs, 2nd Edition, Mintek Special Publication No. 14, pp 66 -68; 76 – 93

SGS Rocks to Results, 2014: A Practical Guide to Laboratory Operations, 5th Edition

Simpson, B. M. and MacDonald, N. J., (2010): Report on cyanide leach testing of three different gold ore composite samples from the Amulsar Deposit, Armenia (unpublished).

Ulsen, C., Kahn, H., Nery, G., Uliana, D., Antoniassi, J.L., (2015). Gold Characterization by MLA and Technological Tests: Discussion of Sample Preparation and Results. In F. Dong (ed.), Proceedings of the 11th International Congress for Applied Mineralogy (ICAM), Springer Geochemistry/Mineralogy, DOI 10.1007/978-3-319-13948-7_5

Weiss, N. I., (1985): Mineral Processing Handbook by American Institute of Mining Metallurgical and Petroleum Engineering Incorporated in the United States of America by Kings Port Press.

Zho, J., Jago, B., & Martin, C., 2004, Establishing the Process Mineralogy of Gold Ores, SGS Minerals Technical Bulletin 2004-03

Unuevho, *et al* (2021) Nigerian Mining Journal, (19) 7 - 18

Lithologic, Petrographic and Geochemical Search for By-passed Gold Mineralization within Mutumdaya Gold Field in Minna outskirts, North-Central Nigeria

Unuevho, O. M.[1], Ako, T. A.[2], Unuevho, C. I.[2*], Ejepu, S. J.[2], Akobundu, N. A.[2], Tahir, A.[1] and Jatau, B. S.[3]

[1] *PW Nigeria Ltd, Minng Division, Minna*

[2] *Department of Geology, Federal University of Technology, Minna*

[3] *Department of Geology and Mining, Nassarawa State University, Keffi*

[*] *Correspondence email:* c.unuevho@futminna.edu.ng

Abstract

By wildcat pitting, local artisanal miners established a lode gold mine within Mutumdaya in the Northern Nigerian Massif. The mine is now abandoned after a few years of mining. Wildcat pitting lacks the benefits of geoscientific investigations, and the mines so found remain unassessed discoveries. Some untapped gold mineralization does remain around such mines when abandoned. The mineralization constitutes by-passed gold mineralization. Lode gold mining will continue in Mutumdaya if by-passed gold mineralization is found within vicinity of the abandoned mine. This study identified by-passed gold mineralization prospects in immediate vicinity of the abandoned mine. This was achieved by searching for rocks that share similar lithologic, petrographic and geochemical attributes as rocks within the abandoned mine site. It involved surface lithologic mapping, thin section petrographic analysis, and elemental gold concentration analysis in rock samples, using X-Ray Fluorescence Spectrophotometer. The rock bodies were found to be kyanite schist, amphibole schist, quartz schist, and quartzite intruded by syntectonic biotite granite bodies. The quartz schist attained greenschist metamorphic grade, while kyanite schist and amphibole schist attained amphibolite facies metamorphic grade. The kyanite schist at the abandoned mine site contains 0.058 ppm gold concentration. This is 29 times average crustal gold abundance of 0.0000002 %. Outside the abandoned mine site, kyanite schist and amphibole schist contain 0.066 and 0.021 ppm gold concentration. They are respectively 33 and 11 times gold enriched. Gold was undetected in the quartz schist, quartzite and granite bodies. The kyanite schist outside the abandoned mine site is more enriched in elemental gold than the rock body that constitute gold ore within the mine. Apparently, rock bodies in the amphibolite metamorphic facies status constitute prospects for by-pass lode mineralization within the immediate vicinity of the abandoned gold mine. These prospects are at location 9°40'05"N, 6°48'50" E, and location 9°39'05"N, 6°48'40"E. Abandoned artisanal gold mines in the Northern Nigerian Massif and in other developing economies should be searched for by-pass lode gold mineralization, using integrated geoscientific methods.

Keywords: Wildcat pitting, by-passed gold mineralization, metamorphic facies, elemental gold concentration

INTRODUCTION

Informal artisanal mining dots the stretch of land from Minna through Gwada to Gurmana in North Central Nigeria (Kankara and Darma, 2016). Mutumdaya lies within Latitudes 9°39' 30" N to 9°40'12" N and Longitudes 6°48'35" E to 6°49'30" E on this stretch of land, where it constitutes part of the Basement Complex in the Northern Nigeria Massif (Figure 1). Main lithologic units within the basement complex are polymetamorphic migmatite-gneiss-quartzite complex of Archean to Middle Proterozoic age, Upper Proterozoic metasediments and metaigneous rocks, and Pan African intrusives generally called Older Granites (Woakes *et al.*, 1987).

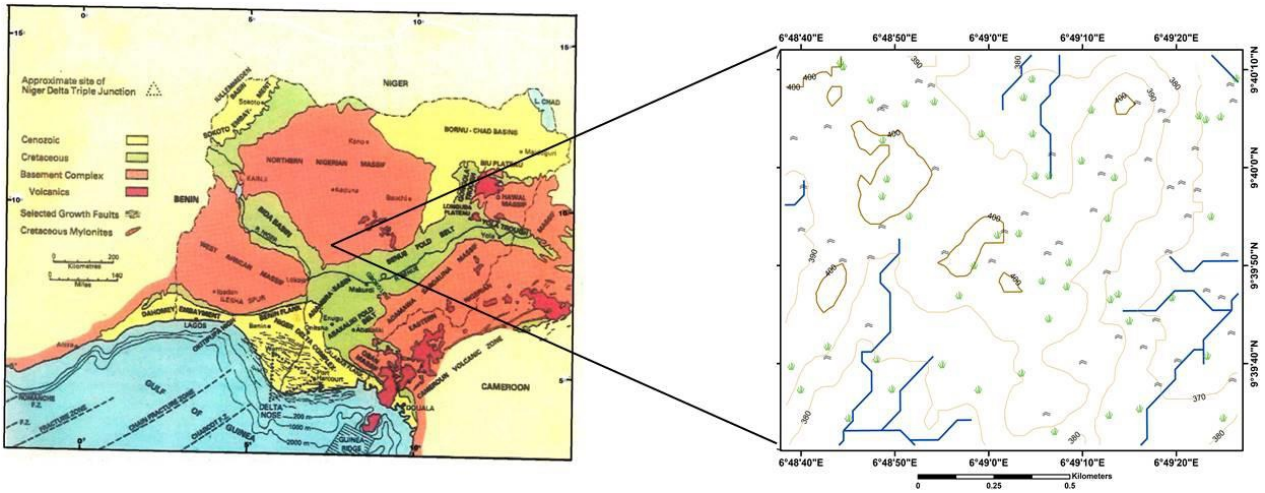

Figure 1: Location of Mutumdaya within Northern Nigerian Massif

According to McCurry (1989), Woakes *et al.* (1987) and Ajibade *et al.* (2008), the Archean to Middle Proterozoic rocks achieved high grade metamorphic status (upper amphibolite – granulite facies) while the Upper Proterozoic rocks belong to lower metamorphic grade (greenschist to low amphibolite facies). The Upper Proterozoic rocks form N – S trending schist belts. Their lithologic units include banded iron formation, schist, amphibolite and quartzite. The Older Granite intruded the Archean and Upper Proterozoic rocks during the Pan African orogeny (McCurry, 1989; Ajibade *et al.*, 2008; Obaje, 2013). The formation of ore deposits is often linked with hydrothermal fluids that commonly originate from igneous activity (Murphy, 2016; Revuelta, 2018). Thus, metamorphic rocks in the vicinity of igneous intrusives are potential ore deposit bearers. Most of the gold deposits in Minna lies within the Kushaka Schist Belt and adjoining Pan-African migmatite and granite bodies (Garba, 2002; Ajibade *et al.,* 2008). Mutumdaya gold field is within the Kushaka Schist Belt, and is regionally encompassed by Migmatite-Gneiss Complex, Older Granite and other schist belts (Unuevho, 2018).

Mining of lode gold deposits (gold mineralization within bedrock or weathered detritus) within Mutundaya gold field took place at a mine site located within Latitudes 9°39' 50" N to 9°39' 55" N and Longitudes 6°49'0" E to 6°50'0" E (Figure 2). This mine site together with its immediate vicinity constitutes the area studied, and covers a spatial extent of 3.3 km^2. Local artisanal miners found the mine by wildcat pitting. The approach lacks the benefits of geoscientific investigation, and this places the mine deposit among chance finds of Nwabufo-Ene and Mbonu (1988).

Figure 2: Lode gold mining at Location 9°39'55.3" 6°49'02.4" E

Figure 3: Mutundaya gold mine at location 9°39'55.3"N 6°49'02.4"E, presently in abandoned state

The mine is now abandoned (Figure 3), thereby creating a mining sustainability challenge in Mutundaya. Gold mineralization in mine found by wildcat pitting of artisans are unassessed discoveries. Some untapped gold mineralization does remain in the vicinity of such mines when abandoned. The mineralization constitutes by-passed gold mineralization. The term 'by-passed gold mineralization' is used in parallel sense to the term 'by-passed hydrocarbon deposit' employed in the petroleum industry to describe hydrocarbons trapped in inadvertently undeveloped reservoirs.

Identification of the by-passed gold mineralization will provide an opportunity for sustaining mining in the Mutundaya gold field. Searching for by-passed gold mineralization within immediate vicinity of an abandoned mine site found by wildcat pitting, requires lithologic, petrographic and geochemical characterization of the rocks at the mine site, and searching for immediate vicinity of the site with similar geoscientific attributes. This study pioneers in such rock characterization in Mutundaya gold field, and its objective is to identify by-passed gold mineralization in the mine's immediate vicinity. Establishing a host rock is an essential aspect of mineral prospecting. Gold mining in developing countries is significantly contributed to by artisanal miners, who are sparingly educated youth struggling to eke out livelihood by exploiting solid mineral resources. Like the Mutundaya gold field miners, they search for deposits by wildcat pitting. Consequently, there are chances of leaving behind by –passed mineralization in mine vicinity when the mines are abandoned. Thus the results of this study should be internationally significant in driving prospectors to deploy integrated geosciences techniques to investigate the vicinity of abandoned mines for possible by –passed gold mineralization.

Groves and Forster (1993) recounted that gold mineralization exists in geological settings that vary from sub-greenschist to upper amphibolite facies. They however remarked that at different localities, gold mineralization selectively occurs in lithologic units. This emphasizes that gold prospecting will be more successful at the local scale if metamorphic facies selected for its mineralization is identified (Sillitoe, 2006; Robert *et al*., 2007). Eskola (1920) first introduced metamorphic facies concept to differentiate rock associations within regionally metamorphosed terrains, using mineral assemblages that attained equilibrium at similar lithostatic pressure and temperature. Some of his metamorphic facies are greenschist facies and amphibolite facies. Bucher and Grapes (2011) as well as Penchuk (2021) defined metamorphic facies as metamorphic rocks that are genetically related in terms of lithostatic temperature and pressure. Winter (2020) emphasized that the prevalent lithostatic pressure and temperature constrain the mineral assemblage that develops during a metamorphic process. Sahin and Erkan (1999) used the presence of biotite, garnet, staurolite and orthoclase to differentiate metamorphic facies in Central Anatolia massif in Turkey. They associated kyanite and biotite with amphibolite facies. Mibel (2014) grouped quartz, feldspar and muscovite as comparatively universal minerals because they remain stable in wide temperature – pressure conditions, and as such inappropriate for facies definition. He emphasized the use of index minerals which he arranged in metamorphic upgrade direction as chlorite, biotite, garnet, staurolite, kyanite and sillimanite.

Groves and Forster (1993) also recounted that most gold deposits were discovered by combining basic surface geological mapping with either geochemical exploration or geophysical exploration or both. They stressed that many gold mines in Western Australia were discovered by drilling geochemical anomalies. According to Murphy (2016), the Prospector's Dictum is that gold is the best pathfinder for gold. Timkin *et al* (2016) employed lithochemical surveys to evaluate gold bearing potential in Akimov ore bearing area of Gory Atlas in the Russian Federation. They delineated gold-silver ore within the anomalous geochemical field. Noor *et al.* (2016) included petrography and X-ray fluorescence in their procedure for ascertaining facies of gold- hosted metamorphic rocks in Rock District of Malukul. Unuevho *et al* (2018) included lithochemical data, in the form of elemental composition, among the geoscientific data employed in the search for ore deposits in Garatu, North Central Nigeria. They established that spatial concentration of gold was

above 900ppm, which far exceed the average crustal concentration (0.0000002%) within a considerable portion of the area.

METHODOLOGY

The first step towards achieving the study's objective was surface lithologic mapping. Lithologies of rock fragments obtained from the mine, and outcropping rock bodies within the mine site vicinity, were first identified in hand specimen, using texture and mafic colour index (MCI). The geographical co-ordinates of locations of the mine site and rock outcrops were obtained using Etrex version of hand held GPS (Geographical Positioning System). Six rock samples that represent the mine rock fragments and outcropping rock bodies within the mine site vicinity, were selected for thin section analysis and whole rock geochemistry. The six rock samples represent 3.3 km^2 spatial extent, which is the areal coverage of the studied mine's immediate vicinity. They constitute an average sampling density of about 2 samples per km^2. This is considered adequate in searching for by-passed gold mineralization within immediate vicinity of a once active gold mine. In thin section, the samples were examined with plane polarized light and cross polarized light of MEIJI manufactured petrographic microscope (N_p– 107B model and serial number 000341) to improve on rock identification made in hand specimen. The identified lithologic units were plotted on a topographic base map and the surface geological map was completed on 1:20,000 scale. Metamorphic facies were identified using Figure 4 as a template.

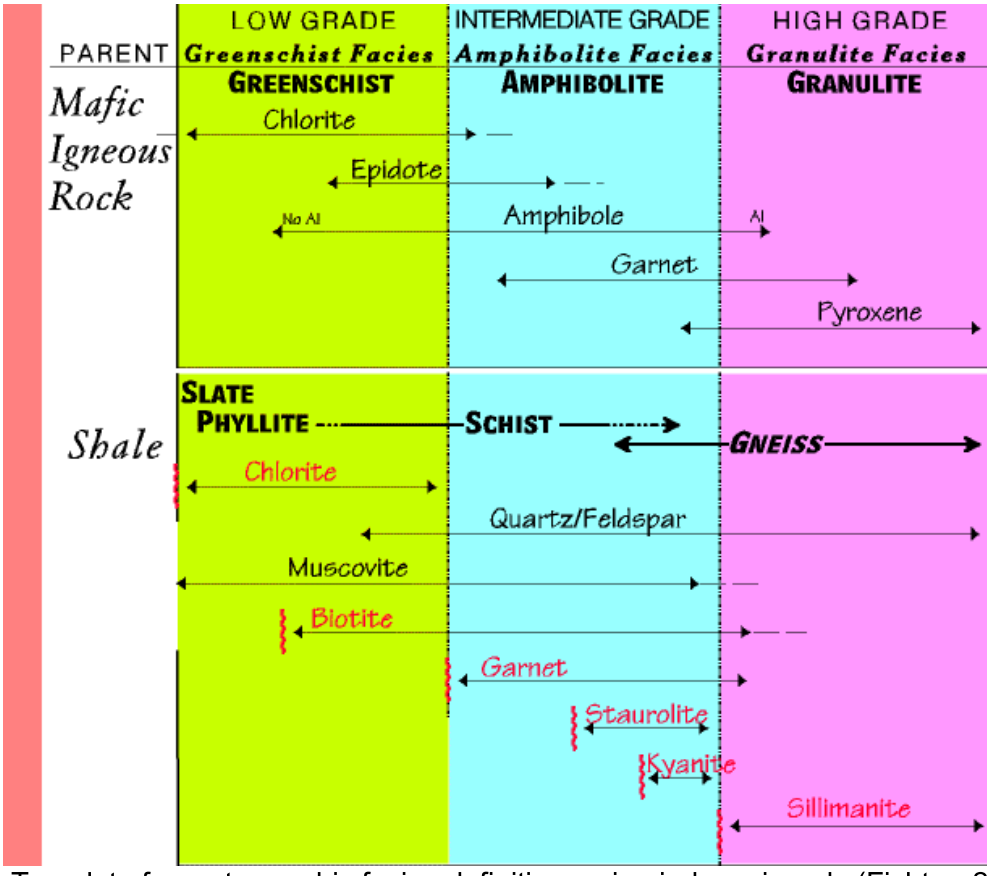

Figure 4: Template for metamorphic facies definition, using index minerals (Fichter, 2000)

Whole rock geochemistry of the representative lithologic samples was investigated at the geochemical laboratory of the Geological Survey Agency of Nigeria, Kaduna, using X- Ray Fluorescence Spectrophotometer, to obtain elemental gold concentration data. Each sample was pulverized and then homogenized in preparation for the elemental concentration determination.

RESULTS AND DISCUSSION

Figure 5 is a rock fragment dug up from the mine site. Quartz (Q), biotite (B), orthoclase (ORT) and

kyanite (K) were seen in thin section view (Plates 1 and 2) of the sample (Sample 1) for the rock fragment. It was identified as kyanite schist in upper amphibolite metamorphic facies by virtue of observed schistose texture and presence of kyanite, in conformity with facies template given in Figure 4.

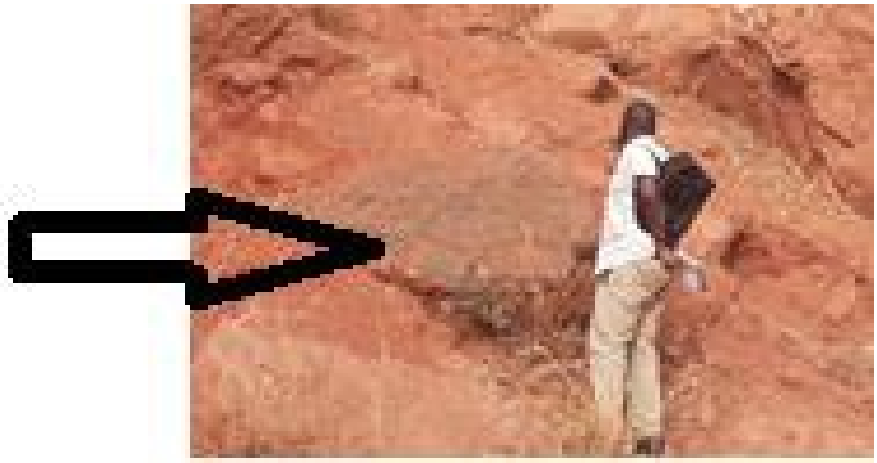

Figure 5: Kyanite schist at Mutumdaya mine pit (9°39'55.3" N; 6°49'0.24" E)

Its photomicrographs under plane polarized light (PPL) and cross polarized light (XPL) are plates 1 and 2 respectively.

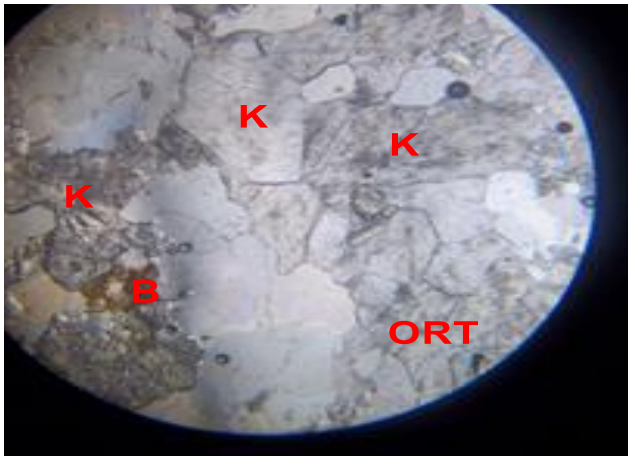

Plate 1: Photomicrograph (PPL) M40 for Sample1

Plate 2: Photomicrograph (XPL) M40 for Sample 1

Figure 6 is an outcrop at Latitude 9°39'52"N and Longitude 6º49'02"E, in the environs of the mine. Quartz, orthoclase and amphibole were observed in thin section (Plates 3 and 4) of its sample (Sample 2). It was identified as amphibole schist on account of its schistosity and dominant amphibole. The outcrop is in the amphibolite facies by virtue of the presence of amphibole, in with the facies template (Figure 4).

Figure 6: Amphibole schist at 9°39'52"N; 6°49'02"E

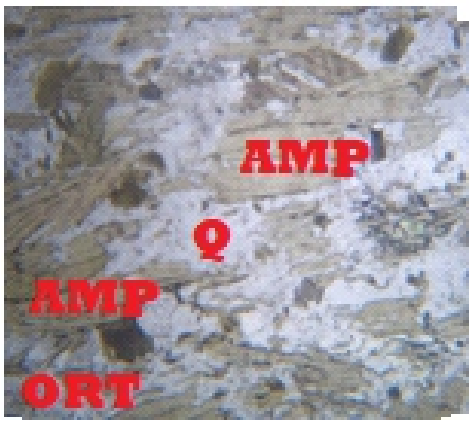

Plate 3: Photomicrograph (PPL) M40 for Sample 2

Plate 4: Photomicrograph (XPL) M40 for Sample 2

Figure 7 is a rock sample from a very poor exposure at Lat. N9°40'04" and Long E 6°48'50". Minerals observed in its thin section (Plates 5 and 6) are quartz, cummingtonite and kyanite (Sample 3). The schistose texture and presence of cummingtonite (an amphibole) and kyanite makes it amphibole schist in the amphibolite facies metamorphic grade.

Figure 7: Kyanite schist at 9°40'04"N and 6°48'50"E

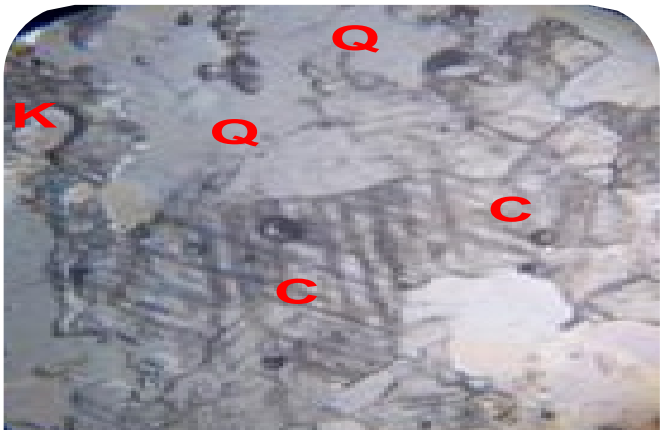

Plate 5: Photomicrograph (PPL)M40 for Sample 3

Plate 6: Photomicrograph of sample 3 (XPL) M40

Figure 8 is a quartz schist outcrop at Latitude N 9°39'50.9'' and Longitude E6°49'3.7''. Photomicrographs (Plates 7 and 8) of a vein filling (Sample 4) in the schistose outcrop shows the presence of quartz, biotite and orthoclase. The combination of quartz, biotite and orthoclase places this rock in the upper greenschist facies, in conformity with the facies template in Figure 4.

Figure 8: Quartz schist outcrop at N9°39'50.9"49'3.7"E

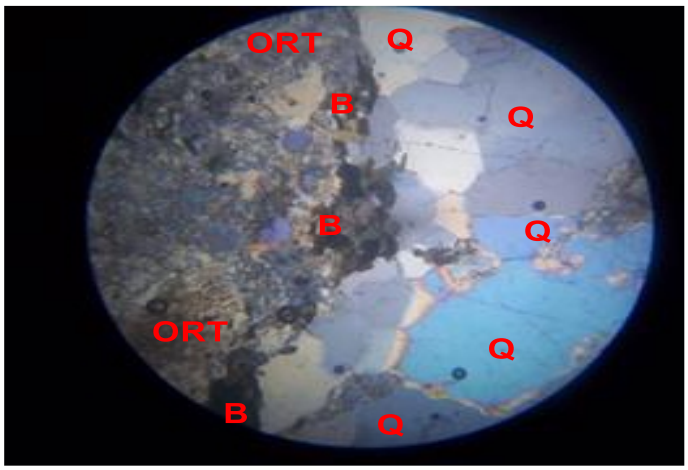

Plate 8: Photomicrograph of sample 4 (XPL) M40

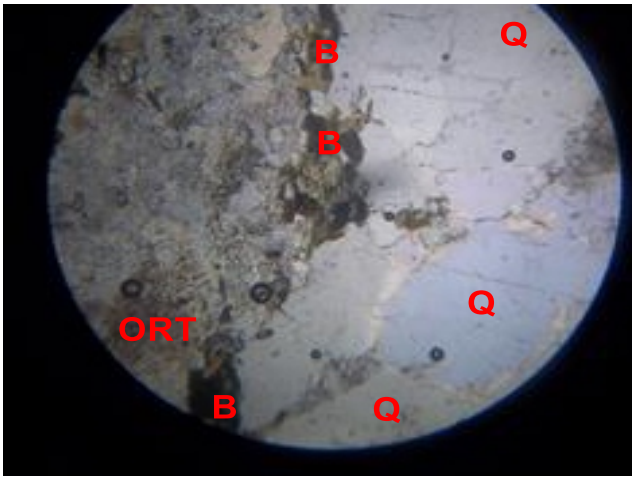

Plate 7: Photomicrograph (PPL) M40 for Sample 4

Figure 9 is quartzite outcrop at Lat. 9°40'01.4"N and Long 6°49'15.1"E.

Figure 9: Quarztite outcrop at Latitude N9°40'01.4"; Longitude E6°49'15.1"

The quartzite body is unferruginised, unlike most quartzite bodies in Minna and environs.

Both the schist and quartzite outcrops were intruded by medium to coarse grained biotite granite (Figure 10). The granite body is slightly foliated and therefore identified as syntectonic biotite granite.

Figure 10: Granite body at Latitude N9°40' 03.3" and Longitude E6°49'12.9"

Photomicrograph of the thin section from the granite sample – Sample 5 (Plates 9 and 10) - shows quartz, biotite and orthoclase.

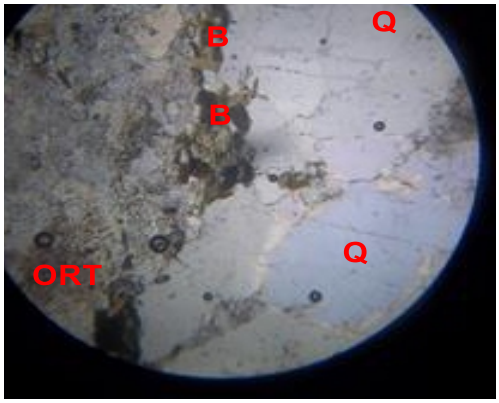

Plate 9: Photomicrograph of granite (PPL) M40 (Sample 5)

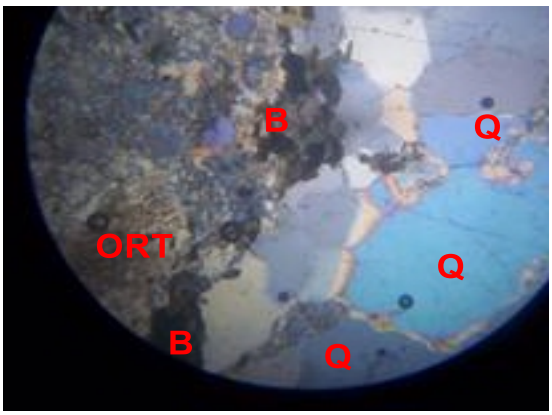

Plate 10: Photomicrograph of granite (XPL) M40

Figure 11 is the geological map produced from the lithological units.

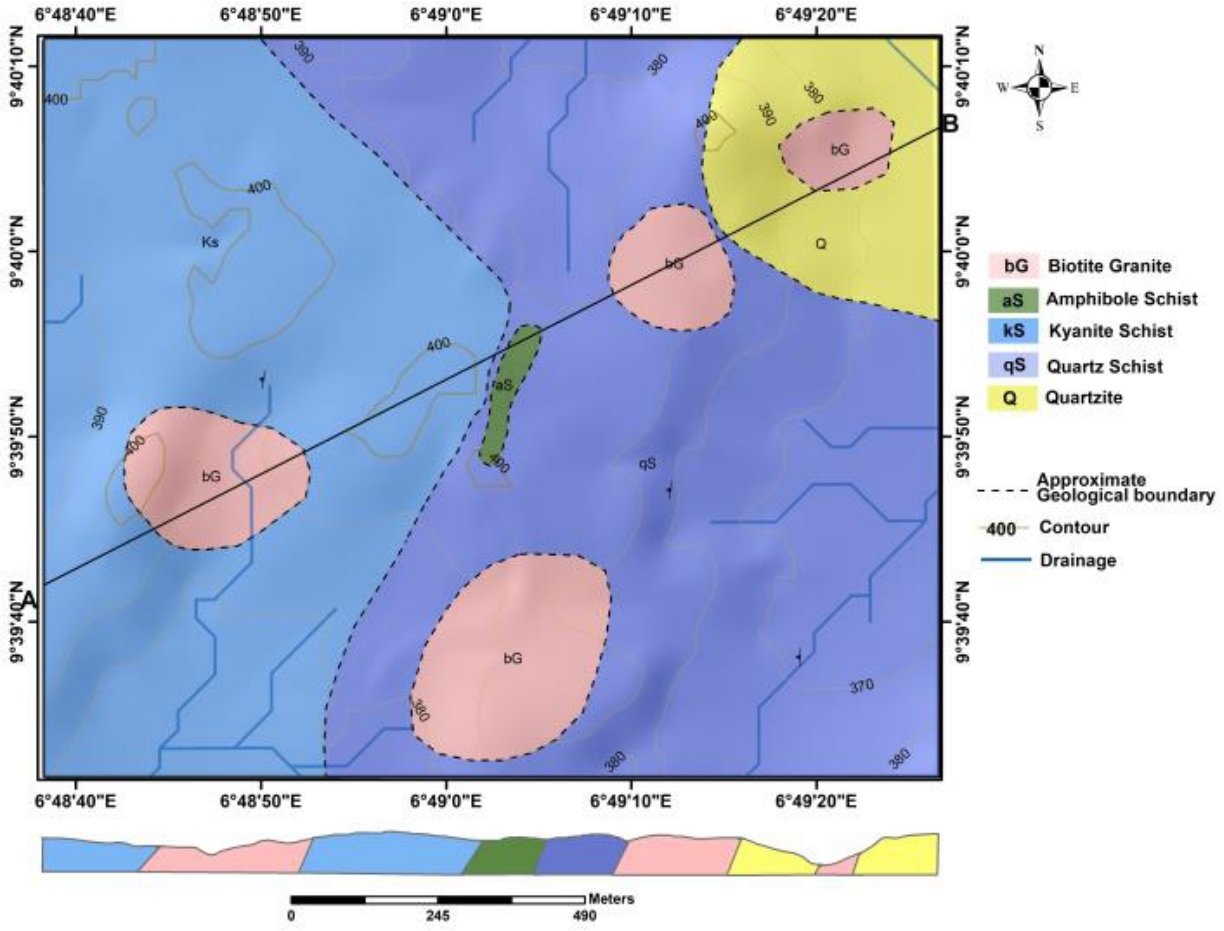

Figure 11: Geological map of Mutumdaya

Results of the X-Ray Fluorescence spectrophotometer analysis for gold concentration (in ppm) in the lithologic samples are presented in Table 1.

Table 1: Trace Element Concentration (in ppm) of some lithologic samples

SAMPLE	LATITUDE	LONGITUDE	Au	ROCK TYPE
1	9° 39'55.3"N	6° 49'0.24"E	0.058	KYANITE SCHIST
2	9° 39'05"N	6° 48'40"E	0.021	AMPHIBOLE SCHIST
3	9° 40'05"N	6° 48'50"E	0.066	KYANITE SCHIST
4	9° 39'50.9"N	6° 49'3.7"E	ND	UPPER GREENSCHIST FACIES SCHIST
5	9° 40'01.4"N	6° 49'15.1"E	ND	QUARZITE
6	9° 40'03.3"N	6° 49'12.9"E	ND	GRANITE

ND means Not Detected

The S1 sample is a kyanite schist fragment obtained from the exhausted mine site. The kyanite content places the schist in upper amphibolite facies metamorphic grade. Its elemental Au concentration is 0.058 ppm. This gives a gold enrichment factor of 29 when divided by an average crustal abundance of gold (0.0000002 %).

Rock sample S3 is from a schist outcrop at Latitude N9° 40'04" and Longitude E6° 48'50". The elemental Au concentration obtained for this sample is 0.066 ppm. Gold is 33 times enriched in this schist than its average crustal composition. Its enrichment factor (33) is higher than the enrichment factor (29) that characterise the rock fragment from the

exhausted mines. Like rock fragments from the exhausted mine site, the S3 rock sample contains kyanite and thus is in upper amphibolite facies metamorphic grade. Elemental gold concentration is 0.032 ppm for the amphibole schist (sample 2) at Latitude N9° 39'52" and Longitude E6° 40'02". Gold is 15 times enriched in this rock body, which is also in the amphibolite facies. Thus all rock bodies in the amphibolite metamorphic facies status constitute prospects for by-pass lode gold mineralization within the immediate vicinity of the abandoned gold mine. Lode gold mineralization hosted in amphibolite facies have been reported by some workers, among whom are Ridley *et al.*(1998), Simard *et al.*(2013), and Kalinin *et al.*(2019). Gold was undetected in the schist outcrop in upper greenschist facies, as well as in the quartzite and granite rock bodies. Since gold is the best pathfinder for gold (Murphy, 2016), the quartzite, granite and upper greenschist facies schist in Mutundaya are barren of gold mineralization. Figure 12 shows positions of the abandoned gold mine and proposed new gold mine for by-passed gold mineralization in Mutundaya.

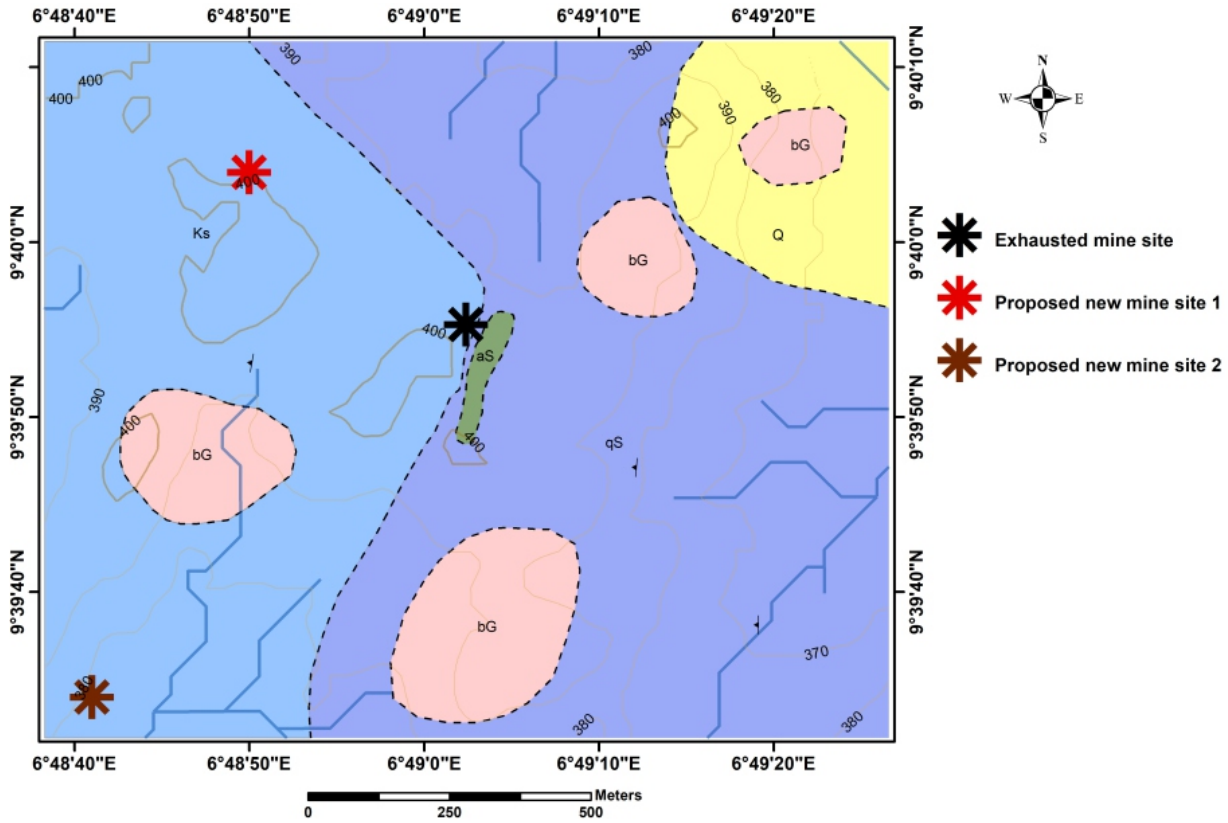

Figure 12: Locations of abandoned gold mine and proposed new gold mine for by-passed gold mineralization in Mutundaya

CONCLUSION

Textural and mafic colour index analysis of rock samples in hand specimen, as well as thin section petrographic analysis revealed the rock bodies within the mine and its immediate vicinity to be kyanite schist, amphibole schist, quartz schist, unferruginized quartzite and syntectonic biotite granite. Observed field relationship showed that the syntectonic biotite granite intruded the schist bodies and the quartzite. By virtue of kyanite being an index mineral, the kyanite schist achieved amphibolite metamorphic facies status. The presence of orthoclase and amphibole in the amphibole schist revealed that the schist attained the upper greenschist facies status. Elemental gold concentration varies from 0.032 to 0.066 ppm in the amphibolite facies schist, and is higher than the elemental gold concentration of 0.055 ppm in the mine rock body at some locations. The gold enrichment in these schist bodies ranges from 15 to 33 times higher than the average crustal elemental gold concentration. The schist in amphibolite facies

metamorphic grade constitutes by-passed lode gold mineralization bodies within the immediate vicinity of the abandoned gold mine. It is recommended that all abandoned gold mines once operated by artisanal miners should be explored for by-passed gold deposits in the vicinity of the mines, in the Northern Nigerian Massif and in countries with significant artisanal mining, using integrated geoscientific methods.

REFERENCES

Ajibade, A.C., Anyanwu, N.P.C., Okoro, A.U. and Nwajide, C.S. (2008). The geology of Minna Area, Geological Survey Agency of Nigeria, Madol Press, Abuja112p.

Al-Sayid, K.Z. (2019). Geological and geochemical techniques.

Bucher, K. and Grapes, R. (2011). Petrogenesis of metamorphic rocks, 8th Edition, Springer-Verlag, Berlin, 419p.

Eskola, P. (1920). The mineral facies of rocks. Norsk. Geol. Tidsskr.6(1922), 143 – 194

Fichter, L.S. (2000). Barrovian metamorphism and metamorphic grade. Jmu geology.

Csmgeo.csm.jmu.edu/geollab/fichter/metarx/barrovian.htl

Garba, I. (2002). Late PanAfrican tectonics and origin of gold mineralization and rare- metal pegmatites in Kushaka Schist Belt, Northwestern Nigeria. J. Mining and Geology, v.8, 1-12.

Groves, D.I. and Foster, K.P. (1991). Archean lode gold deposits. In: Gold metallogeny and exploration. Springer, Boston. https://doi.org/10.1007/979-1-14613-0497-5-3

Haldar, S. (2018). Mineral Exploration, 2nd Edition, Elsevier, 370p.

Kalinin, A.A., Kazanov, O.V., Bezrukov, V.I. and Prokofiev, V. Yu. (2019). Minerals, 9(3), https://doi.org/10.3390/min 9030137

Kankara, I. and Darma, M.R. (2016). A review of gold metallogeny in Nigeria. International Journal of Research in Chemical, Metallurgical and Civil Engineering, 3(2), 49-57.

Mc Curry, P. (1989). A general review of the Geology of the Precambrian to Lower Paleozoic rocks of Northern Nigeria.In: Geology of Nigeria. Ed. Kogbe, C.A., 2nd Ed., pp13 – 37.

Mibel, G. (2014). Introduction to types and classification of rocks. Short Course IX on Exploration for Geothermal Resources. UNU – GTP and Kengen, Kenya

Murphy, M.E. (2016). The trace element chemistry of arsenopyrite and its potential use as an indicator mineral for gold deposit exploration in Australia. PhD thesis unpublished. The University of Western Australia, 357p.

Noor, M., Tonggirch, A. and Mulana, A. (2016). Type of gold hydrothermal deposits in Metamorphic Rock District, Buru Province, Malukul. International Journal of Engineering, 3, 39 – 45.

Nwabufo-Ene, K.E. and Mbonu, W,C. (1988). The metasedimentary belts of the Nigerian Basement Complex – Facts, Fallacies and new Frontiers. In: Precambrian Geology of Nigeria. Eds: Oluyide, P.O., Mbonu, W.C., Ogezi, A.E., Egbuniwe, I.G., Ajibade, A.C., Umeji, A.C., pp 35-65.

Obaje, N.G. (2013). Updates on the geology and mineral resources of Nigeria. Onaivi printing and publishing Co, Abuja, 213 p.

Panchuk, K. (2021). Physical Geology. First University of Saskatchewan Edition

Revuelta ,M.B. (2018). Mineral Resources, Springer Nature, Switzerland, 641p

Ridley, J., Groves, D.I. and Knight, J. H. (1998). Dold deposits in Amphibolite and Granulite Facies Terranes of Archean Yilgam Craton, western Australia: Evidence and implications of synmetamorphism mineralization. Doi:https//doi.org/10.5382/Rev/11.12

Robert, F., Brommeckar, R., Bourne, B.T., Dobak, P.T.,McEwan, C.T., Rowe, R.R. and Zhou, X. (2017). Models and Exploration models for major Gold Deposit Types. In: Proceedings of Exploration 07: Fifth Decennial International Conference in Mineral Exploration. Eds: Mikerett, B., 6991-711.

Sahin, M.B. and Erkan, Y. (1999). Nineral Res Expl., 121, 83-100

Sillitoe, R.H. and Thompson, J.F.H. (2006). Changes in Exploration Practice: consequences for discovery. Society of Economic Geologists Special Publication 12,

193-219.

Timkin, T., Voroshilov, V., Yanchenko, T. (2016). IOP conference : Earth Enviroon.Sci

430120B. Geology, geochemistry and gold-ore potential assessment within Akinmov ore-bearing zone, the Altai territory, Russia.

Unuevho, O.M. (2018). Geology and Geochemistry of Rocks around Mutundaya Gold Mine, Sheet 164SW, North- Central Nigeria. Unpublished BTech Geology Thesis, Federal University of Technology, Minna, Nigeria, 51p.

Unuevho, C.I**.,** Oragba, F.U., Umar, B.S., Oduleke. R.B., Saliu, S., & Udensi, E.E (2018). Geological, Geochemical, and Geoelectrical Prospecting for Ore Mineral Resources in Garatu, North- Central Nigeria*. International Journal of Geology and Earth Sciences ,4(1)*,30-44.

Winter, J.D. (2020). Metamorphic Grades, Zones, Facies and Facies Series: in principles of

Igneous and metamorphic petrology. IUGS – SCRM: https/:www.bjs.ac.uk/scmr/home.html

Woakes, M., Rahaman, M.A. and Ajibade, A.C. (1987). Some metallogenetic features of the Nigerian Basement Complex. Journal of African Earth Science, 16(5), 655-664.

Oyeladun, *et al* (2021) Nigerian Mining Journal, (19) 19 - 28

Beneficiation of Jaruwa Iron Ore for the Production of Super Iron Concentrate

Oyeladun, O. A. W., Tolu, S. and Salawu A. O.
Department of Mineral and Petroleum Resources Engineering, Kaduna Polytechnic, Kaduna
Corresponding author: oawoyeladun@gmail.com, *+2348023636689*

Abstract

Upgrading of iron ore to meet up with production of super iron concentrate industry is necessary. Hence, the beneficiation of Jaruwa iron ore using jigging operation followed by reverse froth flotation were carried out. The chemical analysis of the iron ore head sample revealed the ore contains 52.65%Fe and 22.46%Si. The mineralogical composition of the ore revealed the presence of magnetite and other associated minerals such as quartz and cordierite. The concentration was carried out using jigging operation followed by reverse froth flotation. The results of the concentration processes revealed using jigging operation was 62.49% and recovery of 81.20% which was followed by froth flotation process with concentration of 69.21% and recovery of 89.67%. The super iron concentrate could be used MIDREX production of iron.

Keywords: Beneficiation, jigging operation, froth flotation process

1.0. INTRODUCTION

1.1 Background

Iron (Fe) is one of the most abundant rock-forming elements, constituting about 5% of the Earth crust. It is the fourth most abundant element after oxygen, silicon and aluminum, after aluminum, the most abundant and widely distributed metal. Iron ores are rocks from which metallic iron can be economically extracted. These rocks are usually found in the form of hematite (Fe_2O_3), magnetite (Fe_3O_4) and siderite ($FeCO_3$) (Paul, 2004).

Also, the primary use of iron ore the production of iron, about 98% of world iron ore production is used to make iron in the form of steel. Most of steel is used to make automobiles, locomotives, ships, beams used in buildings, furniture, paper clips, tools, reinforcing rods for concrete, bicycles, and thousands of other items. It is the most-used metal by both tonnage and purpose (Yaro, 2001).

Furthermore, steel is the most useful metal known being used 20 times more than all other metals put together. Steel is strong, durable and extremely versatile. The many different kinds of steel consist almost entirely of iron with the addition of small amounts of carbon (usually less than 1%) and of other metals to form different alloys (e.g. stainless steel). Pure iron is quite soft, but adding a small amount of carbon makes it significantly harder and stronger. Most of the additional elements in steel are added deliberately in the steelmaking process (e.g. chromium, manganese, nickel, molybdenum). By changing the proportions of these additional elements, it is possible to make steel suitable for a great variety of uses (Thomas, 2001).

However, iron ore form nearly all of earth's major ore rocks that formed over 1.8 billion years ago. At that time, Earth's oceans contained abundant dissolved iron and almost no dissolved oxygen. The iron ore deposits began forming when the first organisms capable of photosynthesis began releasing oxygen into the waters. This oxygen immediately combined with the abundant dissolved iron to produce hematite or magnetite. These minerals deposited on the sea floor in great abundance, forming what are now known as the "banded iron formations." The rocks are "banded" because the iron minerals deposited in alternating bands with silica and sometimes shale. The banding might have resulted from seasonal changes in organism activity (Thomas and Yaro, 2001).

Nigeria is among the African countries with vast iron ore deposits which can be found in some states in the country. Itakpe in Kogi State is

believed to have the highest number of deposits of iron ore and other states where it is deposited includes: Enugu, Niger, Zamfara, Kaduna, Abia, Anambra, Bauchi, Benue, Kwara, Plateau and Nasarawa States.

Moreover, there are four main types of iron oxides deposits solely dependent on the mineralogy and geology of the ore deposits in form of magnetite (Fe_3O_4.), hematite (Fe_2O_3), goethite (FeO.(OH)), limonite (FeO.(OH).n(H_20)) siderite ($FeCO_3$), etc. The ore usually is rich in iron and vary in color from dark grey, bright yellow, or deep purple to rusty red.

1.2 Location and Accessibility

The iron ore deposit is located at Jaruwa village, Birnin Gwari L.G.A, Kaduna State with Coordinates 11'03 28N and 6'57 08E

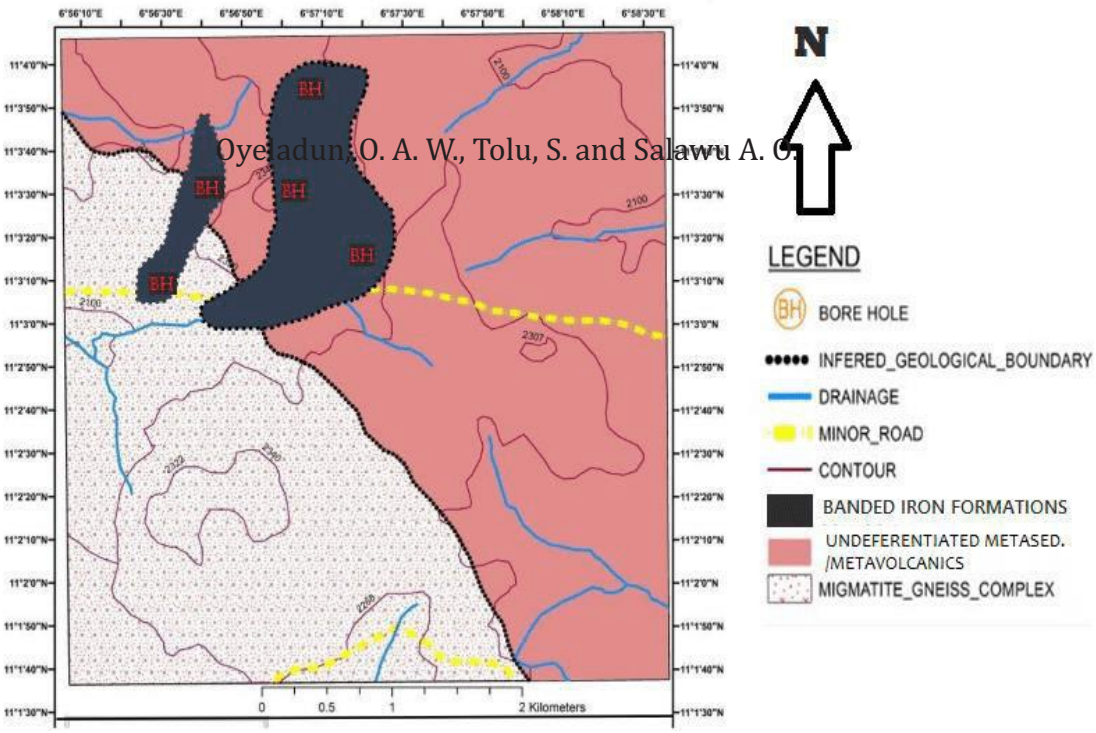

Fig 2.1: Geological map of the study area located around Jaruwa

1.3 Geology of the Area

The entire Kaduna State is underlain by a basement complex of igneous and metamorphic rocks of mainly Jurassic to Pre-Cambrian ages. The basement complex rocks are essentially granite gneisses, migmatites, schists and quartzites (Benett, 1979). The geology of Kaduna North is predominantly metamorphic rocks of the Nigerian basement complex consisting of biotite gneisses and older granites (Kaduna State, 2003).

The topographical relief is relatively flat, having an elevation of between 600 and 650metres in large areas of the local government. It is over 650 metres above mean sea level (a.m.s.l.) in some places, and below 500 metres in places that slope downward towards the river.

1.4 Occurrence of Iron Ore in Nigeria.

It has been proven that Nigeria is blessed with numerous mineral resources, these include Banded Iron Formation (BIF) which occur in metamorphosed folded bands and lenses associated with the Precambrian metasedimentary schist belts which include low grade metasediments, high grade schist, gneisses and migmatites, these are interbedded with pelitic and semi politic phyllites and schists. prominently outcropping in the western half of the country: including Tajimi, Itakpe, Ajabanoko, Ochokochoko Toto, Farin Ruwa, Birnin Gwari , Maru,Jamare, Kaura Namoda, Kakun, Isanlu, Roni and Ogbomoso areas, and the Cretaceous sedimentary (oolitic) iron deposits which occur prominently around Agbaja, Koton karfi, Nsudde areas in the North central and south eastern

zones of the Nigeria respectively. Iron ore reserves in Nigeria were estimated at 11000 million tonnes. Today however, available data has shown that Nigeria has about 2.5 billion metric tons of iron ore reserve, this placed the country as the 12th largest iron ore resource country in the world and the second largest in Africa, but about 70 percent of the deposits are yet to be proven (Yaro 1997).

1.5. Beneficiation of Iron ore

Beneficiation or concentration involves the separation of valuable minerals from the other raw materials received from the grinding mill. In large-scale operations, this is accomplished by taking advantage of the different properties of the minerals to be separated. These properties can be color (optical sorting), density (gravity separation), magnetic or electric (magnetic and electrostatic separation), and physicochemical (flotation).

Different beneficiation methods of iron ore have been developed for different types of iron ore taken cognizance of the grade, and associated tailing. These physical processes include magnetic separation, gravity separation, froth flotation and combination of these techniques. The susceptibility of any iron ore to beneficiation by one of these techniques a major determination into the development of process route for it concentration. The amenability of any types of ore to beneficiation depends on its mineralogical characteristic (Will, 2007).

1.5.1 Gravity Concentration

Gravity concentration method is separating of minerals of different specific gravity by their relative movement in response to gravity and other force (the resistance to motion offered by a viscous fluid such as water or air). It is important for effective separation that marked density differences exist between the mineral and gangue.

Gravity method operate by virtue of the difference in density of various minerals; the greater the difference between two mineral, the easier they can be separated by gravity methods. The laws of free and hindered setting are also very important in the theory of gravity concentration, (Will, 2007). Gravity concentration process are those processes for the separation of minerals of different specific gravity by including variance movement in responses to the force of gravity and one or more forces natural or applied with the assistance of a flowing film. In particular, magnetic separation, floatation and chemical treatment. The major demerit of gravity separation process itself. Even with advanced (or more sophisticated) slime gravity concentrators the practical lower limit of particle size, which can be handled is still about 10μm (Yaro 1997).

A. Principle of Gravity Concentration

1. Concentration Criterion

Some idea of the amenability of separation of two minerals can be obtained from the concentration criterion, which is usually defined as: The specific gravity of the heavy species minus the density of the suspending fluid, divided by the specific gravity of the light species minus the density of the suspending fluid.

The determining criteria, are the relative density of value and gangue minerals modified by the media density, the particle size range, degree of liberation and the particle shape. It is difficult to account for all these factors in a single expression to determine whether gravity separation is possible (Abouzeid, 1990). A simple relative density difference criterion known as gravity concentration criterion C has been suggested as a rough measure for the possibility of gravity separation (Abouzeid, 1990).

Algebraically: using mathematical equation

$$\text{Gravity concentration criterion, C} = \frac{\rho h - \rho f}{\rho l - \rho f}$$

Where:

ρh is density or specific gravity of heavy mineral

ρl is density of light mineral

ρf is the density of media

According to Vijayendra (2001) if this ratio is negative or a positive number greater than 2.5, separation in water is easy at all sizes down to the finest sands. When the criterion value between 1.75 and 1.50 separation is possible down to 210 μm.

At ratio 1.25, good separation is difficult, below which commercial separations by gravity

concentration without differential weight modification is not possible. The laws of free and hindered settling are also very important in the theory of gravity concentration.

In order to allow for difference in particle shape, the Concentration Criterion must be multiplied by a shape ratio factor. This factor is the quotient of the shape settling factor for the heavy mineral and the shape settling factor for the light mineral.

The shape settling factor is the ratio of terminal velocities of two particles of the same mineral of the same measured particle size but different shape; the first particle to be that for which the ratio is required and the second a sphere. Provided particle shape is taken into account, the Concentration Criterion can be quite useful. If shape is ignored, mineral processor may well be in for some unpleasant surprises.

B. Mechanisms of Concentration

The various mechanisms are represented pictorially below:

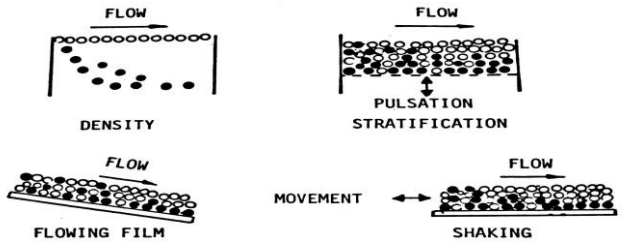

Figure 2.3 the Various Mechanisms of Gravity Concentration

a. Density: The viscous fluid used has a density or apparent density in between that of the minerals to be separated, such that one mineral(s) will have a net positive buoyancy and will float, whilst the other(s) will have a net negative buoyancy and will sink. Into this classification fits heavy medium separation, one of the most important of all gravity concentration processes as well as magnet-hydrostatic separation.

b. Stratification: The various mineral constituents are stratified by being subjected to an intermittent fluidization caused by the pulsation of the fluid in a vertical plane. This classification is represented by jigs of which there are a wide range and number.

c. Flowing film: The various constituents are separated by their relative movement through a stream of slurry which is flowing down a plane by the action of gravity. Flowing film concentration is the oldest process used in gravity concentration and remains of major importance, with such units as the sluice or palong, pinched sluice. Reichert cone, and, by including lateral movement caused by the addition of centrifugal force, the spiral.

d. Shaking: The mineral components are stratified by superimposing on the flowing film, a horizontal shear force, whether it be oscillating as in a shaking table, or orbital, as is the case on the Bartles-Mozley separator or Crossbelt concentrator.

1.5.2 Flotation Process

Flotation or more specifically froth flotation is both a physical and chemical process of concentrating finely ground ores that depends on the selective adhesion to air of specific minerals while others remain submerged in the pulp.

The process involves treatment with suitable reagents of an ore pulp to create conditions favorable for the attachment of certain (hydrophobic) mineral particles to air bubbles and render the other solids hydrophilic or water - loving.

The air bubbles carry the selected minerals to the surface of the pulp and form a stabilized froth, which is skimmed off while the other minerals remain submerged in the pulp. (Wills.2007).

Although flotation was originally developed in the mineral industry, the process has been gradually extended to other fields.

In general, mineral particles coarser than 48 mesh (about 295 microns or 0.295 mm in diameter) cannot be effectively recovered; consequently, an ore that is to be floated must first be ground fine enough so that the desired mineral is all, smaller than this limiting size.

Flotation is a selective process and can be used to achieve specific separations in complex ores. It is best applied to very fine particles of minerals so that downward pull of gravity will be insufficient to overcome its adhesion to an air-water interface.

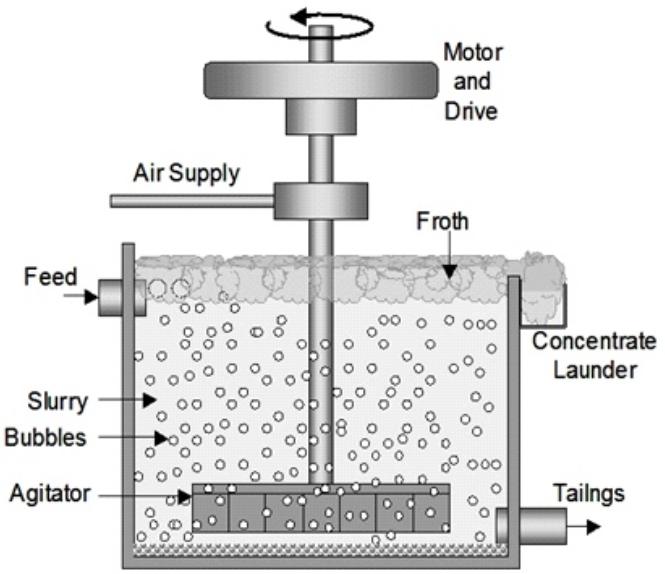

Figure. 2.6 Froth Flotation Machine

A. Principle of Flotation

There is a complexity in the theory of froth flotation, but nevertheless, the mechanism involved is simple. The essential mechanism of flotation involves the attachment of mineral particles to air bubbles in such a manner that the particles are carried to surface of the ore pulp, where they can be removed (Will. 1992)

In general, mineral, which in its natural state are not hydrophobic, or aerophilic is made to develop the required contact angle by the reagent for easy adhesion of the air bubbles for flotation (Wills, 1985)

B. Types of Flotation

There are various types of flotation concentration process, which include the following

a) Direct Flotation: Flotation of the valuable mineral

b) Reverse Flotation: Flotation of the gangue mineral

c) Roughing: Floatation to obtain concentrate from the first few cells of a bank of cells which is usually refloated to obtain higher grade concentrate.

d) Scavenging: Middling which are weak aerophilic mineral particles

e) Cleaning: Refloating the rough concentrate in another cell to obtain a high-grade concentrate

Meanwhile, reverse or indirect flotation process is best used in the flotation of iron ore (Wills, 2007)

C. Flotation Agent

Flotation agents or reagents are substances added to the mineral pulp prior to or during flotation in order to make possible or to facilitate the process.

Flotation agents or reagents may be classified as Collectors, Frothers and Modifiers.

- Collector or promoters: Examples are oils, organic bases, and organic acids and their salt.
- Frother: Examples are Amyl Alcohol $C_5H_{11}OH$, Cresol $CH_3C_6H_4OH$ in cresylic acid, Terpinol$C_{10}H_{17}OH$ in pine oil
- Modifiers or regulator: Examples are grouped into depressants, activator, pH regulator and dispersants.

1.6. The Requirements of Iron Super Concentrates

The requirement of grades of iron super concentrate are magnetite (Fe_3O_4. 68 – 72.49%Fe), hematite (Fe_2O_3, 67 – 69.9%Fe), goethite (FeO.(OH), 62.9% Fe), limonite (FeO.(OH).n(H_20), 559% Fe) siderite ($FeCO_3$, 48.2% Fe), etc. (Ola et al, 2009; Wang and Yang, 2011)

2.0. MATERIALS AND METHODS

2.1 Equipment

The equipment used in carrying out this research work include the following; sledge hammer, laboratory jaw crusher, pulverizer (grinding), ball mill grinding machine, sieves, sieve shaker, weighing machine, X-RAY fluoresce (XRF) machine, X- RAY Diffraction (XRD) machine, jigging machine and froth flotation machine.

2.2 Sample Collection

The iron ore sample used for this project was obtained from Jaruwa village of Birnin Gwari Local Government in Kaduna State. Grab method of sampling was used to collect the sample. The

sample was collected from (4) four points at interval of 100m at 3m depth.

2.3 Sample Preparation

Representative sample weighing 5kg were collected from the site location, in lumps size undergo comminution process. The ore was broken into the size that could be fed into a jaw crusher using a sledge hammer. Crushing of the ore was carried out in the laboratory jaw crusher. After crushing, the samples were taken for pulverizing machine for further reduction of size. Since the size of the crusher is not suitable for the sieves analysis as well as gravity separation, the grinding is carried out in a ball mil. The ball mill was allowed to run for (20)minutes as the mill rotates the ore samples is ground by combined effects of impacts and abrasion forces.

2.4 Chemical composition of the Head sample using XRF

X-ray fluorescence, process whereby electrons are displaced from their atomic orbital positions, releasing a burst of energy that is characterize of a specific element. The x-ray beam is then emitted from the front end of the handheld XRF analyzer.

2.5 Mineralogical analysis of the Head sample

Part of the sample was analyzed to determine the mineralogical properties of the ore using XRD, it can be used to identify crystals which are present in a mixture. Crystalline sample is place in the path of an x-ray beam. X-rays diffract through the crystal and into a detector.

2.6 Particle Sieves Size Analysis

The sieves apertures were arranged using the principle of root ($\sqrt{2}$) finest sieve aperture) or ($\sqrt{2}$/coarsest sieves aperture). The sieves were arranged from the coarsest sieve at the top (Control sieve) which was 355um down to the finest sieve (90um) and the pan at the bottom. 500g of the ore was introduce into top sieve size and machine was allowed to vibrate 20 minutes, samples were collected and analyzed using X-ray fluorescence (XRF).

2.7 Jigging Concentration

The jigging machine was first cleaned to remove all possible dirt from the machine. A thick bed coarse heavy particles (ragging) was placed on a perforated horizontal jig screen. The feed (Iron ore) was poured from the top. Water was pulsated up and down (the jigging action) by pneumatic or mechanical plugger. The feed moves across the jig bed. The heavier particles penetrate through and screen to settle down quickly as concentrate. The concentrate was removed from the bottom of the device. The jigging action causes the lighter particles to be carried away by the cross flow supplemented by a large amount of water continuously supplied to the concentrate chamber. This was repeated 3 times at interval of 10 minutes. The product (concentrate and tailing) were collected and dried, samples were analyzed using X-ray fluorescence (XRF) technique.

2.8 Reverse Froth flotation

The flotation was carried out at different reagents of pine oil as frother and kerosene as collector. The pulp 40% solid by weight was prepared; the pulp was conditioned for 10-20 minutes to ensure proper mixing. The reagents were then added at different collector dosage to the mineral pulp and the air bubbles were introduced by the flotation machine. The froth was then collected. The concentrate and tailing were dried in an oven and analyzed using X-ray Fluorescence.

3.0. RESULT AND DISCUSSION

3.1 Chemical Composition of Head Sample Using X-Ray Fluorescence

Table 1: Chemical composition of the Head sample of Jaruwa iron ore

Element	Al	**Si**	Mn	**Fe**	P	Co	Ba	Cu
% Composition	7.17	**22.46**	11.17	**52.65**	0.05	0.17	0.10	0.04
Element	Cl	S	K	Zn	Ca	Ti	Nb	V
% Composition	0.74	0.19	0.24	0.10	3.26	1.61	0.13	0.11

3.2. Mineralogical Analysis of Head Sample

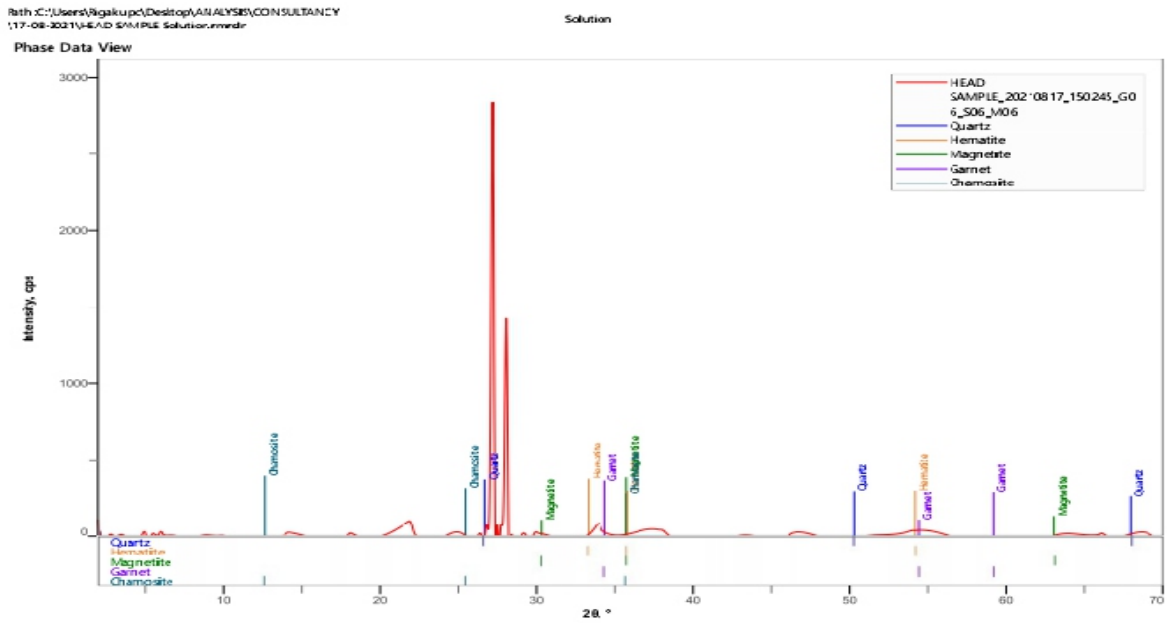

Figure 1: Mineralogical composition of Jaruwa iron head sample

Table 2: Mineralogical Composition Using X-ray diffraction

DB Card Number	Phase name	Formula	Figure of merit
00-002-0471	Quartz	SiO_2	2.850
00-006-0502	Hematite	Fe_2O_3	2.850
01-075-0449	Magnetite	Fe_3O_4	2.770
00-002-0981	Garnet	3 (Ca, Fe, Mg) O. (Al,Fe...	2.850
00-003-0063	Chamosite	Fe-Mg-Al-Si-O-OH	2.850

From Table 2, the Jaruwa iron ore contain silica, Hematite, Garnet and Chamosite as the major mineral while magnetite is minor mineral. These findings compared favorably with similar works done by Ndaliman, et al (2013), Yaro and Dungka (2009) and Salawu et al, (2016) where they stated that the iron ore minerals within the Kaduna schist are predominantly hematite and magnetite in association with calcium, aluminum and silica as gangues. This confirm the result of XRF analysis that the major iron bearing mineral present in Jaruwa iron ore are hematite and magnetite. Hence, the need for the beneficiation of the ore in order to upgrade its iron content.

Table 3 presents chemical analysis of the various particle sizes. The result reveals that at 355µm contains 53.82%Fe, 17.24 of Si, at 250µm contains 57.87%Fe, 15.86% of Si, at 180µm contains 51.52 %Fe, 18.51% of Si at 125µm contains 51.91%Fe, 23.92% of Si at 90µm contains 50.41%Fe, 26.00 % Si and pan 53.64%Fe, 20.98% of Si.

Table 4 presents the results obtained from the particle size analysis of the ore. The various size fraction obtained from the particle size analysis were subjected to chemical analysis. Sieve size 250µm gives the highest assay of Feas 57.87 %.

From Tables 3, 4 and Figure 2, the iron and silica minerals distributed itself normally. This trend compared favourably with works done by Weiss, (1985) and Wills, (2006) where they also observed similar trends. Furthermore, the liberation size of the iron ore is found to be 250µm being the sieve size with the highest assay value of the total iron content of 57.87%Fe and distribution of 20.06% as defined (Wills, 2006; Mills, 2014).

3.3. Particle Size Analysis of Jaruwa Iron Ore

Table 3: Chemical Analysis of the Various Particle Size

Element	**Pan**	**90um**	**120um**	**180um**	**250um**	**355um**
Al	7.65	7.55	7.44	7.98	6.31	7.49
Si	**20.98**	**26.00**	**23.92**	**18.51**	**15.86**	**17.24**
P	0.04	0.12	0.04	0.01	0.07	0.05
K	0.51	0.47	0.49	0.58	0.31	0.47
Ca	1.12	1.22	1.27	3.32	1.89	2.72
Ti	1.82	1.59	1.56	1.27	1.37	1.86
V	0.13	0.09	0.06	0.06	0.07	0.09
Cr	0.02	0.03	0.01	0.01	0.02	0.00
Mn	12.41	11.54	12.34	14.81	15.28	15.15
Fe	**53.64**	**50.41**	**51.91**	**51.52**	**57.87**	**53.82**
Co	0.19	0.14	0.15	0.14	0.15	0.16
Cu	0.08	0.06	0.04	0.04	0.05	0.08
Zn	0.05	0.05	0.04	0.05	0.04	0.05
Rb	0.23	0.20	0.22	0.20	0.18	0.24
Zr	0.06	0.02	0.06	0.10	0.03	0.04
Nb	0.52	0.13	0.15	1.05	0.15	0.14
Ba	0.45	0.28	0.19	0.25	0.12	0.25
Ta	0.01	0.00	0.00	0.03	0.04	0.03
W	0.10	0.10	0.09	0.06	0.20	0.13

Table 4: Sieves Size Analysis of Jaruwa Iron Ore

Sieves (μm)	Normal Aperture (μm)	Weight retained (g)	Percentage weight retained (%)	Cumulative wt. retained (%)	Cumulative wt. passing (%)	Assay of Fe
+355	355	40.7	8.28	8.28	91.72	53.82
-355+250	250	98.6	20.06	28.34	71.659	57.87
-250+180	180	55.7	11.33	39.67	60.326	51.52
-180+125	125	115.7	23.54	63.21	36.786	51.91
-125+90	90	75.2	15.30	78.51	21.486	50.41
Pan		105.6	21.49	100.00	0.00	53.64

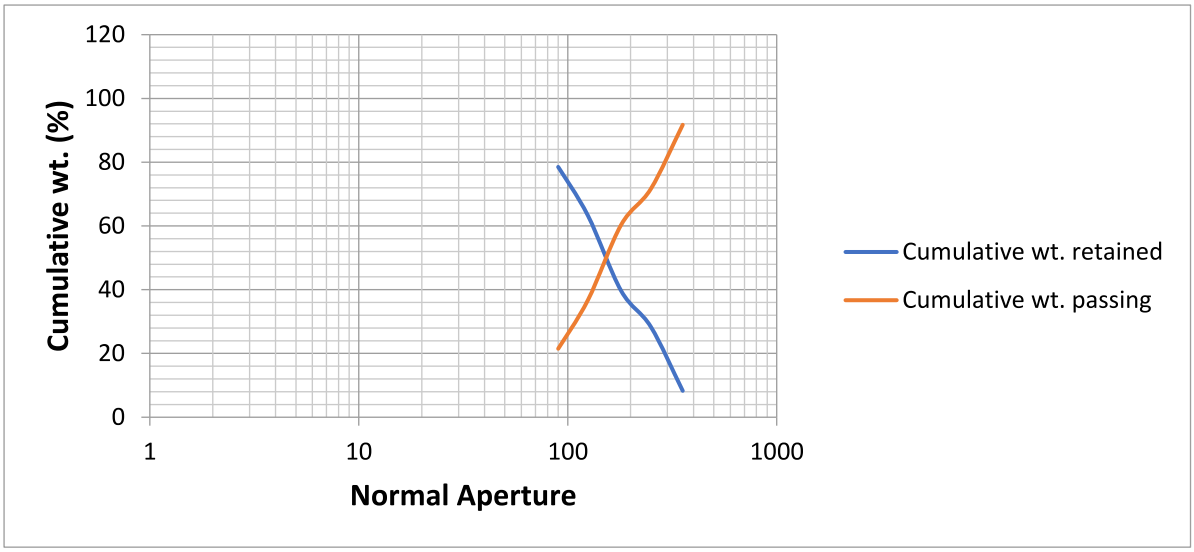

Figure 2: Particle Size Analysis of Jaruwa Iron Ore

3.5. Result of Jigging Operation

Table 5: Elemental Composition of Jigging products using X-Ray Fluorescence (XRF)

Element	Al	**Si**	Mn	**Fe**	P	Co	Ba	Cu
Concentrate (%)	5.36	**13.77**	11.54	62.49	0.04	0.21	0.27	0.04
Tailings (%)	8.85	**24.34**	15.23	43.86	0.10	0.12	1.38	0.08
Element	Cl	S	K	Zn	Ca	Ti	Nb	V
Concentrate (%)	0.94	0.15	0.15	0.09	1.38	1.91	0.38	0.09
Tailings (%)	0.84	0.51	0.59	0.49	1.93	1.12	0.30	0.06

From Table 5, Jaruwa iron ore after undergoing jigging operation contains 62.09%Fe and 13.77%Si in the concentrate, 43.86%Fe and 24.34%Si was found in the tailings. This result conforms to the requirement of iron concentrate for blast furnace technology and is in line with result in literatures.

3.6. Result of Froth Flotation of Jaruwa Iron Concentrate

Table 6: Elemental Composition of Froth flotation products using X-Ray Fluorescence (XRF)

Element	Al	**Si**	Mn	**Fe**	P	Co	Ba	Cu
Concentrate (%)	4.86	**3.33**	14.63	**69.21**	0.12	0.18	0.59	0.05
Tailings (%)	6.15	**38.96**	6.12	**33.91**	0.06	0.17	0.05	0.05
Element	Cl	S	K	Zn	Ca	Ti	Nb	V
Concentrate (%)	0.96	0.22	0.12	0.10	1.96	1.96	0.46	0.10
Tailings (%)	0.94	0.22	0.14	0.08	1.40	1.17	0.00	0.11

From Table 6, Jaruwa iron ore after undergoing jigging operation followed by froth flotation, it was revealed that Jaruwa iron ore concentrate contains 69.21%Fe and 3.33%Si, while 33.91%Fe and 38.96%Si was found in the tailings. This result conforms to the requirement of iron super concentrate for MIDREX process and is in line with result in literatures.

3.7 Recovery Permutation

The recovery in a mineral concentrating operation is the percentage of total metal content in the ore that is recovered in concentrate. The purpose of calculating is to determine the distribution of the metal in the feed or heads among the various product of the mineral concentrating operation. Below is the permutation for the recovery of the minerals of

interest (Iron Fe).

Mathematical equation

Metallurgical accounting of concentration using jigging operation

$$\text{Recovery, R} = \frac{c(f-t)*100}{f(c-t)}$$

$$\text{R} = \frac{62.49(57.87-43.86)*100}{57.87(62.43.86)} = 81.20\%$$

Metallurgical accounting of concentration using froth flotation process

$$\text{R} = \frac{69.21(62.49-33.91)*100}{62.4(69.21-33.91)} = 89.67\%$$

The recovery indicates that the concentrate produce (69.21% assay) meet up with the grade require for Midrex process and other process which require higher concentrate for the extraction of iron, this is in line with literature and ASM standards.

4.0. CONCLUSION AND RECOMMENDATION

4.1 Conclusion

The beneficiation of Jaruwa iron ore has been carried out and the following conclusions were drawn:

i. That chemical analysis revealed that the ore contains 52.65%Fe and 22.46%Si.

ii. The mineralogical composition of the ore revealed the presence of hematite, magnetite and other associated minerals such as quartz and chamosite.

iii. The particle size distribution reveal the presence of 53.82%Fe in +355µm, 57.87% of Fe, -355+250µm, 51.52%Fe in -250µm+180µm, 51.92%Fe in -180+125µm, 50.41%Fe in -125+90µm and 53.64%Fe in pan.

iv. That concentration of iron ore using jigging operation was 62.49% and recovery of 81.20% which was followed by froth flotation process with concentration of 69.21% and recovery of 89.67%.

4.2 Recommendation

The exploitation of Jaruwa iron should be carried out using jigging operation followed by reverse froth flotation in order to produce super iron concentration.

References

Adeniyi, O.O. (1987). Gravity survey of older granite plutons in Zaria area of Kaduna State, Nigeria, Ahmadu Bello University Zaria, Nigeria (unpublished Thesis).

Ajakaiye, D.F. (1974). A gravity survey over the Nigerian younger granite province: in C.A. Kogbe (ed) Geology of Nigeria, Elizabethan Publishing Co.

Gaudin, A. M. (1957) Flotation, Second Edition, McGraw-Hill Book Company, Inc., New York.

Gordon, Robert B. (1996), American Iron 1607-1900, the Johns Hopkins University Press.

Kirk R.E. and Othner, D.F. (1951). Inter-science, Vol. 6, pp. 595-614

Leja J.and Schulman, J.H. (Feb., 1954). "Flotation Theory-Molecular Interactions between Frothers and Collectors", Min. Eng., 221-28

Ministry of Mines and Steel Development (2012)

Ndaliman B. I. Dungka G. T. and Yaro, S. A. (2013). Determination of the Liberation Size of Koton Karfe Iron Ore Deposit, Nigerian Mining Journal, Vol. 11, No 1 p 41 – 47

Ola S. A., Usman G. A., Odunaike A. A., Kollere S. M., Ajiboye P. O. and Adeleke A. O. (2009) Froth Flotation Studies to Upgrade Nigerian Itakpe Sinter Grade Iron Ore to a Midrex Grade Super Concentrate, Journal of Minerals & Materials Characterization and Engineering Vol. 8 No. 5 pp 405 – 416.

Ramanaidou, E. R. and Wells, M. A. (2014). Sedimentary Hosted Iron Ores. In: Holland, H. D. and Turekian, K. K. Eds., Treatise on Geochemistry (Second Edition). Oxford: Elsevier. 313-355.

Salawu A. O., Amoka I. S. and Thomas D. G. (2016) Mineralogical and Chemical Characterization of Gujeni Iron Ore, North Western Nigeria, Nigerian Mining Journal, Vol. 14, No 1 p 60 – 64

Spedden H.R. (1951) "Flotation", in Encyclopedia of Chemical Technology (ed).

Srobade (1997) Magnetic method of treatment of mineral, development in mineral processing Vol. 8 Elsevier Science Publisher, Amsterdam

Utherland K.L. and Wark I.W. (1955) Principles of Flotation, Australia Institute of Mining and Metallurgy pp. 102-12.

Wang, W. and Yang C. (2011) Application of Super Iron Concentrate and its Beneficiation Technology, Key Engineering Materials Vol. 480 – 481 Trans Tech Publications, Switzerland, pp 1442-1445

Wills B.A. (2007); Mineral processing technology, 7th Edition, Pengamon Press korea. pp 46, 90,108-153.

Yaro S. A. and Dungka G. T. (2009). Chemical and Mineralogical Characterization of Koton Karfe Iron Ore, Journal of Engineering and Technology (JET), Bayero University, Kano Vol. 4, No 1 pp 65 – 71

Achuenu, *et al* (2021) Nigerian Mining Journal, (19) 29 - 41

Appraisal of Kuru-Jentar Cassiterite using Mathematical Modeling Approach with respect to Certain High Field Strength Elements

Achuenu I.[a], Akinola A. P. and Komolafe K.

Department of Mining Engineering, Faculty of Engineering, University of Jos, Plateau State, Nigeria.

Corresponding email: achuenuifeanyi@gmail.com, *akinolaa@unijos.edu.ng*

Abstract

The main purpose of this study was to assess Kuru – Jentar Cassiterite ore, using mathematical modeling approach with respect to certain selected minerals of high field strength elements (HFSE) and how they control the formation of cassiterite during crystallization of magma. The effectiveness of Cassiterite ore in Extractive Industry depends on the properties of these minerals of HFSE that composed the Cassiterite during crystallization of magma and can be mathematically expressed as $Z[X_{n-x}Y_x]O_6$,$[X_{n-x}Y_x]O_4$ and, $[X_{n-x}Y_x]O_3$ *as n ranges from 0 to 5 where x depends on' n'*. These minerals contain HFES and are those that essentially partitioned along the silicate minerals. Methodologically, 20kg of cassiterite was crushed and pulverized in the laboratory mill machine for an hour, before sized by sieving into number of size fractions using the automatic sieve shaker for 15 minutes, after processing using high intensity magnetic separator and with the help of ordinary hand magnet of about 0.01Tesla, relative density measure, the relationship between minerals of HFSE can be mathematically established using a *Cassiterete* model. The findings shown that, the minerals obtained from Kuru-Jentar cassiterite during processing are mainly minerals of HFSE such as tin, ilmenite, columbite, zircon, and as such classified as Ilmeno-Columbite Cassiterite type and chemical analysis using XRF revealed the following chemical compositions of cassiterite; SnO_2, TiO_2, Fe_2O_3/Fe_3O_4, Nb_2O_6, ZrO_2. In conclusion after the comparative analysis among the minerals of HFSE in cassiterite using matrix equations and certain measures such as density, magnetic susceptibility, and their electrical conductivity, it is observed that, the type of reactions that take place during the formation of Cassiterite are oxidized and isomorrphous which include oxidation, isovalent and heterovalent reactions, as a result of this, concise valuable substantive empirical novel model was developed and can be employed to study cassiterite ore. This concise empirical novel model was, "*Cassiterite"* model designed with the aid of: Matrix equation, Oxidation and the isomorphic process, *and* can be recommended to study the Casssiterite and the application can improve mineral processing in extractive Industry.

Keywords*:* HFSE, Kuru-Jenta, Cassiterite, Isovalent, Heterovalent, Complex

1.0 INTRODUCTION

1.1 Background to the Study.

Jenta-Kuru Cassiterite is generally defined as an ore of tin, mathematically with associated minerals of certain HFSE. These HFSE possess characteristics of large ionic charge, with intermediate to greater ionic potential and these elements are partitioned along the aqueous phase, if both the aqueous phase and silicate phase coexist together during the crystallization of magma. These HFSE are the major elements in Cassiterite ore and minor elements in the source rock, e.g., Biotite or Syenite and Pegmatite. These certain HFSE including tin, iron; niobium, tantalum, and zircon are incompatible trace elements because of their inability to achieve a charge balance with silicate structure (SiO_4) in the silicate magma phase. Ebikemefa (2020) has shown that, the concentration of certain selected oxides of HFSE such as iron oxide in cassiterite is about 16%, titanium oxide is 15%, niobium oxide is 11%, tantalum oxide is 1%, zirconium oxide is 9% and then the hafnium oxide is 0.4%. The above elements of these oxides except iron oxide have their ionic potential greater than 3, with their ionic charge greater 4. Except for iron, these elements do not exist as free ions in the magma but form

complexes with oxygen in the magma during crystallization. Because cassiterite is a primary phase in pegmatite and can incorporate Nb, Ta, Zr, and Hf into its structure, it is expected that the Nb/Ta and Zr/Hf ratios of the cassiterite potentially reflect the Nb-Ta and Zr-Hf fractionation of the pegmatite melts as in this case. Cerny et al also suggested that the compositional trend of cassiterite is from Nb-rich to Ta- rich cassiterite in lepidolite- subtype pegmatites.

In this study, XRF analysis show that the concentrations LILE.REE, Y,U,Th and Pb are extremely low in Kuru – Jenta Cassiterite and do not show any distinct variation patterns. Therefore, we only focus on elements including Zr, Hf, Nb, Ta, W, Sn, Ti and Sc that are commonly present in cassiterite, especially in Jenta-Kuru Cassiterite.

Gonçalves *et al* (2015), pointed out that such fractionation trends were likely due to different solubilities of the end-member phase in CGM and zircon respectively. According to their study, columbite and zircon have lower solubility than tantalite and hafnon respectively, in metaluminouss to peraluminous granite melts, the granite melts would be Ta-and Hf-richer with increasing fractionation degree. Recently, Van lichtervelde *et al*., (2017), argued that isothermal Nb-Ta fractionation cannot be explained by solubility differences. Rather disequilibrium crystallization at supersaturation should be the reason for extreme of Ta enrichment in residual melts

Rocks contain thousands of tiny ferrimagnetic minerals grains. The compositions of ferrimagnetic minerals are mostly transition metals in which oxygen atoms fill the lattice space of the metal. These are iron (Fe), titanium (Ti), manganese (Mn), cobalt (Co) Nickel (Ni), Zircon (Zr), Niobium (Nb) and tantalum (Ta). These are magnetic elements, because of the presence of extra electrons in the d-orbital below the outer orbital (Burns, *et al.,* 1964). The magnetic minerals to be modeled are: Wustite (FeO), Rutile (TiO_2), Magnetite (Fe_3O_4), Haematite (Fe_2O_3), Ulvospinel (Fe_2TiO_4), and COLTAN

Krumbein and Grayhill (1965) have distinguished three types of models in geology: (1) scale-models; (2) conceptual models; and (3) mathematical models. Traditionally, geologists have been concerned with scale-models and conceptual models mainly.

Examples of scale-models are the geological map and cross-sections where the spatial variability of attributes is represented at a reduced scale for topographic surface and vertical planes, respectively. Geological processes also can be represented by scale-models. A classic discussion of this subject was given by Hubbert (1937). Conceptual models are mental images of variables and constants. They are statistical or deterministic depending on whether one or more random variables are used in the equation or systems of equations to express uncertainty. Mathematical equations generally can be represented geometrically by curves or surfaces.

The three types of models listed are not mutually exclusive. Scale-models can be based on mathematical criteria and conceptual models may be partly or entirely quantitative. Most mathematical models in geology have some important aspects of uncertainty and for this reason, are statistical. The problem may consist of eliminating the random variations from data so that a deterministic expression is retained representing the relationship between averages for assemblages of attribute rather than between single features. Statistical components or the uncertainty provide a way of expressing a range of different extrapolations for single features, all of which are possible, but with different probabilities of occurrence. This method replaces that of extrapolating a phenomenon with absolute certainty.

Geology differs from physics, chemistry and other sciences in that the possibility of doing controlled experiment is more limited. The observations are restricted to a record of past events, making geology a historical science. Generally, the final product of many interrelated processes is exposed at the surface of the earth in an imperfect manner. These mainly physical-chemical processes seldom reached a state

Younger igneous rocks, consisting largely of plutonic and volcanic components, form the

Jurassic alkaline ring complexes of Jos Plateau, which are the major sources of the Nigerian tin and associated ores, iron ores (Macleod, et al., 1971).The bulk of the cassiterite was obtained from alluvial deposit on Jos Plateau general considered to be derived from the Jurassic biotite granites of the ring complexes. Only very few economic deposits of tin were known in the older basement rocks. The ore is currently being processed using magnetic and gravity methods. The presence of columbite and tantalite in cassiterite depends on the ratio niobium to tantalum and their genetic environment as shown in table 2. The geochemical behavior of niobium and tantalum in granitic rocks depends to a certain extent on the paragenesis of the titanium minerals. Monozite bearing granites containing ilmenite and rutile commonly niobium and tantalum in accessory biotite, whereas allanite – bearing granites containing sphene and magnetite commonly have niobium and tantalum are concentrated in sphene with only subordinate amounts in the biotite in some granitic rocks, the niobium and tantalum in discrete accessory minerals of these element. Although exceptions occur, niobium and tantalum generally accumulate in the later differentiation during crystallization of granites and there is a tendency for tantalum to be concentrated relative to niobium in certain albitized or greisenized rocks. Separation of niobium from tantalum and the concentration of tantalum are attributed to change in alkalinity-acidity of the crystallizing medium and to the complexing of these elements with fluorine. High concentrations of niobium and tantalum occur in granitic pegmatite both as discrete niobium – tantalum minerals and as minor constituents in the lattices of mica, garnet, tourmaline, ilmenite, zircon and other minerals.

Nepheline syenite is well known for its high concentration of niobium about 12:1 ratio of columbite to tantalite, as in Russia. Nepheline syenites have been studied extensively by Russian geologists and Russian reports dominate the literature on these rocks. According to Es'kova (1960), nepheline syenite comprises about one percent of the igneous rocks of USSR and more than thirty massifs of this type of rock are known to occur there. In eight prominent nepheline syenite massifs the average niobium content ranges from 100 to 900ppm and the average tantalum content ranges from 8 to 70ppm.

As in granitic rocks, niobium and tantalum of nepheline syenite are more highly concentrated in late phases of intrusive that is pegmatite, albitized zones and carbonite and hydrothermal veins such enrichment is several to tens of times the niobium and tantalum contents of parent rocks (Es'kova, 1969).

Niobium occurs in a wide variety of minerals in nepheline syenite and other feature connected with them.

Tantalum was discovered by Anders G. Ekeberg in 1802 in Uppsalaa, Sweden, in the minerals tantalite from Finland and yttrotantalite from Sweden. Unfortunately for Ekeberg in 1809, the well-known English chemist, William Wollaston said there had been no discovery and there was no new element.

Granite pegmatites are also the only known commercial source of tantalum. Niobium and tantalum tend to be concentrated in the later products of crystallization of certain types of granite and the rocks tend to be enriched I tantalum with respect to niobium.in most granite, independent accessory minerals of niobium and tantalum are not found, but in pegmatite phases of such granites a wide variety of niobium and tantalum minerals is commonly formed. Niobium and tantalum enter also to a certain degree into the structure of other pegmatite minerals such as mica, garnet, tourmaline, ilmenite and zircon. Kuz'menko (1961) such that niobium is preferentially taken into the mica structure leaving tantalum to accumulates and form independent minerals of its own such as microlite and tantalite. The presence of lithium -bearing micas in pegmatite has significance in the formation of separate tantalum deposits. The content of tantalum with respect to niobium tends to increase from the earliest to the latest phases of pegmatite development. Such an increase in tantalum from wall zones to cores of pegmatite is reflected by the progressive increase in specific

gravity in columbite- tantalite of the quartz.

Wollaston in year 1800 claimed, Ekeberg's new element was actually niobium, which had also been discovered in 1802. The scientific community came to believe Wollaston was right and that Ekeberg claim for new element had been a mistake.

Tantalum and niobium are in fact hard to separate from one another, which led to Wollaston error.

In 1846 German mineralogist Heinrich Rose finally proved beyond doubt that tantalum and niobium were different elements.

1.2 Modeling.

A model is a simplified version of reality that is useful as a tool. There are primarily two types of models namely qualitative and quantitative models. Qualitative models are mostly descriptive and use of standard geological techniques of mapping and construction of cross-sections. The quantitative models are broadly of two types: deterministic and probabilistic models. According to Yukler and Welte, (1980); Welte and Yukler, (1981); Nakayama and Vansiclen, (1981); Ungerer et al., (1984), deterministic models seek to identify and quantify all variables of the system and thus predict its behavior by establishing values or limit for each system. They require large number of input data and therefore worthwhile only when extensive exploration has already been carried out. In probabilistic models, both input and output data are presented as probability distributions as according to Bishop et al., (1983); Sluijk and Nederlof, (1984).

A successful model strikes a balance between realism and practicality. Geologic maps constitute a familiar class of models. To map sedimentary section, a geologist collects data at certain outcrops. He casts his observations in terms of the local stratigraphy, which is itself a model that simplifies reality by allowing groups of sediments to be lumped together into formations. He then interpolates among his data point and projects beneath them to infer positions for formation contacts, faults and so on across his study area.

The first and most critical step in developing a geochemical model is conceptualizing the system or process of interest in a useful manner. By system, we simply mean the portion of the universe that we decide is relevant. The composition of a closed system is fixed, but mass can enter and leave an open system. A system has an extent, the amount of fluid and mineral considered in calculation.

The “art” of geochemical modeling is conceptualizing the model in a useful way as shown in Figure 6. This figure shows schematically the basis for constructing a geochemical model. The heart of the model is equilibrium system, which remains in some forms of chemical equilibrium, throughout the calculation. The equilibrium system contains an aqueous fluid and optionally one or more minerals. The temperature and composition of the equilibrium system are known at beginning of the model which shows the system's equilibrium state to be calculated Pressure also affects the equilibrium state, but usually in a minor way under near-surface condition, (Helgeson, 1969 but also Hemley *et.al,* 1989), unless a gas phase is present.

In the simplest class of geochemical models, the equilibrium exists as a closed system at a known temperature. Such equilibrium models predict the distribution of mass among species and minerals as well as species activities, the fluid saturation state with respect to various minerals and fugacities of different gases that can exist in the chemical system. In this case the initial equilibrium system contributes the entire geochemical model.

Conceptualizing a geochemical model is a matter of defining:

- The nature of equilibrium to be maintained
- The initial composition and temperature of the equilibrium system.
- The mass transfer or temperature variation to occur over the course of the reaction process envisioned.

1.3 Equilibrium Modeling

According to Pitzer and Brewer, (1961), and

Denbigh (1971), a system is in equilibrium when it occupies a specific region of space within which there is no spontaneous tendency for change to occur.

Geochemical models can be conceptualized in terms of certain false equilibrium states (Barton et.al, 1963; Helgeson, 1968). A system is in metastable equilibrium when one or more reactions proceed toward equilibrium at rates that are vanishingly small on the time scale of interest. Metastable equilibrium commonly Figure in geochemical model. In calculating the equilibrium state of natural water from a reliable chemical analysis, for example, we may find that the water is supersaturated with respect to one or more minerals. The calculation predicts that the reaction to precipitate these minerals have not progressed to equilibrium.

1.4 Classification of Elements in Periodic Table

Goldchmidt (1947), classifies chemical elements within the Earth according to their preferred host phases into lithophile (rock-loving), siderophile (iron- loving), chalcophile (ore – loving) and atmophile (gas- loving).

Mendeleev (1869) arranged 63 elements according to their increasing atomic number in several columns, noting recurring chemical properties across them.

Alexandre (1862), a geologist arranged elements in a spiral on a cylinder by order of increasing atomic weight.

1.5. Minerals of *HFSE* in Kuru-Jentar Cassiterite.

At rhyolitic and basaltic melt temperatures, magmas behave like weak electrolyte, especially on a microscopic scale and are applicable to principle of electroneutrality (Denbigh, 1971). The electrolytic value of magma increases as magma becomes more aqueous. High field strength, hydrophile and lithophile elements with intermediate ionic potential (I = 3 to 9.5) such as niobium, tantalum, tin, zircon, hafnium, titanium and iron are partitioned along this aqueous phase and maintain equilibrium with silicate melt. Since they cannot be partitioned along the silicate phase, they are *INCOMPATIBLE* trace elements, because of their inability to achieve a charge balance with those elements that partitioned along the silicate phase with charge of +2 such as magnesium, calcium and barium if the crystal phase and aqueous phase coexist (Whittaker and Muntus, 1970), but incorporate into cassiterite structure as shown in equation 1. The precipitation of HFSE from the aqueous phase is very much modified by the presence of water making them hydrophilic elements. Therefore, when silicate magma coexists with an aqueous fluid, HFSE would be strongly partitioned in the aqueous phase. This affinity of water is almost certainly responsible for the concentration of HFSE and its ore, cassiterite in pegmatite and hydrothermally altered rock At an igneous temperature, there is a mobility of ions or atoms in the molten magma, since it behaves like a weak electrolyte under electrolytic condition according to Faraday second law of electrolysis, within the magma, so that ions or atoms with an ionic charge less than 3 tend to exist as free ions in the magma and then partition along the silicate phase but those with ionic charge greater than 3 and some of the smaller trivalent ions, will form a complexes with oxygen and then partitioned along the aqueous phase. These complexes maintain their identity during crystallization process. In this case under control condition of temperature, ions or atoms of the same charge or similar size must find themselves and occupy a lattice position to form crystals (Goldschmidt, 1937), which set in matrix (Cayley, 1895), to form rock of a particular composition. The rock formed would reduce to an ore whenever there is a weathering breakdown, such that high temperature minerals are more susceptible to weathering breakdown and would have gone into solution leaving behind low temperature minerals (Goldic 1988). .

2.0 RESEARCH METHODOLOGY

Sample of fresh cassiterite was obtained from Jos Plateau state. 50kg of cassiterite sample was obtained for the study. The sample of cassiterite was taken and broken manually with a sledge hammer to provide the required size

acceptable to laboratory jaw crusher. The sample was crushed and pulverized, part of pulverized sample was weighed for sieve analysis and processing using magnetic separator. The procedure is as follows.

1. 20kg of cassiterite was crushed and pulverized in the laboratory mill machine for an hour,
2. Cassiterite was taken and sized by sieving into a number of size fraction using the automatic sieve shaker for 15 minutes.
3. Cassiterite was gathered together and introduced into the laboratory mill machine and ground for 15 minutes.
4. The cassiterite from the laboratory ball mill machine was sized and each sieve fractions were weighed and the value noted as the product or discharge.
5. Sieve analysis. The ground samples were sieved into the following sieve size fractions; + 365 µm, 355 µm, +250 µm, -250 µm, +180 µm, -180 µm, +125 µm, -125 µm, +90 µm, -90 µm, +63 µm, -63 µm using automatic sieve shaker for 15 minutes.
6. The discharged product of cassiterite was taken to magnetic separator for processing.
7. Ordinary bar magnet of about 0.01 Tesla which produces 650 magnetic field lines is used to measure the magnetic property of the COLTAN in cassiterite obtained from the sources, that is cassiterite from Jos plateau state
8. Relative densities of each of the minerals from the processed cassiterite were measured using Archimedes' principle and their specific gravities were calculated
9. Mathematical equations were also used to achieve this research

3.0 RESULTS AND DISCUSSION

3.1 Results

Ebikemefa (2020), noted that there is high concentration of tin (iv) oxide, Niobium (v), iron (iii) oxide, zirconium(iv) oxide and titanium(iv) oxide, but low concentration of tantalum(v) and hafnium(iv) oxide at Kuru-Jentar as shown in Table 1.

The minerals processed from cassiterite were mainly minerals of HFSE which include tin, iron ore, columbite, zircon, monazite and sand and their chemical compositions are presented in Table 1.

3.2. Kuru-Jentar Cassiterite Model

Cassiterite is an ore of tin that is stable at room temperature, not oxidized by air, not hydrolysed by water vapour and do not disproportionate or decomposed at normal temperature. Minerals of cassiterite contain HFSE that have ionic potentials greater than 3.5 and hence have similar stability limit. These HFSE are of higher oxidation states and formed stable complexes in cassiterite at normal temperature. They are small, highly charged ions and have vacant low energy orbitals to accept lone pairs of electrons donated by other groups or ligands and form complexes during crystallization of magma. These HFSE are called hard acids and their corresponding ligands or radicals are called hard bases.

Determinant matrix is used to construct *Cassiterite* model according to tantalum to niobium and titanium to iron ratio with respect to its genetic origin in which titanium and tantalum are determinant factors and niobium and iron are constant variables and are expressed as follow from equations (33) and (42). For isovalent substitution as shown in equation (42), the determinant matrix is always equal to zero, because there is always complete substitution of one HFSE to another in solid solution during crystallization of magma, which involves atoms of the same charge and similar size thereby making the two elements to be isomorphic and for heterovalent substitution as shown in equation (42), the determinant matrix is always equal to 2, because there is always partial substitution of one HFSE to another in solid solution during crystallization of magma, which involves atoms of different charges and similar size thereby making the two elements to be isomorphous. Figure 2, has shown that Cassiterite is grouped into three according to its origin with respect to the ratio of niobium to tantalum and that of the ratio of tantalum to titanium. These are niobium

– iron rich cassiterite, titanium – niobium rich and tantalum - titanium rich Cassiterite and therefore formed the minerals in the upper part of the table such as the magnetite, haematite, hafnon and columbite and the minerals in the lower part of the table such as the ulvospinel, ilmenite, zircon and tantalite. The elements that formed complexes with oxygen formed minerals like monazite and sand.

A. Determinant Matrix

1. Using determinant matrix to classify cassiterite according to its origin with respect to iron and titanium into groups;

Using determinant matrix to resolve equation (29) into equation (51)

Table 1: Analyzed Cassiterite Sample at Kuru-Jentar

Oxide composition (%)	CEB6	CEB7	CEB8	CEB9	CEB10
SiO_2	ND	6.00	14.00	12.74	8.24
Cl	ND	0.94	ND	ND	ND
K_2O	0.99	0.94	ND	0.76	ND
CaO	0.20	0.20	0.61	0.20	ND
TiO_2	17.00	15.20	13.80	15.90	14.70
MnO	0.75	0.66	0.59	0.65	0.61
Fe_2O_3	16.67	15.81	14.22	17.02	15.57
CuO	0.23	0.17	0.21	0.14	0.22
ZnO	ND	ND	0.087	0.084	0.088
SeO_2	ND	ND	ND	0.004	ND
Ga_2O_3	0.070	ND	0.048	ND	ND
As_2O_3	0.028	0.008	ND	ND	0.02
Y_2O_3	0.832	0.653	0.696	0.832	0.738
ZrO_2	9.71	9.56	9.15	9.09	10.10
Nb_2O_5	11.20	10.60	10.20	9.42	11.00
SnO_2	32.20	30.00	30.44	24.00	28.20
BaO	1.80	2.20	1.20	2.40	1.10
CeO_2	2.10	2.00	1.90	2.20	2.30
Nd_2O_3	0.26	0.40	0.20	0.51	0.19
Eu_2O_3	0.40	0.37	0.52	0.48	0.50
HfO_2	ND	0.41	0.26	0.40	0.39
Ta_2O_5	1.00	1.33	0.79	1.18	1.11
WO_3	ND	ND	0.22	ND	0.16
PbO	0.13	0.15	0.26	0.17	0.59
ThO_2	1.53	1.44	ND	1.62	1.47
LOI	2.90	0.90	0.60	0.20	2.70

Source: Ebikemefa (2020)

$$\begin{pmatrix}3, & 0\\ 2, & 0\end{pmatrix} + \begin{pmatrix}2,1\\ 1,1\end{pmatrix} = \begin{pmatrix}5,1\\ 3,1\end{pmatrix}$$

$$[0] + [1] = [2] \quad \ldots(51)$$

Therefore;

$$\begin{pmatrix}Magnetite\\ Haematite\end{pmatrix} = \begin{pmatrix}3, & 0\\ 2, & 0\end{pmatrix}$$ *= Sedimentary rock*

$$\begin{pmatrix}Ulvospinel\\ Ilmenite\end{pmatrix} = \begin{pmatrix}2,1\\ 1,1\end{pmatrix}$$ *= Igneous rock*

$$\begin{pmatrix}\text{Titanomagnetite}\\ \text{Titanohaematite}\end{pmatrix} = \begin{pmatrix}2,1\\ 1,1\end{pmatrix} = Igneous\ rock$$

From equation (32) and (33);

- Iron ore in basalt = magnetite and haematite, no cassiterite
- Iron ore in sedimentary = magnetite and haematite, no cassiterite
- Iron ore in granite = ilmanite and ulvospinel in cassiterite
- Iron ore in andesite = titano – maghaematite in cassiterite

From above statement, cassiterite is originated from magmatic melt, e.g., granite or syenite and hydrothermal fluid, e.g., lithium pegmatite but not sediment e.g., sedimentary rock. Because sedimentary rock does not contain most of these minerals of HFSE as igneous rock does, sedimentary rock does not host cassiterite, as igneous rock does.

1. Using determinant matrix to classify cassiterite according its origin into Niobium rich cassiterite and Tantalum rich cassiterite groups;

Using determinant matrix to resolve equation (43) into equation (52)

$$\begin{pmatrix}3, & 0\\ 2, & 0\end{pmatrix} + \begin{pmatrix}2,1\\ 1,1\end{pmatrix} = \begin{pmatrix}5,1\\ 3,1\end{pmatrix}$$

$$[0] + [1] = [2] \quad \ldots(51)$$

Therefore;

$$\begin{pmatrix}Magnetite\\ Haematite\end{pmatrix} = \begin{pmatrix}3, & 0\\ 2, & 0\end{pmatrix}$$ *= Sedimentary rock*

$$\begin{pmatrix}Ulvospinel\\ Ilmenite\end{pmatrix} = \begin{pmatrix}2,1\\ 1,1\end{pmatrix}$$ *= Igneous rock*

$$\begin{pmatrix}\text{Titanomagnetite}\\ \text{Titanohaematite}\end{pmatrix} = \begin{pmatrix}2,1\\ 1,1\end{pmatrix} = Igneous\ rock$$

From equation (32) and (33);

From equations (36), (37), (38) and (39),

- Coltan type cassiterite in syenite = columbite
- Coltan type cassiterite in pegmatite = tantalite
- Coltan type cassiterite in syenite-pegmatite = coltan

A. Isovalent Substitution using Determinant Matrix

For isovalent substitution, using determinant matrix

$$\begin{pmatrix}5, & 0\\ 4, & 0\end{pmatrix} + \begin{pmatrix}0,5\\ 0,4\end{pmatrix} = \begin{pmatrix}5,5\\ 4,4\end{pmatrix}$$

$[0] + [0] = [0]$ *shows that there is a complete substitution of niobium by tantalum in solid solution during crystallization of magma*

***B.* Heterovalent Substitution, using Determinant Matrix**

$$\begin{pmatrix}3, & 0\\ 2, & 0\end{pmatrix} + \begin{pmatrix}2,1\\ 1,1\end{pmatrix} = \begin{pmatrix}5,1\\ 3,1\end{pmatrix}$$

$[0] + [1] = [2]$ *shows that there is a partial substitution of iron by titanium in solid solution during crystallization of magma.*

Ø **Niobium - iron rich Cassiterite**: In this group, the amounts of tantalum and titanium atoms are zero, and niobium and iron atoms increase from +2 to +5 across the figure from left to right with a general Gibbs free energy numerically $\Delta G > 0$ and has not been affected by tantalum and titanium with ratio of niobium to tantalum to be 5:0 and that of that of iron to titanium is 3:0 for magnetite and 2:0 for haematite. Minerals in this group are relatively

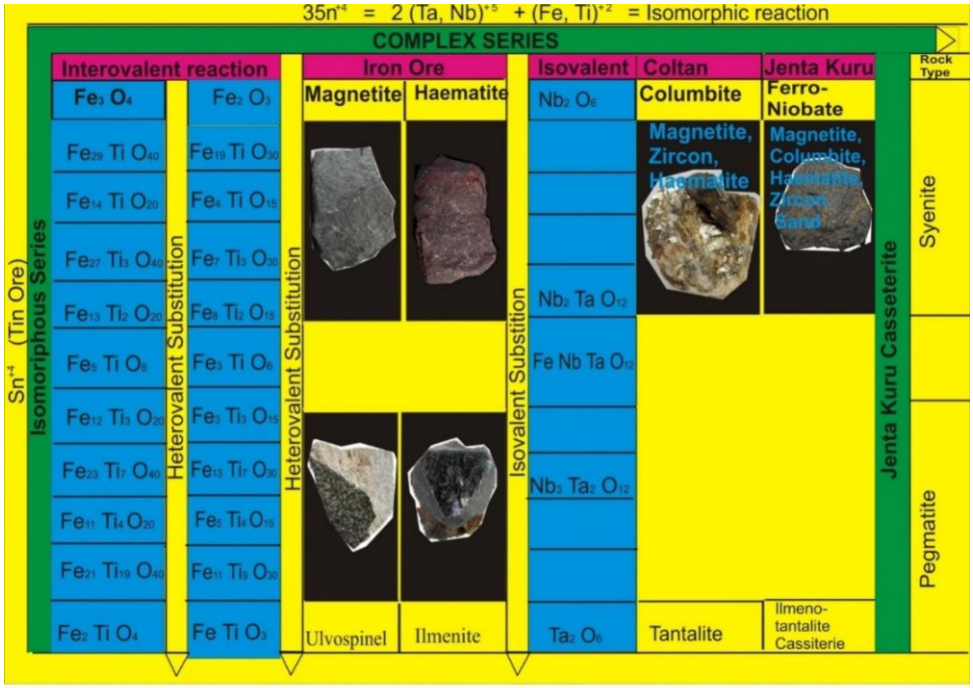

Figure 2: Jenta Kuru Cassiterite Model

resistant to weathering during weathering breakdown and first weathered under weathering condition when compared with tantalum and titanium rich cassiterite, according to Goldich (1988). The rock types of this group of cassiterite are basalt and syenite.

Ø **Tantalum – titanium rich Cassiterite**: In this group, the amounts of tantalum and titanium atom increase down the group with decreasing number of atoms of niobium and iron to the point where niobium is completely replaced by tantalum with the ratio of niobium to tantalum atom to be 0:5 and iron is partially replaced by titanium with the ratio of iron to titanium to be 2:1 for ulvospinel and 1:1 for ilmenite. Minerals in this group are highly resistant to weathering during weathering breakdown and least weathered under weathering condition when compared with niobium and iron rich cassiterite, according to Goldich (1988). The rock types of this group of cassiterite are granite and pegmatite.

3.3: Application of Mathematical Model to Kuru-Jentar Cassiterite using certain HFSE.

Ebikemefa (2020) as shown in Table 1, observed that the concentration of certain selected oxides of HFSE such as iron oxide in cassiterite is about 16%, titanium oxide is 15%, niobium oxide is 11%, tantalum oxide is 1%, zirconium oxide is 9% and then the hafnium oxide is 0.4%. The above elements of these oxides except iron oxide have their ionic potential greater than 3, with their ionic charge greater 4. They have smaller ionic radius with larger atomic number than those of s and p block elements which make them HFSE with larger ionic charge. These oxides are represented empirically in Table 2, and their mathematical representations give them the IUPAC name, which is an expression of a system of model of computation of numerical values to chemical elements in their algebraic form to produce a material of a particular IUPAC nomenclature according to Achuenu and Komolafe (2021), e.g., ferrohexaoxoniobate (v) is the *IUPAC* name for Columbite ($FeNb_2O_6$) and that of ferrohexaoxotantalate (v) is Tantalite ($FeTa_2O_6$) as well as iron (ii) and iron (iii) oxides for Haematite and Ilmenite.

Given that, the concentration of iron (iii) oxide in Kuru –Jentar cassiterite is 16% and that of titanium oxide is 15%, then, mathematically;

$$Fe = 52, Ti = 44$$

$$Fe_2O_3 = 16/52$$

$$Fe = 0.31$$

$$TiO_2 = 15/44$$

$$Ti = 0.34$$

Therefore, mathematically, $[Fe_{1-x}Ti_x]O_{n.}$ = $\{Fe:Ti\}O_n$

Then the atomic ratio, Fe:Ti = 0.31 :0.34

= 0.31/0.31:0.34/0.31

Fe:Ti = 1:1

Since oxidation state of Fe is +3, then n = 3, then;

$\{Fe:Ti\}O_3 = \{FeTi\}O_3$

$\{FeTi\}O_3$ = ilmenite

2) Given that, the concentration of niobium oxide is 11% and that of tantalum oxide is 1%, then mathematically;

Nb =82, Ta = 146

Nb = 11/82

Nb = 0.134

Ta = 1/146

Ta = 0.0068

Therefore, mathematically, $[Nb_{1-x}Ta_x]O_{n.}$ = $\{Nb:Ta\}O_n$

Then the atomic ratio, Nb:Ta = 0.134 :0.0068

= 0.134/0.0068:0.0068/0.0068

Nb:Ta = 20;1

Since the oxidation state of Nb = +5, then n = 5

$[Nb_{2-x}Ta_x]O_5 = [Nb_{20}Ta]O_{50}$

$\{Nb:Ta\}O_5 = \{Nb_{50}Ta\}O_{50}$

As $\{Nb_{20}Ta\}O_{50}$ Lim→ $\{Nb_2\}O_5$, if Ta ≈ Nb, since Ta is very small then,

Ta ≈ 0

Nb_2O_5 = columbite

In the presence of iron oxide, $Nb_2O_5 = FeNb_2O_6$

$FeNb_5O_6$ = columbite

$\{FeTi\}O_3$ = ilmenite

3) Given that, the concentration of zirconium oxide is 9% and that of hafnium oxide is 0.292%, then mathematically;

Zr = 80, and Hf = 144

Zr = 9/80

Zr = 0.113

Hf = 0.292/144

Hf = 0.002

Therefore, mathematically, $[Zr_{1-x}Hf_x]O_n$

= $\{Zr:Hf\}O_n$

Then the atomic ratio, Zr:Hf = 0.113:0.002

= 0.113/0.002:0.02/0.002

Zr:Hf = 57;1

$\{Zr:Hf\}O = \{Zr_{57}Hf\}O_{114}$

As $\{Zr_{57}Hf\}O_{114}$ lim→ $\{Zr\}O_2$, if Hf ≈ Zr, since Hf is very small then;

Hf ≈ 0

ZrO_2 = Zircon

4) Since the silica content of the Kuru-Jentar cassiterite is less than 40%, then there is no silica rich mineral such as sand (SiO_2) in Kuru-Jentar cassiterite.

Table2: Empirical Representation of Kuru – Jenta Cassiterite Obtained from Table1

Element	Iron Ore		COLTAN		Zircon		Tin Ore	Others
Percentage composition (%)	Fe	Ti	Nb	Ta	Zr	Hf	Sn	
	16	15	11	1	9	0.4	32	16
Atomic Number	56	47	82	146	80	144	50	
Mole Ratio	0.31	0.34	0.134	0.006	0.133	0.003		
Mole Ratio/smallest	1	1	20	1	38	1		
Empirical Formula	Fe	Ti	Nb_{20}	Ta	Zr_{38}	Hf		
Oxidation Number	+3	+4	+5	+5	+4	+4	+4	
Number of Oxygen Atom	3	4	5	5	4	4	4	
Molecular Oxygen Formula	O_3	O_4	O_5	O_5	O_4	O_4	O_4	
Chemical Formula	$FeTiO_3$		$Nb_{20}TaO_{50}$		$Zr_{38}HfO_{80}$		SnO_2	
	$FeTiO_3$		Nb_2O_5		ZrO_2			
Genetic Name	Ilmenite		Columbite		Zircon		Tin Ore	

From the empirical expression in Table 2, the minerals obtained from Kuru-Jentar cassiterite using mathematical method includes;

i. Tin Ore

ii. Columbite

iii. Ilmenite

iv. Zircon

These are the minerals in Kuru-Jentar cassiterite that can be processed during mineral processing. Therefore, iron ore in granite, either in biotite or diorite rich cassiterite is ilmenite and is in group 1 iron ore according to Achuenu and Komolafe (2021) Table 3, as represented in equation (54), (55) and (56) below.

Since the ratio of iron to titanium is 1:1, therefore;

Fe:Ti = 1:1

Fe:Ti = $FeTiO_3$ = granite

If Granite = biotite or syenite, then from equation (31)

Haematite + Ilmenite = Titanohaemite . ... (54)

$Fe_2O_{3(S)} + FeTiO_{3(s)} = Fe_3TiO_{6(s)}$ ...(55)

Basalt + Granite = Andesite …(56)

Therefore, COLTAN in granite, either in Nepheline Syenite or Lithium pegmatite rich cassiterite is columbite and is in Niobate group COLTAN according to Achuenu and Komolafe (2021) Table 3, as represented in equations (57), (58), and (59) bellow.

Since the ratio of noibium to tantalum is 20:1, therefore;

Nb:Ta = 20:1

Nb:Ta = $Nb_{20}TaO_{50}$ and

$Nb_{20}TaO_{50}$ is very small to Nb_2O_5,

then,

$Nb_{20}TaO_{50} = Nb_2O_5$ = granite

From equation (45);

Columbite + tantalite = Coltan …(57)

Granite + Pegmatite = Granite Pegmatite ...(58)

$FeNb_2O_6 + FeTa_2O_6 = Fe[NbTa]_2O_6$ … (59)

From equation (54), ilmenite is found in granitic rock which could be either biotite granite or syenitic granite

From equation (58), columbite is found in syenite granite or Diorite.

At a given Gibbs free energy, each of these minerals of HFSE maintains their highest oxidation states under standard conditions of temperature and pressure as shown in Table 5. From table 5, the following deductions were made;

1. Iron and Titanium have different oxidation states of +3 and +4. Hence undergo heterovalent substitution during crystallization of magma. Since the ratio of iron to titanium is 1:1, therefore the number of oxygen atoms would be 3, and then the molecular formula would be given as $FeTiO_3$. At a given equilibrium, $FeTiO_3$, would be stable, and has minimum free Gibbs energy, numerically $\Delta G > 0$, under standard conditions of temperature and pressure. Therefore, the type of iron ore in Kuru- Jentar cassiterite is ilmenite and it belongs to group 1 iron ore in periodic table of an iron ore according to Achuenu and Komolafe (2021).

2. The oxidation state of niobium and tantalum is +5, therefore the number of atoms oxygen in this case would be 5. Since the ratio of niobium to tantalum is 20:1, then the molecular formula would be $Nb_{20}TaO_{50}$. At a given free Gibbs energy, $Nb_{20}TaO_{50}$ is limiting to Nb_2O_5, $\Delta G = 0$, this means that Nb_2O_5 is stable but not with minimum Gibbs free energy under standard conditions. Therefore, further oxidation of Nb_2O_5 will produce a more stable crystal with the formula of $FeNb_2O_6$ as shown in equation (56).

$Nb_2O_{5(s)} + FeO_{(s)} \rightarrow FeNb_2O_{6(s)}$ …(56)

Therefore, at equilibrium, Nb_2O_5 reacts with FeO in hydrothermally altered rock to produce $FeNb_2O_6$ as shown in equation (56). $FeNb_2O_6$ reaches its minimum Gibbs free energy under standard conditions of temperature and pressure, numerically $\Delta G > 0$.

Therefore the type of COLTAN in Kuru-Jentar cassiterite is columbite and it belongs to Niobate –group COLTAN as shown in COLTAN model Table 2 according to Achuenu and Komolafe (2021)..

3. The oxidation states of zirconium and hafnium is +4, therefore the number of oxygen atoms would be 4. Since the ratio of zirconium to hafnium is 38:1 as shown in Table5, then the molecular formula is $Zr_{38}HfO_{80}$. As the $Zr_{38}HfO_{80}$ is limiting to Zr_2O_4, the free Gibbs energy of Zr_2O_4 is minimum under standard conditions. Therefore, the Kuru-Jentar cassiterite is a zircon – cassiterite type.

In conclusion, ilmeno-columbite rich cassiterite is granitic rock origin; therefore, this defines the geology of Kuru-Jentar of Jos Plateau. In this case, the geology of Kuru-Jentar of Jos Plateau is mainly Ilmeno- Columbite bearing Biotite and Syenite granite. Large commercial deposite of columbite-tantaalite occur in biotite granite (magmatic type) of Nigeria as well in placer (exogenic type) derived from such rocks and pegmatites (Kuz'menko1959, 60). Kuz'menko (1959) classified columbite of Jos Plateau state as Biotite granite and alkali granites with riebeckite and pyrochlore.

4.0 CONCLUTION

Using mathematical modeling approach to appraise Kuru-Jentar cassiterite with respect to HFSE, it could be concluded that the presence of HFSE in Cassiterite affirms the genetic origin of cassiterite from granite and syenite to pegmatite, such that iron – niobium rich cassiterite is basalt, titanium-niobium rich cassiterite as shown in Figure 2, Table 1 and 2 and titanium – tantalum rich cassiterite is pegmatite. The ratio of columbite to tantalite in Kuru-Jentar cassiterite is 20:1, and iron to titanium ratio in Kuru-Jentar cassiterite is 1:1 as shown in Table 2. Kuz'menko (1950) shows that the columbite to tantalite ratio in Jos Plateau state is about 4:1 The weak magnetization of these minerals makes them to be concentrated in the high intensity magnetic separator during mineral processing of cassiterite and paramagnetic at room temperature at 1atm. Finally, the presence or absence of titanium and tantalum in cassiterite determines their cassiterite type, either ferro/ferric - niobium rich type cassiterite, or titanium - tantalum rich type cassiterite, as well as their genetic rock origin, in which the amount of titanium and tantalum in cassiteriteincreases from alkaline rock e.g. syenite to more silicic rock e.g. granite, such as pegmatite which gives the account that maghaematite and columbite are found in nepheline syenite and ulvospinel, ilmenite and tantalite are found in lithium pegmatite such that the weathering of syenite would give magnetite, haematite, and columbite and that of pegmatite would give tantalite.

Mathematically, this shows that Kuru-Jentar is expected to be Ilmeno-columbite bearing Cassiterite, because, iron, niobium, and tin meet the percentage requirement for an ore of tin to form, therefore the rocks expected in Kuru-Jentar are Biotite granite and syenite which speak the geology of the area. Therefore the minerals to be processed from Kuru- Jentar Cassiterite include; Ilmenite, tin, columbite and other associated minerals like zircon. In this case the Cassiterite type in Kuru-Jentar is ilmenite-columbite Cassiterite as shown in Figure 2.

REFERENCES

Burns, R. G., Clark, R. H.«and Fyfe, W. S., 1964, Crystal-field theory and application to / problems in geochemistry, in *Chemistry of the Earth's Crust,* Vemadsky Centennial Symposium. Vol. 2 (Vinogradov, ed.), Moscow, pp. 88-106.

Burns, R. G., and Fyfe, W. S., 1966, Distribution of elements in geological processes, *t^/Chem. Geol.,* 1, 49-56. *BumS,* R. G., and Fyfe, W. S., 1967, Trace element distribution rules and their significance, *Chem. Geol.,* 2, 89-104. Burns, R. G., and Fyfe, W. S., 1967, Crystal-field theory and the geochemistry of transition elements, in *Researches in Geochemistry,* Vol. 2, (Abelson, ed.), Wiley, New ^ York, pp. 259-285.

Chayes, F. (1965) Titania and alumina content of oceanic and circumoceanic basalt. Mag., 34, 126-31

Denbigh, K.G., and J.C.R Turner., (1971). Chemical Reactor Theory – An Introduction (Second Ed.). Cambridge, UK: Cambridge Univ. Press (1971).

Goldschmidt, V. M., 1926, Geochemische Verteilungsyesetze der Elemente VII. Die Gesetze der Kristallochemie, *Skrfler Norske Videnskaps-Akad. Oslo,'I, Mat. Naturv.* Kl, 2,5-116.

Gonçalves, G., Lana, C., Scholz, R., Buick, I., Gerdes, A., Kamo, S., Corfu, F., Marinho, M., de Oliveira Chaves, A., Valeriano, C. and Nalini Jr, H. (2015). An assessment of monazite from the Itambé pegmatite district for use as U–Pb isotope reference material for microanalysis and implications for the origin of the "Moacyr" monazite. Chemical Geology. 424. 10.1016/j.chemgeo.2015.12.019.

Kuz'menko, M.V., 1961, Role of micas in the process of Ta enrichment: Akad. Nauk SSSR Doklady, V.140,P.1411-14114 (in Russian).

Mendele'ev D. (1877). Entstehungund Vorkommen des materials Dtsch. Chem.Gas. Ber; 10, 229.

Mendele'ev D. (1902). The principle of chemistry, 2nd English ed; Vol.1, (Translated from 6th Russian ed;) Collier, New York.

Marieke, V. L., Alexis, G., Michel, de S. B., Philippe, O., Axel, G., Paquette, J., Melgarejo, J., Druguet, E., and Alfonso, P. (2017). U-Pb geochronology on zircon and columbite-group minerals of the Cap de Creus pegmatites, NE Spain. Mineralogy and Petrology. 111. 10.1007/s00710-016-0455-1.

Ringwood, A. E., 1955a, the principles governing trace element distribution during mag- /matic crystallization. Part I. The influence of electronegativity, *Geochim. Cosmo- ^ chim. Acta,* 7, 189-202. Ringwood, A. E., 1955b, the principles governing trace element behavior during magmatic allization. Part II. The role of complex formation, *Geochim. Cosmochim. Acta,* 7,242-254

Ringwood, A.E. 1962. A Model for the Upper Mantle. J. Geophys. Res. 67, 4473 - 4477.

Ringwood, A.E. 1975. Composition and Petrology of the Earth's Mantle.McGraw-Hill, New York.

Aluwong, *et al* (2021) Nigerian Mining Journal, (19) 42 - 49

Value Addition to Cab Quality Gemstones using Cabochon

Aluwong K. C., Basu M.M., Akinola A.P [a], and Amuga, K.G.
Department of Mining Engineering, University of Jos, Plateau, Nigeria
[a] ***Email***: wok_harat@yahoo.com, akinolaa@unijos.edu.ng

Abstract
Gemstones are naturally occurring mineral crystals of precious stones found underneath the Earth; they are substances of pristine beauty when cut and polished for jewellery and are part of alternative and complementary medicine from pre-historic times. This research was carried out to assess how much value can be added to gemstones with inclusions through cabbing – a particular form of gemstone polishing – by analyzing the methods used in mining gemstones and identifying their inclusions. Recognized rock samples with inclusion were polished in the lapidary utilizing the technique known as "cabbing" on a cabbing machine. First, it involves the grinding process that shapes the cabochon and removes any surface irregularities, smoothing and further shaping the stone. The resin wheels sand and smoothen away flat spots, scratches, and tiny bumps left behind, and lastly, the final polish is carried out on a flat polishing lap disc. The resulting polished gemstones were significantly enhanced due to their super smooth surfaces that reflect light easily and exude both beauty and exquisite shape, thus attracting a higher percentage of sell-on profits – depending on the degree and perfection of treatment. Conclusively, the value addition of gemstones is sure to raise the gain of artisanal miners and, thus, a better quality of life. Government can also benefit through investments in the solid mineral sector, as miners will pay more taxes.

Keywords: Gemstone, Cabochon, Lapidary, Faceting, Cabbing Machine

1.0 INTRODUCTION

Gemstones are natural inorganic matter, minerals, or stones available in igneous rocks and alluvial gravels. Gemstones occur in most major geological environments. Each domain tends to have a unique suite of gem materials; when cut and polished, gemstones are used to make ornaments or other adornments. The geological environment in which they are found or mined is known as the gemstone occurrences, and most gemstones are available at the in-situ site. However, agents of denudation transport some gemstones from their place of in-situ – these are known as alluvial gem deposits. Compared with several other countries where gemstones are mined, processed, and sold for foreign exchange, Nigeria's gem mineral industry will require tidying up; from a geological point of view. Nigeria's gemstone potential displays a favourable competition with other gemstones producing countries such as Tanzania, Zambia, South Africa, Brazil, and Madagascar, as Nigeria is known for the presence of different gemstones in appreciable quantities, including Corundum, Beryl, Quartz and its varieties, Tourmaline, Garnet, Aquamarine, Topaz, and Spinel (Olade, 2022).

In Nigeria, gems exist within four distinct units; Basement, Younger Granite complexes, Sedimentary basins, recent lavas and volcanic pipes. Many gemstones have been found in locations within the Nigerian pegmatite belt. Common gems that have been discovered in Nigeria include; Amethyst, Tourmaline, Aquamarine, Topaz, Sapphire, Ruby, Garnet, Quartz, and Zircon. These gems have been found to occur individually and jointly in various localities, but many are of low grade, usually with inclusions. The artisanal miners have little idea how value can be added to the gemstones with inclusions since they just mined them out and sold the excellent grade, leaving the low-grade behind on the site. Therefore, they are not gaining as much as they should. Thus, the paper aims to assess how much value can be added to gemstones with inclusions through cabbing. Also, to analyze the methods used in mining gems, identify those with inclusions polish gemstones with inclusions in the lapidary using the cabbing Machine, and educate the miner about the great benefits of the gemstone industry in the country at large.

The business community of the gemstone

industry in Nigeria has been found wanting in its contribution to revenue generation (Fayemi, 2015). He further said that Nigeria's solid minerals sector makes up about 0.34% of Gross Domestic Product (GDP), smaller than its real potential. The effect was that the industry has been operating below capacity as mostly artisanal and small-scale miners are mainly engaged in mining operations in the country, consequently dominating gemstone production. There are possibilities for developing the local gemstone business in Nigeria as there is a high international demand for gems from Nigeria. There has been a lamentable lack of active, proactive progress concerning mitigation factors that degrade vulnerable regional environments. The gemstone industry in Nigeria is presently at an embryonic stage, with an enormous potential for growth, foreign exchange earnings, revenue generation, poverty eradication, and job creation.

1.1 Gemstone Formation

Gemstones are formed below the Earth's surface. They sometimes show traces of other minerals called inclusions; these are tiny crystals of other minerals caught up in the growth of the larger host crystal or formed as it grew. Internal fractures that have been partially healed during growth or traces of earlier growth stages are marked by zoning; the inclusions can sometimes identify gemstones and prove whether the stone is natural or synthetic and tell us where a gemstone originated. (Stachel *et al*., 2005). Some gemstones like diamond and zircon are formed deep in the Earth and brought to the surface by explosions of molten rock. In contrast, many, like topaz, tourmaline and aquamarine, crystallize slowly from hot fluids and gases as they cool and solidify far below the Earth's surface. Others formed from liquids filtered into cracks and pockets in rocks. Like garnet and jade, some form when rocks are heated and pressurized by earth movements and recombine to form new, different minerals (Groat, 2007).

1.2 Cabbing Machine

The Cabbing Machine is a combination unit designed to grind and polish gemstones. The cabbing Machine is stainless steel and features an electric motor, a lamp, water control knob, drip pan, stone tray base board, wheels, space between wheels, and diamond wheels. The wheels are of different grits; 80-grit hard, 220-grit hard, 360-grit soft, 600-grit soft, 1200-grit soft and 3000-grit soft. The wheels are changeable with a universal base unit for 6- or 8-inch wheels. The machines with the switch located at the front for easy access are designed to run at two different speeds. The 1/2 horse motor is pulley driven and water-resistant. The cabbing Machine's overall size is 32" x 25" x 12" and is placed on a wooden base. It grinds and polishes all kinds of shapes and designs out of rock, glass, synthetic material and metal, with its most popular use being the making of cabochons.

Plate 1: Cabbing Machine

1.3 Gemstone Polishing

Gemstone polishing increases the value of a gemstone by transforming a rough gemstone into something more beautiful than the previous. The most common and valuable way to process a stone is to facet it; this puts a series of flat facets on a gemstone, allowing light to reflect through the gemstone and back to the eye in a pleasing manner. It is only possible to cut transparent material this way, as less translucent or opaque material will not be able to reflect the light properly, making the gemstone appear dull and without sparkle. Instead, these near or non-gem products can be cut into cabochons, beads, or carvings, or they can be sold as rough material; this can be done differently. However, a significant note is that not all gemstones can be cut economically as the rough material may carry greater value.

1.4 Cabochon

Cabochon is a stone that is smoothly rounded and polished on top and relatively flattish, and it is either flat or slightly rounded at the bottom. This form of cutting is often used for dense or translucent stones, but it is also frequently used for transparent materials with too many inclusions to yield a good faceted stone. Cabochon cutting or cabbing is often done by simply holding the stone between the fingers by doping the stone onto a wooden or metal dope stick. The process facilitates twirling the stone to produce smooth curves and avoid flat areas during grinding, sanding, and polishing. A typical cabbing machine holds several wheels representing a progressive diamond or silicon carbide grit series. They are turned by a common motor and water supply that serves as coolant/lubricant to wash away cuttings and keep the stone from overheating; it is ground and sanded progressively on finer wheels.

2.0 METHODS

2.1 Data Collection Technique

The extraction of gemstone from the host rock body in placer or primary deposit or fresh rock is done through open-pit mining, tunnelling, and panning. Gemstone mining varies depending on the type of gemstone: open–surface mining (stream sediment digging/excavation) is being practised in part of the active alluvial sediments. Such mining practice is very common and extensive.

2.1.1 Fieldwork/Geological mapping

The Geological mapping of the study area was carried out, and it lies between Northings N08˚ 51' - N08˚ 45' and Eastings E007˚ 45' - E008˚ 00' of North Central part of Keffi, Nasarawa State, Nigeria. The methods of study involved desk study, fieldwork and lapidary work. The mapping was done with a Global Positioning System (GPS). During the fieldwork, questions such as the quantity, quality and prices of the gemstones were asked.

2.1.2 Equipment used during fieldwork

The field instruments used in the course of the mapping exercise are:

(i) Satellite Map for locating areas to be mapped.

(ii) Field Note Book for jotting down features seen in the location.

(iii) Sample Bags for collecting gemstone samples in the field.

(iv) Camera for taking photographs of the environment

(v) Waterproof marker for sample labelling.

(vi) Global Positioning System (GPS) for taking coordinates and elevation of the study area

2.2 Processing

Gemstone sorting and grading in the mining site were carried out by handpicking - a process that is economically viable in countries with low wages. The difference in specific gravity (weight) between the gems and other minerals (sand and stones) allows them to be separated by gravity. The rocks are sorted according to their grades: grade A is clear and free from inclusions and cracks; grade B is slightly included, and; grade C, also referred to as cab quality, is heavily included.

Figure 3.0 Processes involved in the extraction of gemstone: (a) shows an artisanal miner in the process of exploiting gemstone in sediments within the mining site (b) an artisanal miner sorting the gems from the rubble (c) some gems shown off (d) breaking off of rocks containing gems.

2.3 Equipment Used in the Lapidary

(i) Cabbing machine (ii) Safety goggles (iii) Apron

2.3.1 Cutting cabochons

The lapidary used for the research is the Nigerian Institutes of Mining and Geosciences Lapidary Jos, Plateau State. The procedure is discussed as follows:

Step 1

After deciding on the shape to cab the stone, one starts the electroplated diamond wheels on the left shaft to start the grinding process. The grinding process shapes the cabochon and removes any surface irregularities so that the stone can be smoothed and polished. The cutting begins with the 80-grit electroplated diamond wheel; complete and thorough grinding of the stone's surface is carried out using adequate water as coolant while ensuring that scratching does not occur. Cabochon is frequently dried with a paper towel or clean rag to reveal the remaining scratches while at work.

Step 2

This step further smoothens and shapes the surface of the stone. All the edges and scratches that the 80-grit could not smoothen will be removed using the 220-grit electroplated diamond wheel.

Steps 1 and 2 are known as grinding.

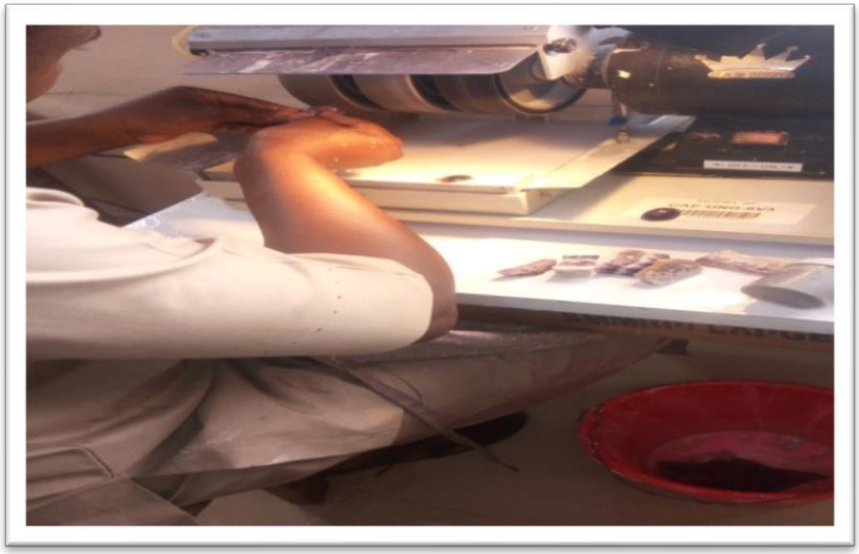

Plate 4: Grinding

Step 3

Once one is done grinding and shaping the cabochon on the 80-grit and 220-grit electroplated diamond wheels, one proceeds to the resin wheel sequence. These wheels sand and smooth away flat spots, scratches and tiny bumps left behind from the grinding wheels in one's stone, resulting in a pre-polished cabochon. The resin wheel sequence starts with the 360-grit resin wheel and proceeds to the 600-grit, 1200-grit and, lastly, the 3000-grit. One thoroughly grinds and smoothes the stone on each wheel, moving onto the next wheel when finished. After completing the resin wheel sequence, the cabochon will be ready for polishing in a step known as pre-polishing. It is essential to adjust the lamp as one works to provide additional light.

Step 4

To put the polish on the stone, one attaches the flat polishing lap disc by screwing it into the end of the proper wheel assembly while the Machine is turned off. After that, the Machine is turned on, and the stone is guarded around the disc for polishing. While polishing, a water spray tube is aimed at the centre of the disc so that when the disc is twirling, the water will spread evenly throughout the surface of the polishing pad, cooling it in the process. The water drip is adjusted to one's preference by moving the water spray tube to the left or right.

3.0 RESULT AND DISCUSSION

3.1 Result

The research used participant observations to gain more insight into the extraction of gemstones. The art of cabbing involves experimentation since every stone is different. The progression attained a certain realization such that different grits may be necessarily used depending on the type of stone and application. As with all stone cutting and cab making, practice and experimentation are keys to success. The research revealed how the value had been added to cab quality gemstones, as seen below. Black tourmaline's colour has been enhanced due to polishing, giving out a lustrous and beautiful sheen and reflecting light, thus capturing the imagination and admiration of all. On processing the crude sapphire and beryl, they show beauty, design, and sheen, which attract higher valuation. Having bought the rough tourmaline weighing 0.5kg at #2000, it later sold for #6200 after being polished, and this shows how much value can be added in monetary terms when gemstones are processed.

Figure 4.0: Rough and Polished black tourmaline

Figure 5.0: Rough and polished sapphire

Figure 6.0: Rough and Polished Beryl

3.2 Discussion

The Nigerian gem industry is operating in an embedded way of doing business. The sector is dominated by Artisanal and Small-Scale Miners that excavate the gems and rough dealers; Nigerian gems are smuggled out of the country as raw materials. The opportunities in this sector, such as employment generation, increased internally generated revenue, reduced poverty, and enhanced foreign exchange earnings, are not harnessed; this is a result of the sector being undeveloped and neglected due to over-dependence on oil.

4.0 CONCLUSION

The gemstone industry in Nigeria is full of opportunities; thus, the availability of adequate information concerning the path and value chain of the gemstone can lead to the positive evolution of the industry. The stages of the gemstone path in Nigeria abruptly stopped with the rough dealers and few gem cutters. As we advance, the other path stages are essential for promoting the nation's economic development. There is a need for government to realize that the sector can contribute immensely to the national economy, as presently, the full contribution of the sector is not captured in the country's GDP. The market for finished gemstones is not fully developed in Nigeria, and as a result, most of the rough gems are smuggled out of the country. Suppose the Nigerian market is developed to purchase homemade processed gems. A multiplier effect will have great economic benefits capable of

inducing development in the mining sector.

5.0 RECOMMENDATIONS

To ensure the gemstone activity in Nigeria is adequately utilized in all the stages of the path, the study recommends:

(i) Establish implementable policies that will improve activities carried out in the sector. The policies should allow the smooth establishment of more training institutes, centres, and gem identification laboratories to ensure skills and capacity development. It will also encourage the miners to be open and pay royalties meant for government coffers.

(ii) This research also recommends creating buying centres in states endowed with gemstones to enable miners to get value for their stones and enable value-added business and economic growth in the gemstone sector.

(iii) There is a need to massively explore and operate the value chain by involving a huge investment in expertise and finance.

(iv) Government should support the existing gemological institutions in the training of artisanal and small-scale miners, cutters, and jewellers to improve the quality of the products and encourage the participation of the local market in the gem business.

(v) Because this research concentrated on cabbing alone, the need for heat treatment of gemstones would need to be studied alongside cabbing to see how much value would be added to them.

Acknowledgement

Our special acknowledgement goes to the Nigerian Institutes of Mining and Geosciences Lapidary Jos, Plateau State, Nigeria, for permitting us to use their Lab facility to carry out cabochon polishing at almost no cost.

References

Dalat G.D and Filaba M.A (2007): Historical Background. In Akwa V.L, Binbol N.L Samaila K.I and Marcus N.D (eds) ***Geographical perspective on Nasarawa State***. A publication of the Department of Geography, Nasarawa State University, Keffi. Onaivi printing and publishing Co. Ltd, Keffi.

Falola T (1992). 'An Ounce Is Enough': The Gold Industry and the Politics of Control in Colonial Western Nigeria. Afr. Econ. Hist. (20):27-50. doi:10.2307/3601628

Fayemi DK (2015). The Role Of Solid Minerals In Nigeria's Economy As We Diversify From https://www.nta.ng/news/investment/2015/12/22-the-role-of-solid-minerals-in-nigerias-economy-as-we-diversify-from-crude-oil-dr-fayemi/

Gaywala MR, Surat N (2014). Gemstone processing. The United States patent application publication.

Groat LA (ed) (2007) Geology of Gem Deposits. Mineralogical Association of Canada Short Course 37, 276 pp

Hausel D.W. (2006). Gemstone Discoveries in Wyoming. The Rocky Mountains Association of Geologists Vol. 55 (3) Newsletter.

Humphries M (2013). Rare earth elements: The global supply chain. Congressional Research Service, 1-31. Retrieved from https://fas.org/sgp/crs/natsec/R41347.pdf

James L, Simon G, Estelle L, Abhijit P, Mattew R (2015, July 16). Due Diligence for Responsible Sourcing of Precious Stones. Retrieved from Sustainable & Responsible Solutions: http://www.estellelevin.com/wp-content/uploads/2016/04/Final-SRSReport.pdf

Kayode A (2018). Opening remarks on the occasion of the first annual general meeting of the Gemstones Miners and Marketers Association of Nigeria. Retrieved from Gemstones Miners and Marketers Association of Nigeria Database

Lyam, A. (2000): Nasarawa State. In Mamman A.B, Oyebaji, J.O. and Peters S.W. (eds) ***Nigeria: A people United, a future assured*. Survey of States.** V0l 2 No2- Millennium edition, Abuja, Federal Ministry for Information: 382-392

Magotra, N., Namga, S., Singh, P., Arora, N., Srivastava, P.K., 2017. A New Classification Scheme of Fluorite Deposits. International Journal of Geosciences, 8, 599-610.

Mudili K, Govindan K, Barve A, Geng Y (2013).

Barriers to green supply chain management in Indian Mining Industries: A graph-theoretic approach. J. Clean. Prod. 47:335-344.

Obaje N.G, Lar U.K, Nzegbuna A. I, Moumouni A, Chaanda M.S and Goki N.G (2007): Geology and Mineral Resources - A preliminary Investigation. In Akwa V.L, Binbol N.L, Samaila K.I. and Marcus N.D (eds)

Geographical perspective on Nasarawa State. A publication of the Department of Geography, Nasarawa State University, Keffi. Onaivi printing and publishing Co Ltd, Keffi.

Olade, Moses. (2022). Overview of Nigeria's Mineral Resources in the Context of Africa's Mineral Wealth.

Olaniyi R (2011). West African' stone boys and the making of the Ibadan mining frontiers since the 1990s. Department of History, University of Ibadan. Retrieved from www.afdb.org

Basau, *et al* (2021) Nigerian Mining Journal, (19) 50 - 73

Experimental Investigation into the Mechanical Behaviour of a Mine Backfill Material

Basu, M. M., Akinola, A. P.[a], Jacob A. A. and Joro. J.
Department of Mining Engineering, University of Jos, Plateau, Nigeria
[a] Email: wok_harat@yahoo.com, akinolaa@unijos.edu.ng

Abstract
This research focused on the mechanical properties of the mine material used in the backfilling of mine sites, and this is very significant because the fact that these reclaimed sites will be opened for future usage; a solid base ensures safety of both life and property. The project examined the suitability of the backfill material found within the case study areas. Samples were obtained from various locations at Gwol in Barkin Ladi LGA, Plateau state. Sample A, B, C and D was used in mechanical behaviour determination. These samples were subjected to various laboratory tests which included: Sieve Particle Analysis Test, Atterberg Limit Test, Specific Gravity Test and Compaction Test. From the undertaken tests, the compaction test revealed the optimum moisture content of the four samples: samples A, B, C and D were found to be 18.03%, 17.99%, 18.24% and 14.52% respectively. This is a clear indication that the soil samples are inorganic clayey-silty soil. The sieve analysis results indicate that 80% of cumulative percent passing through the resulting sieve size distribution of 2.00mm soil size are samples A, B and D. While for sample C the major soil distribution is 4.75mm. Specific gravity result for the sample A, B, C and D were 2.50, 2.55, 2.42 and 2.53 respectively. From the results of the tests carried out, it was found out that the soil samples A, B, and C are more suitable for backfilling due to their soil sizes and moisture content.

Keywords: Backfilling, compatibility, shear strength, void ratio, permeability

1.0 Background

Mining is the extraction of profitable and valuable minerals or geologic materials from the earth, which can either be done on the surface or underground. Mining activities occur in five (5) stages, namely: prospection, exploration, development, exploitation, and reclamation. At the prospecting stage, geologists use visual inspection and physical measurements of the earth's properties to discover mineral deposits. The prospecting stage is mostly physical labour, which involves traversing (traditionally on foot or on horseback) the intended area of coverage, panning, and sifting and outcrop investigation, looking for signs of mineralization. In some areas, a prospector must also make claims by erecting post with the appropriate placards on all four corners of a desired land in which one wish to prospect within, and register the claim before they may take samples. In other areas, publicly held lands are open to prospecting, by staking a mining claim (Canine, 2019). Newman *et al* (2010) described the exploration stage as the value determination of mineral deposits through drilling of holes to estimate the mineral concentration and its variability throughout the ore-body. He also explained the development stage as the transitional period when the mine planning studies is translated into mine design by determining the mining method, estimating production capacity infrastructure capital and performing detailed engineering design.

Howard and Jan (2007) explained that during the exploitation stage, ore is removed from the ground via surface and (or) underground mining methods, usually in large quantities as the mine begins producing, and depleting down the line as earlier envisioned. And they also revealed that the reclamation of mines consists of restoring the area in which mining occurred to its natural state to the extent possible.

Backfilling is a form of reclamation, and it is defined as any material, mine waste or rock used to refill a mining opening /to provide support after ores have been removed (Wu *et. al.,* 2017). Also backfilling operations have

been used for effective and safe underground mining for many years. Frequently, the tailings are classified with cyclones where the coarser fractions of the tailings stream are used for backfill, with the balance (referred to as slimes) being deposited on the surface (Williams, 2016). It is absolutely important and that any material or waste rock that will be used for backfilling must undergo various mechanical behavioural tests to guaranty the mine site geologic stability (Huang *et.al.,* 2018).

The backfilling of mines is an integral part of the mining process, requiring the same level of attention generally afforded to the more commonly recognised "profit-producing" parts of the operation (Zhou *et al*, 2013). The change in perception of backfilling from an additional cost to mining operations, to one of a pre-profit activity, will aid the required advancement in technology required for backfill (Rankine et. al, 2007). Backfilling is required for the continuance and efficiency of mining operations. Additional benefits include: improved regional and local rock stability through the support provided by the backfill, reduced costs of building significant tailings disposal structures on the surface, and the reduced environmental impacts by the underground containment of waste material. All these focus the operation towards the overall design objective of a safe, environmentally sound and aesthetically satisfactory post-operational mine-site (Rankine *et al.*, 2007). Backfilling mining method is widely used in underground mine for overlying strata control, and the overlying strata are supported by solid backfilling materials. This mining method effectively prevents the rupture of overlying strata and then decreases the geological disasters in mine (Huang *et al*, 2018). The support ability of backfilling body depends on the mechanical characteristics of materials (Zhou *et al*, 2013), which are usually composed of gangue, fly ash, tailings, or limes (Wu *et al.*, 2017).

Since when the tin rush mining operation of the 1950's took place in Jos, Plateau state, the mining industry has become more progressive across the state and in Nigeria in general. In terms of domestic contribution, mining and its related industries contributed millions of Naira to the Gross Domestic Product (GDP) of Nigeria before the discovery of oil.

However, alongside the prominent contribution of the mining industry to the Nigerian economy, there had been consequential problems to the environment such as land subsidence – leading to the endangerment of lives and properties – resulting from inadequate knowledge of the mechanical properties of the backfill material to be used, rendering land impossible to be used due to void, toxicity of mines residues to natural water and ecosystem; pollution of the environment. (Wireman, 2001).

Thus, this work aims to determine the mechanical behaviour of materials used in backfilling of mine sites and their suitability, by carrying out laboratory tests for optimum moisture content, maximum dry density, grain size distribution, specific gravity, compaction, etc., and the effects that is encountered if inappropriate materials that are not up to the required standard are used to backfill mine sites.

2.0 Description of the Study Area

The samples used for this study is gotten from Gwol, Barkin Ladi of Plateau State, Nigeria. This is as a result of many mining activities that have taken place in this area during the operation of Nigeria Mining Company. The vegetation of Gwol is typical of the Guinea Savannah which is characterized by sparsely distributed shrubs, trees, and short grasses. The area is heavily cultivated both on the highlands and lowlands (Ezekiel, 2008).Gwol area has a ubiquitous and predominantly geographical landscape. Gwol is associated with undulating highlands characterized by hills ranging from 500-1600 metres above sea level, as well as artificial hillocks and mining paddocks/dump (NigeriaRoute.com). The drainage pattern is usually dentritic in nature.

The area is also affected by the Tectonic activities which played a key roles in the shaping of the area, making it very suitable for mining operation. The initial the younger granite intruded into the basement complex but in due course, the case study area was grossly

overshadowed by the intrusion of volcanic rocks covering most part of the area. Subsequently weathering, transportation and deposition of the weathered rocks created very extensive lowlands of Laterites (Ezekiel, 2004).

3.0 Materials and Methods

The backfill material were taken from four different locations in lumps at depth 3 meters, from different locations in the study area. Each sample is tagged sample A, B, C and D. Global Positioning System (GPS) device is used to obtain the coordinates of the points where the samples were taken. Each sample taken was conveyed to the laboratory using the sampling bags.

Sieve Analysis Test.

Material Used are: Mechanical Shakers, Scoop, Sieve brush, metal tray, weighing balance, sieve size of 4.75mm, 2.00mm, 1.18mm, 425µm, 300µm, 150µm and pan.

Sieve particle analysis test, also known as gradation test, a procedure used to assess the particle size distribution of the granular material by allowing the material to pass through series of sieves progressively, the metal tray is placed on the weighing beam and reset to 0.00g, where a measure of the sample is scooped on the metal tray and weighed until an accurate measure of 250g was gotten. A measured sample (the representative sample of 250g) was taken and poured on the mechanical shaker, closed and turned over to shake for five minutes. After five minutes, each sieve size was separated with its soil content. The soil content of 4.75mm sieve was then poured into a container, the sieve and soil content weighed separately and individually to get the sieve weight and the weight of the soil content: this process was repeated for the other sieve sizes of 2.00mm, 1.18mm, 425µm, 300µm, 150µm and pan.

Atterberg Limit Test

Material Used: Casagrande liquid limit apparatus, spatula, weighing balance, metal tray, wash bottle, moisture can, clean flat glass plate and dry oven.

Atterberg limit test used to measure the critical water content of a fine-grained soil is carried out in three (3) stages: liquid limit, plastic limit and shrinkage limit. In The Atterberg Limit Test, samples were sieved using 425µm sieve, where the fine particles were mixed with water and transferred into a polythene leather to stay for 24 hours. The mixture is placed on a metal tray and mixed with small quantity of the dried fine particle soil to thicken the mixture, which is then applied into the brass cup of the Casagrande liquid limit; the soil is demarcated at the centre using the grooving tool, resetting the reading of the blower first to zero. The next step involved turning the handle at two revolutions per second (lifting and dropping the cup) until the two parts of the soil close the groove at the bottom of the cup: the number of blows that caused the closure was recorded.

For plastic limit, the remaining mixture left is rolled into a ball, and pressure is applied, rolling the soil between the finger and thumb into a diameter of 3mm until the soil begins to show signs of longitudinal and transverse crack at the rolled diameter. After that, the sample is gathered and the cracked thread are transferred into moisture cans, and then placed into the oven dryer for 24 hours. After 24 hours, the moisture cans were weighed again to determine the moisture loss of the soil. The graph of moisture contents against the number of drops (blow) was plotted. The moisture content at 25 drops was noted and recorded as the liquid limit from interpolation of the graph.

Specific Gravity Test

Material Used: Density bottles with stopper de-aired distilled water, weighing balance, vacuum pump and 425µm sieve.

Specific gravity of soil is the ratio of the weight of a given volume of soil particles in the air to the weight of an equal volume of distilled water at a temperature of 4°C. It is an important factor required for computing the most important soil properties e.g. void ratio of soil, unit weight, and degree of saturation. To carry out the test, **t**he density bottle is rinsed with distilled water, and a tissue paper is used to clean the density bottle, after which about 10g of soil passing through the 425µm sieve is weighed. The density bottle, the soil, and the bottle with stopper and added

de-aired distilled water to the bottle containing 10g soil is weighed individually on the beam balance. The mixture is shaken until no air is released and left to observe if there's any decrease in water volume. The bottle, stopper and water after the exterior has been dried are weighed. The bottle is thoroughly cleaned and filled with distilled air and allowed it to stand for one (1) hour. The whole operation is repeated twice to get an average.

Compaction Test

Materials Used: Standard proctor mould of 1000CC volume; standard rammer of 2.5kg; a mixing tray; heavy duty straight edge' weighing balance and water.

The compaction test is a laboratory method of experimentally determining the optimal moisture content at which a given soil type will become more dense and achieve maximum dry density. The soil sample is oven dried for 24 hours after which 3kg of soil was emptied into the mould and placed in the mixing tray. 4% of 3kg of the soil which is 240g (or in this case 240ml of water) was taken and mixed with the soil and poured into the mould. The rammer is used to ram the soil 27 times to ensure it is compacted before adding more soil to make sure the compacted soil was filled to the tip of the mould, after which the final compacted layer of soil is scratched off for proper bonding with subsequent layers of which the mould and soil on the beam balance was weighed. The soil specimen is extracted and 2 samples taken for determination of moisture content – tin (that has already been weighed) is provided for the weighing.

Triaxial Compression Test

Material used: compression tester

In the triaxial test, soil samples were air-dried for 24 hours, and then mixed with water until it was evenly wet. Three (3) representing ssamples was taken for moisture content determination andthe specimen was re-molded with dimensions of (76mm length and 38mm diammeter) and each was stored in the desiccator for some period of time. Using the rubber sheath and sucking procedure, I prepared the specimen, capped at the bottom and top by securing them with rubber bungs. The specimen was installed in a loading frame and adjusted until it made contact with loading ram. The air valve was opened and applied round with initial cell pressure of 100KN/m^2, then observed the load and deformation dial gauge readings. The procedure was repeated for initial cell pressure of 200KN/m^2 and 300KN/m^2.

4.0 Result and Discussion

Sieve Analysis Results

The obtained results for **Sample A, B, C and D** is shown below:

Weight of metal pan = 147.32g

Weight of sample = 250g

Table 1**:** Sieve Analysis Table of Sample A

Sieve Number	Weight of sieve + soil	Weight of sieve	Weight of soil retained	Percent retained (%)	Cumulative percent retained	Percent passing (%)
4.75mm	501.46	493.76	7.70	3.08	3.08	96.92
2.00mm	516.59	458.28	58.31	23.29	26.37	73.63
1.18mm	448.49	395.13	53.36	21.31	47.68	52.32
425µm	418.77	339.02	79.75	31.85	79.53	20.47
300µm	334.66	322.57	12.09	4.83	84.36	15.64
150µm	315.75	300.37	15.38	6.15	90.51	9.49
Pan	285.86	262.08	23.78	9.49	100.00	0.00

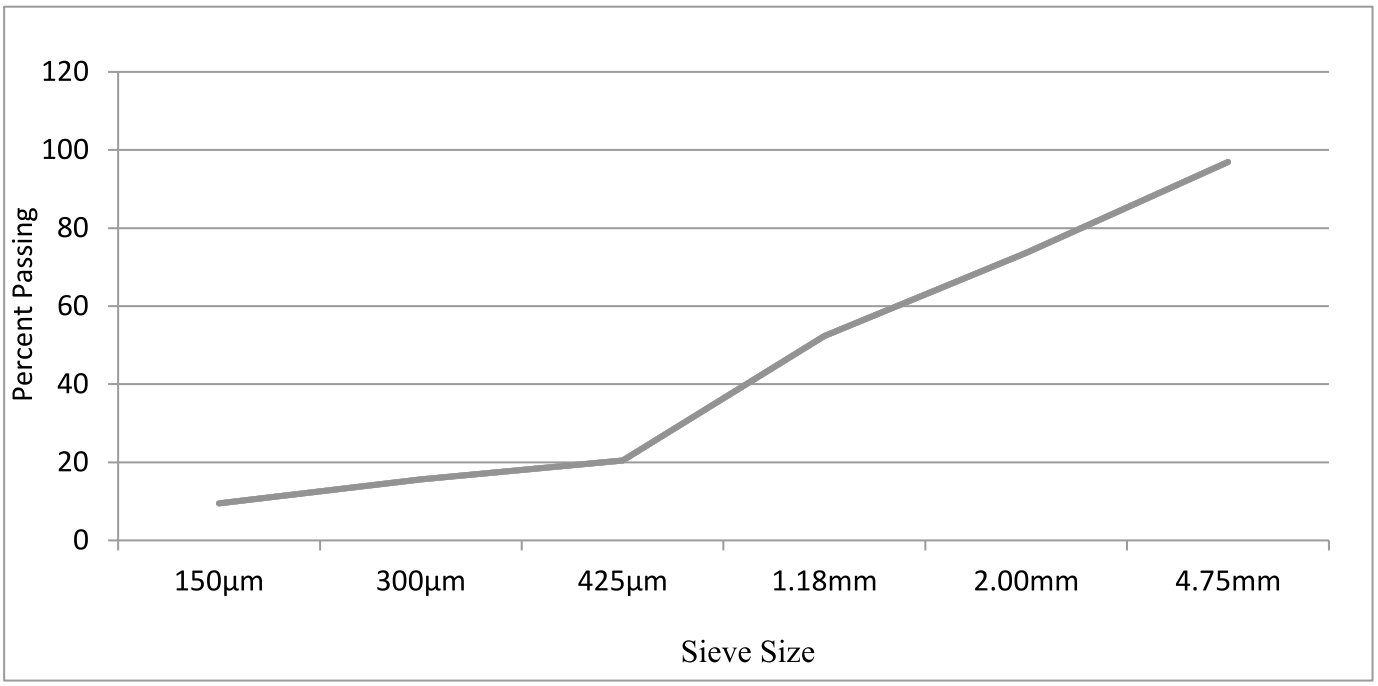

Figure 1: Graph of Sieve Analysis for Sample A

Table 2: Graph of Cumulative Percent Passing Against Sieve Size of Sample B

Sieve Number	Weight of sieve + soil	Weight of sieve	Weight of soil retained	Percent retained	Cumulative percent retained	Percent passing [%]
4.75mm	502.03	493.76	8.27	3.31	3.31	96.69
2.00mm	494.32	458.28	36.04	14.43	17.74	82.26
1.18mm	426.56	395.13	31.43	12.59	30.33	69.67
425µm	415.67	339.02	76.65	30.69	61.02	38.98
300µm	348.49	322.57	25.92	10.38	71.40	28.60
150µm	343.01	300.37	42.64	17.08	88.48	11.52
Pan	290.85	262.08	28.77	11.52	100.00	0.00

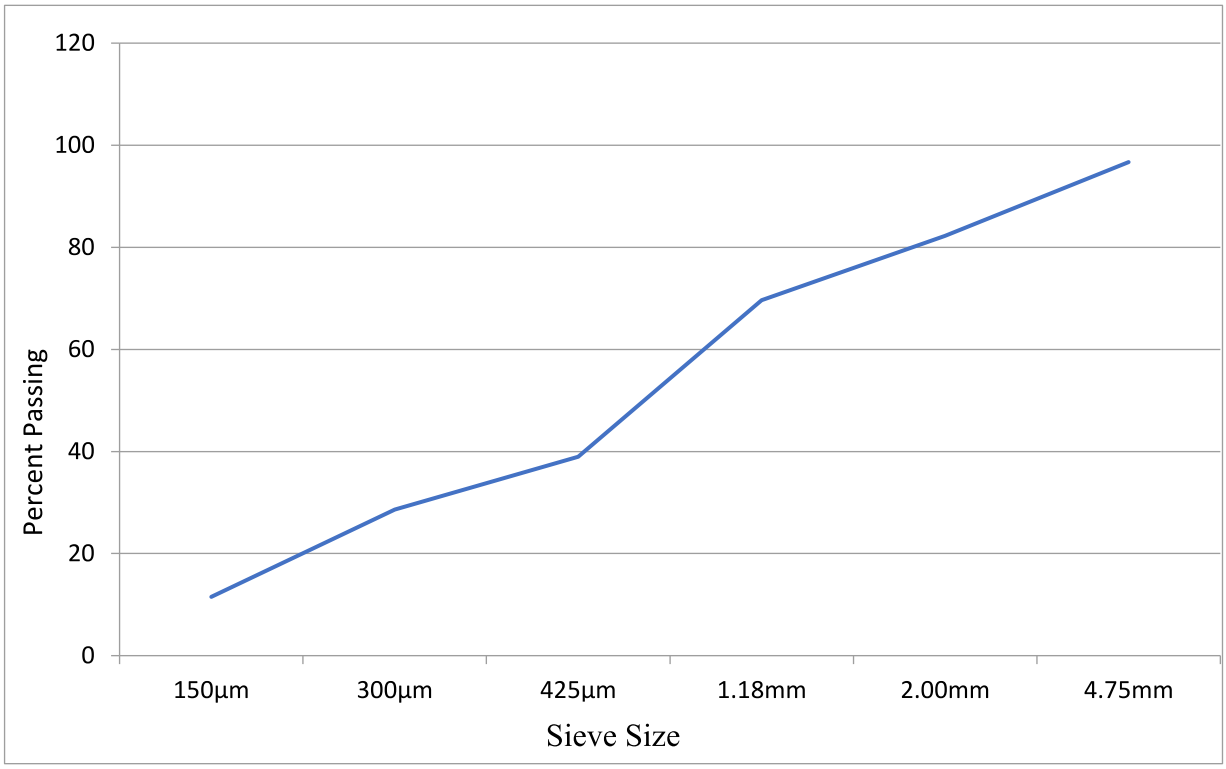

Figure 2: Graph of Cumulative Percent Passing Against Sieve Size of Sample B

Table 3: Sieve Analysis Table of Sample C

Sieve Number	Weight of sieve --++ soil	Weight of sieve	Weight of soil retained	Percent retained	Cumulative percent retained	Percent passing[%]
4.75mm	521.70	493.76	27.94	11.23	11.23	88.77
2.00mm	509.96	458.28	51.68	20.76	31.99	68.01
1.18mm	435.27	395.13	40.14	16.13	48.12	51.88
425µm	420.65	339.02	81.63	32.79	80.91	19.09
300µm	336.18	322.57	13.61	5.49	86.40	13.60
150µm	308.38	300.37	8.01	3.29	89.69	10.31
Pan	287.97	262.08	25.89	10.40	100.00	0.00

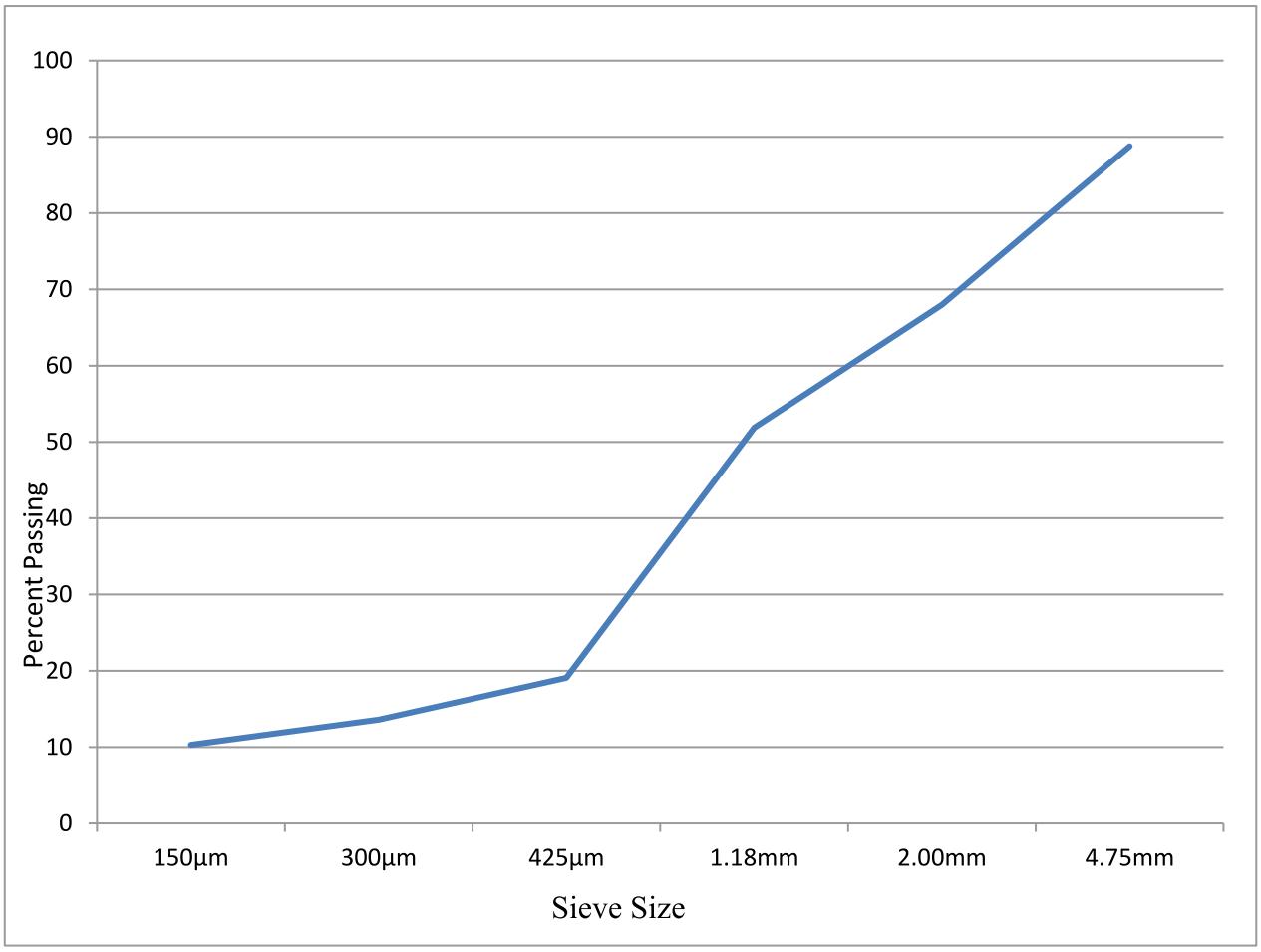

Figure 3: Graph of Cumulative Percent Passing Against Sieve Size of Sample C

Table 4: Sieve Analysis Table of Sample D

Sieve Number	Weight of sieve + soil	Weight of sieve	Weight of soil retained	Percent retained	Cumulative percent retained	Percent passing [%]
4.75mm	499.95	493.76	6.19	2.48	2.48	97.52
2.00mm	499.33	458.28	41.05	16.44	18.92	81.08
1.18mm	442.74	395.13	47.61	19.07	37.99	62.01
425µm	422.98	339.02	83.96	33.63	71.62	28.38
300µm	339.22	322.57	16.64	6.67	78.29	21.71
150µm	326.05	300.37	25.68	10.29	88.58	11.42
Pan	290.59	262.08	28.51	11.42	100.00	0.00

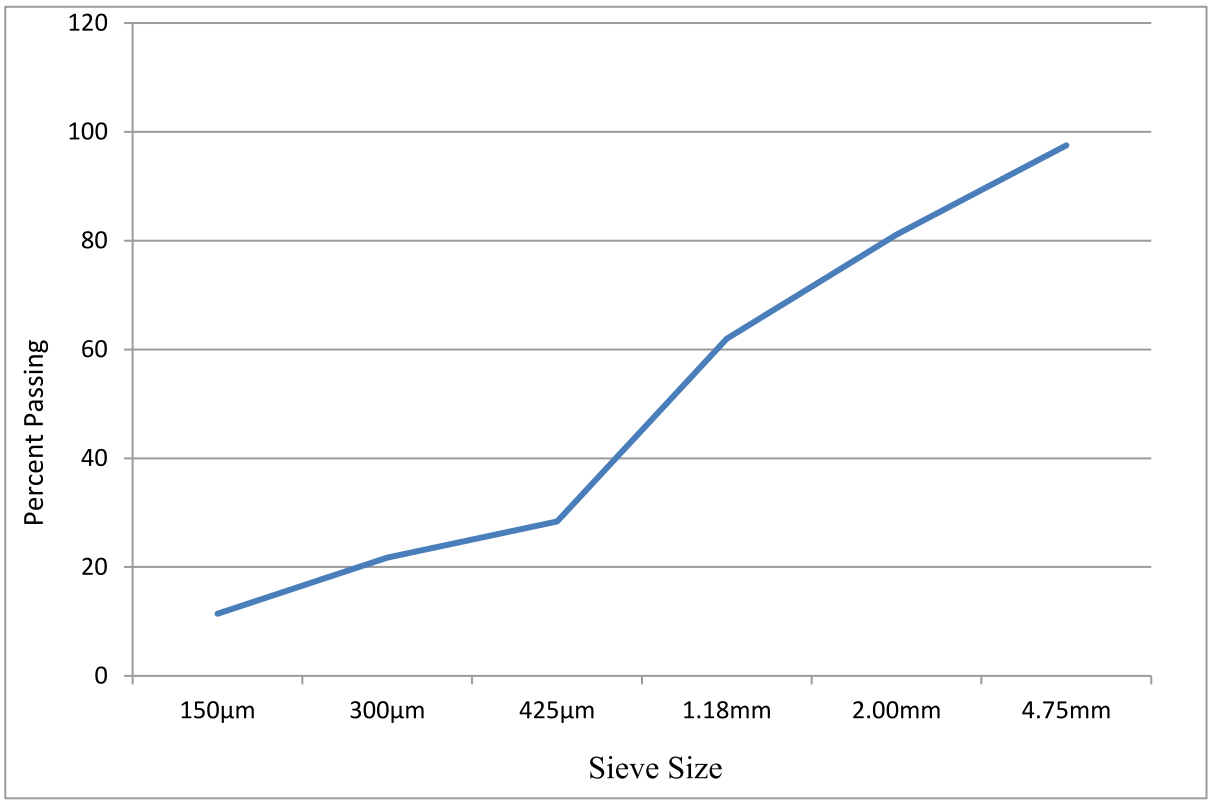

Figure 4: Graph of Cumulative Percent Passing Against Sieve Size of Sample D

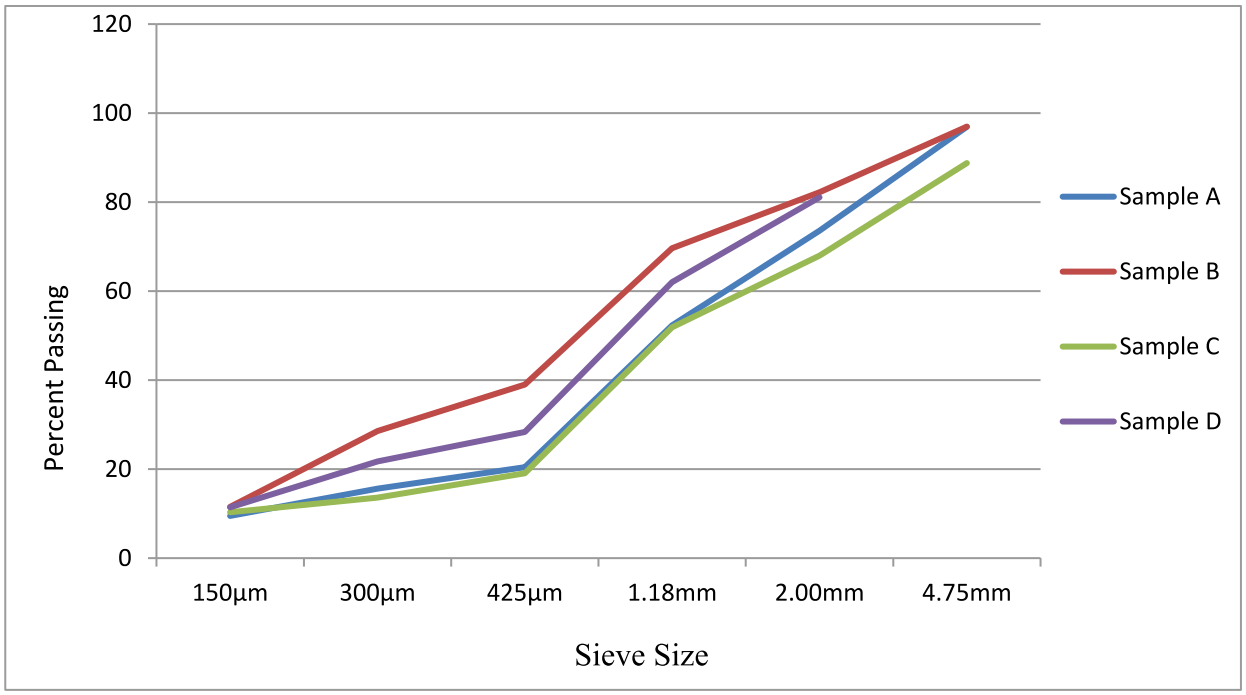

Figure 5: Sieve Particle Test (% Passing against Sieve Size) for all samples

Major division			Group symbol	Typical name	Classification criteria	
Coarse-grained soils (More than 50% retained on No. 200 ASTM sieve)	Gravels 50% or more of coarse fraction retained on No. 4 ASTM sieve	Clean gravels	GW	Well-graded gravels and gravel-sand mixtures, little or no fines.		$U = D_{60}/D_{10}$ greater than 4 $C_c = D^2_{30}/(D_{60} \times D_{20})$ between 1 and 3.
			GP	Poorly-graded gravels and gravel-sand mixtures, little or no fines.	Classification on the basis of percentage of fines. Less than 5% passing No. 200 ASTM sieve—GW, GP, SW, SP. More than 12% passing No. 200 ASTM sieve— GM, GC, SM, SC. 5% to 12% passing No. 200 ASTM sieve—Border-line classification requiring use of dual symbols.	Not meeting both criteria for GW.
		Gravels with fines	GM	Silty gravels, gravel-sand-silt mixtures.		Atterberg limits plot below *A*-line or plasticity index less than 4.
			GC	Clayey gravels, gravel-sand-clay mixtures.		Atterberg limits plot above *A*-line or plasticity index less than 4.
	Sands More than 50% of coarse fraction passes No. 4 ASTM sieve	Clean sands	SW	Well-graded sands and gravelly sands, little or no fines.		U greater than 6 C_c between 1 and 3.
			SP	Poorly-graded sands and gravelly sands, little or no fines.		Not meeting both criteria for SW.
		Sands with fines	SM	Silty sands, and-silt mixtures.		Atterberg limits plot below *A*-line or plasticity index less than 4.
			SC	Clayey sands, sand-clay mixtures.		Atterberg limits plot above *A*-line or plasticity index greater than 7.
Fine-grained soils (50% or more passes No. 200 ASTM Sieve)	Silts and Clays (Liquid limit 50% or less)		ML	Inorganic silts, very fine sands, rock flour, silty or clayey fine sands.	Check Plasticity Chart	
			CL	Inorganic clays or low to medium plasticity, gravelly clays, sandy clays, silty clays, lean clays.		
			OL	Organic silts and organic silty clays of low plasticity.		
	Silts and clays (Liquid limit greater than 50%)		MH	Inorganic silts, micaceous or diatomaceous fine sands or silts, elastic silts.		
			CH	Inorganic clays of high plasticity, fat clays.		
			OH	Organic clays of medium to high plasticity.		
Highly organic clays			P_t	Peat, muck and other highly organic soils.	Fibrous organic matter, will char, burn, or glow. Readily identified by colour, odour, spongy feel, and fibrous texture.	

Figure 6: Unified Soil Classification System. (Source: Bowles, 2012)

The percentages of different sizes of soil particles coarser than 75μm is determined by sieve analysis whereas less than 75μm is determined by hydrometer analysis. Based on the Unified Soil Classification System (USCS) as shown on table 13, soils with > 50 % of sample mass retained on the 0.074 mm sieve is term coarse-grained and if > 50 % of the coarse fraction is retained on 4.76 mm sieve, the soil is classified as gravel but if ≥ 50 % of the coarse fraction passes 4.76 mm sieve, such soil is sandy soil.

From results obtained during the experimental analysis of samples using the 4.76mm sieve, 96.92% of sample A passed through the sieve, 96.69% of sample B passed through the sieve, 88.77% of sample C passed through the sieve and 97.52% of sample D passed through the 4.76mm sieve as well; as such, the materials are sandy soil.

Since ≥ 50 % of the sample mass of soils A, B, C, and D passed through the No 4 sieve of the American Society for Testing and Materials (ASTM), the soil can therefore be classified as fine-grained soil, thus the plasticity index of the soil fine-grained is then plotted against its liquid limit on plasticity chart to further distinguish the soil as silt or clay of low, medium, or high plasticity. From plots and consequent calculation, the plasticity index of the four samples were found to be: sample A is 10.36 (medium plasticity: clay-loamy soil); sample B is 21.64 (high plasticity: silty-clayey soil); sample C is 17.03 (medium plasticity: clay-loamy soil); and sample D is 11.83 (medium plasticity: clay-loamy soil).

Sieve Analysis Test is an important test in assessing the fill's ability to act as a ground support material. In mechanical soil stabilization, the main principle is to mix a few selected soils in such a proportion that a desired grain size distribution is obtained for the design mix. Hence, for proportioning the selected soils, the grain size distribution of each soil is required to be known (Rankine, 2007). An analysis of this property helps to determine whether the design objectives of

the fill will be met. A fill with well-graded particles will offer more resistance to displacement and settlement than one with uniformly graded particles, as it was determined that the finer and well-distributed the grain size, the higher the surface area, and consequently, better compressive strength and bulk density, physical stability of structures and backfilled voids, reduced permeability, and excellent soil texture, cohesiveness and compaction (Raj, 2017).Samples A, C and D having medium plasticity and sample B with high plasticity show that the soils are cohesive due to their low inter-granular spacing and large surface area of particulate contact, and this will make the soils easily compact when used to back-fill mining voids. All the samples' sizes – in combination with their plasticity – can be used make excellent backfill material, as they will yield better compaction and high compressive strength in the voids irrespective of the continuous loads applied – reducing significantly the incidence of subsidence.

Atterberg Limit Test Result

It is carried out in 3 stages: liquid limit, plastic limit and shrinkage limit.

Liquid Limit

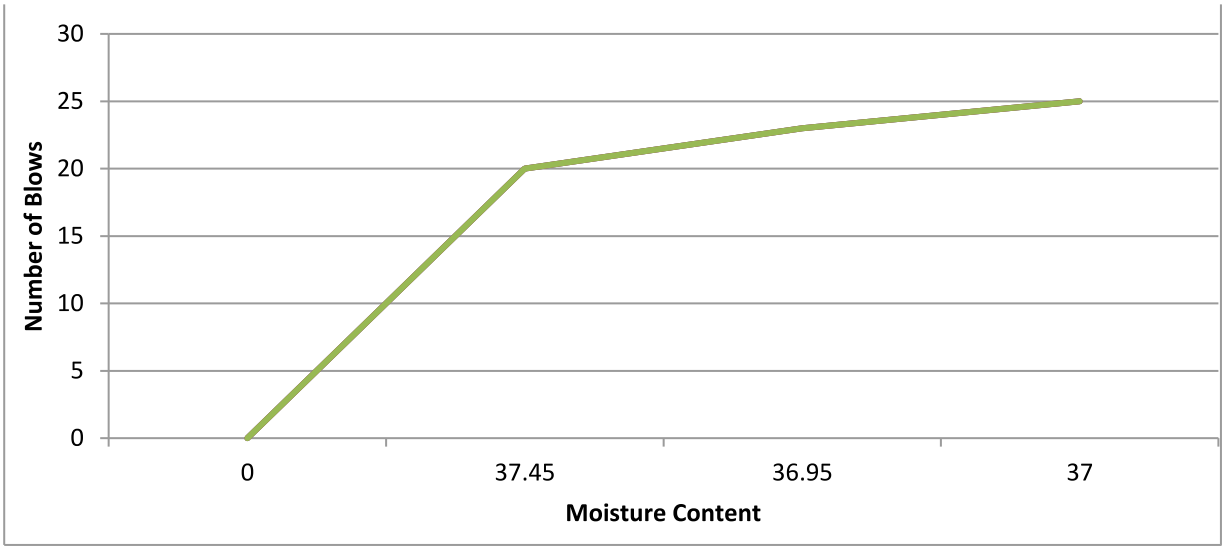

Figure 7: Graph of Number of Blows against Moisture Content of Sample A

Table 5: Atterberg Liquid Limit Table of Sample A

Test Number	1	2	3
Number of Blows	20	23	25
Container Number	13	15	21
Wet soil + Container	38.93	42.83	49.52
Dry soil + Container	30.98	35.69	40.48
Moisture can weight	9.75	16.29	16.05
Dry Soil	21.23	19.40	24.43
Moisture Loss	7.95	7.14	9.04
Moisture Content %	37.45	36.95	37.00

The Liquid Limit was determined by tracing 25 numbers of blows on the graph (fig 3.2) to the moisture content which is 37.00.

Table 6: Plastic Limit of Sample A

Container Number	09	42	47
Wet soil + Container	21.84	20.50	22.29
Dry soil + Container	20.61	19.64	21.14
Container weight	16.65	16.18	16.35
Dry soil	3.96	3.46	4.79
Moisture	1.23	0.86	1.15
Moisture Content %	31.06	24.86	24.01

Plastic Limit

Plastic limit = Average of the moisture content = 26.64

Plastic Index (PI) = Liquid Limit (LL) – Plastic Limit (PL)
PI (sample A)) = 37 – 26.64 = 10.36; this is also done for samples B, C and D.

Result of sample B

Liquid Limit

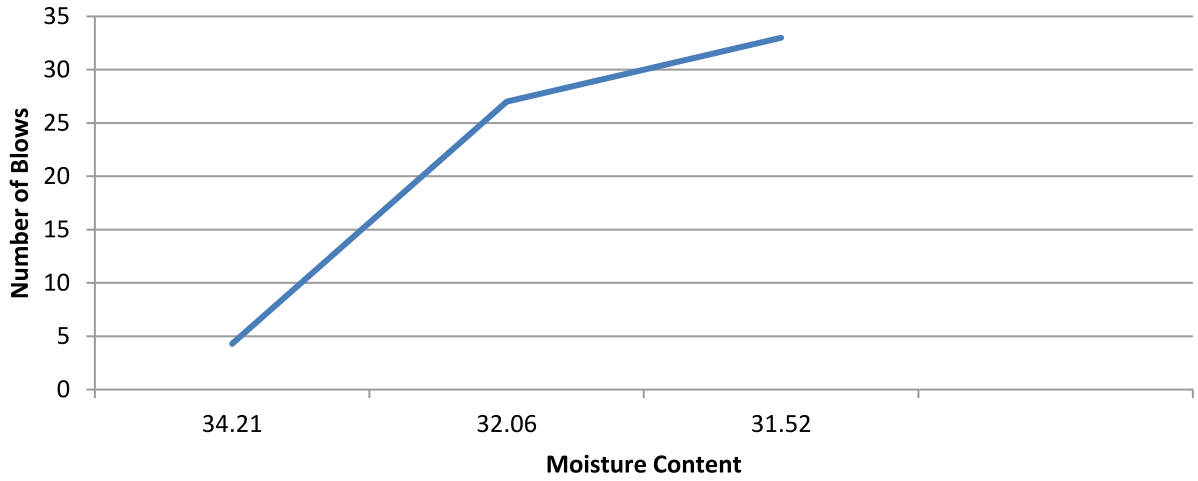

Figure 8: Graph of Number of Blows against Moisture Content of Sample B

Table 7: Atterberg Liquid Limit Table of Sample B

Test Number	1	2	3
Number of Blows	24	27	33
Container Number	04	27	50
Wet soil + Container	39.42	37.83	34.90
Dry soil + Container	33.91	32.55	30.45
Moisture can weight	16.05	16.08	16.33
Dry Soil	17.86	16.47	14.12
Moisture Loss	6.11	5.28	4.45
Moisture Content %	34.21	32.06	31.52

Plastic Limit

Table 8: Plastic Limit of Sample B

Container Number	13	20	41
Wet soil + Container	24.61	24.30	23.28
Dry soil + Container	23.29	23.80	22.83
Container weight	16.13	15.88	15.92
Dry soil	7.16	7.92	6.91
Moisture	1.32	0.50	0.45
Moisture Content %	18.45	6.31	6.51

Result of sample C

Liquid Limit

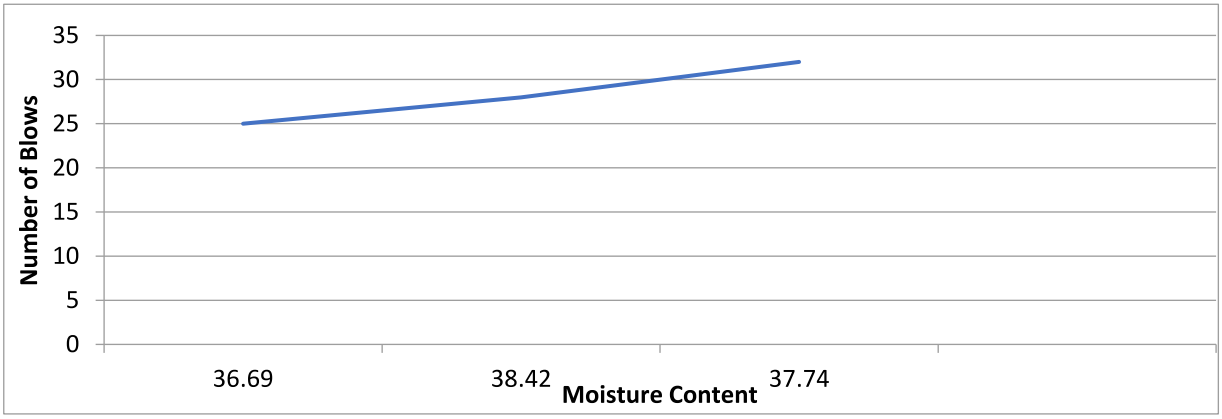

Figure 9: Graph of Number of Blows against Moisture Content of Sample C

Table 9: A Liquid Limit of Sample C

Test Number	1	2	3
Number of Blows	25	28	32
Container Number	38	45	47
Wet soil + Container	29.97	28.45	23.52
Dry soil + Container	26.08	24.83	19.55
Moisture can weight	16.18	16.41	10.03
Dry Soil	10.82	9.42	10.52
Moisture Loss	3.97	3.62	3.97
Moisture Content %	36.69	38.42	37.74

Plastic Limit

Table 10: Atterberg Plastic Limit of Sample C

Container Number	44	24	28
Wet soil + Container	21.22	22.20	24.54
Dry soil + Container	20.35	21.08	23.25
Container weight	15.70	15.94	16.31
Dry soil	4.65	5.14	6.94
Moisture	0.87	1.12	1.29
Moisture Content %	18.59	21.79	18.59

Result of Sample D

Liquid Limit

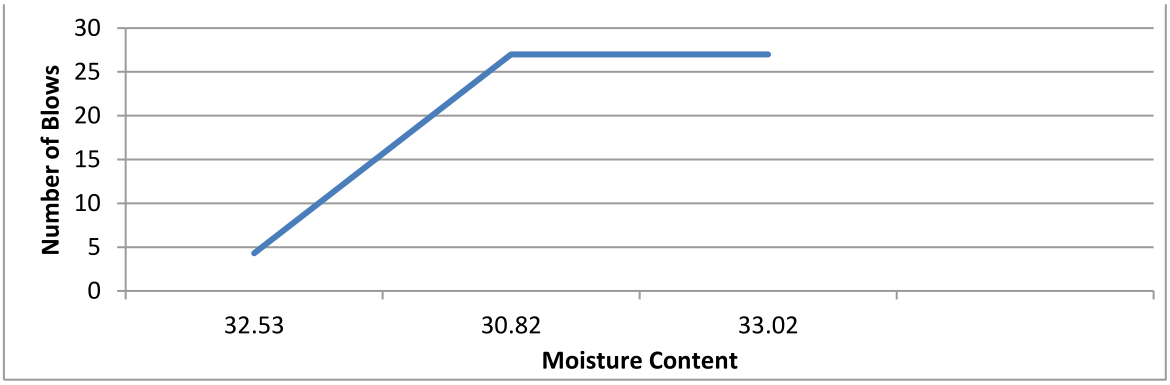

Figure 10: A Graph of Number of Blows Against Moisture Content Sample D

Table 11: Liquid Limit of Sample D

Test Number	**1**	**2**	**3**
Number of Blows	24	27	27
Container Number	06	46	48
Wet soil + Container	27.45	28.62	29.14
Dry soil + Container	24.61	25.73	25.96
Moisture can weight	15.88	16.35	16.33
Dry Soil	8.73	9.38	9.63
Loss	2.84	2.89	3.18
Moisture Content %	32.53	30.81	33.02

Plastic Limit

Table 12: Plastic Limit of Sample D

SAMPLE	PLASTIC INDEX	INDICATION
A	10.36	Medium plasticity (clay-loamy soil)
B	21.64	High plasticity (silty-clay soil)
C	17.03	Medium plasticity (clay-loamy soil)
D	11.83	Medium plasticity (clay-loamy soil)

Table 13: Plasticity index of sampled soils

Container Number	13	26	05
Wet soil + Container	15.99	22.24	22.38
Dry soil + Container	15.01	20.46	21.43
Container weight	9.79	12.91	16.62
Dry soil	5.22	7.55	4.81
Moisture	0.98	1.78	0.95
Moisture Content %	18.77	23.58	19.75

Table 14: standard plasticity index of soils. (Sourced: Bowles, 2012)

Plasticity index (%)	Soil type	Degree of plasticity	Degree of cohesiveness
0	Sand	Non-plastic	Non-cohesive
<7	Silt	Low plastic	Partly cohesive
7-17	Silt clay	Medium plastic	Cohesive
>17	Clay	High plastic	cohesive

The Plasticity index, which expresses (in percent) the dry weight of the soil sample, gives a good measure of the compressibility of the soil. It shows how much clay is contained in the soil, indicating its fineness and capacity to change shape without altering its volume when compressed. A study on slaking as done by Morgenstern and Eigenbrod (1974) indicates that if the range of liquid limits for weathered materials fall between 20 and above, slaking occurs extensively, and the rocks are highly plastic. Nevertheless, an important aspect of backfill materials having plastic properties is that when surplus pore pressures are found in the backfill material, it might not be rapidly dissipated as the materials' stress is increased, impacting compressibility as a result.

COMPACTION TEST

Table 15: Compaction Test Table of Sample A

	8%		4%							
Weight of mould(kg)	1.980		1.980		1.980		1.980		1.980	
Weight of mould + soil	3.532		3.646		3.862		3.975		3.957	
Weight of compacted soil	1.552		1.666		1.882		1.995		1.977	
Bulk density	1.55		1.67		1.88		1.99		1.98	
Dry density	1.44	1.44	1.51	1.51	1.64	1.64	1.69	1.69	1.59	1.59
Tin number	Li22	22B	Am4	PA_{20}	PA_{10}	Sp7c	BH_{17}	B31	L1	BH
Tin weight(g)	23.43	24.31	24.93	23.60	23.56	24.61	24.85	23.83	23.50	24.91
Tin + wet soil(g)	67.57	60.57	68.17	63.52	64.80	66.47	62.36	56.15	61.60	59.91
Tin + dry soil	64.46	58.03	64.11	59.62	59.69	61.19	51.38	56.46	54.22	53.21
Weight of water	3.13	2.54	4.06	3.90	5.21	5.28	4.77	5.90	7.38	6.70
Weight of soil	41.03	33.72	39.18	36.02	36.13	36.58	26.53	32.63	30.72	28.30
Moist. cont. (%)	7.63	7.53	10.36	10.83	14.42	14.43	17.98	18.08	24.02	23.67
Ave moisture cont.		7.58		10.59		14.43		18.03		23.85

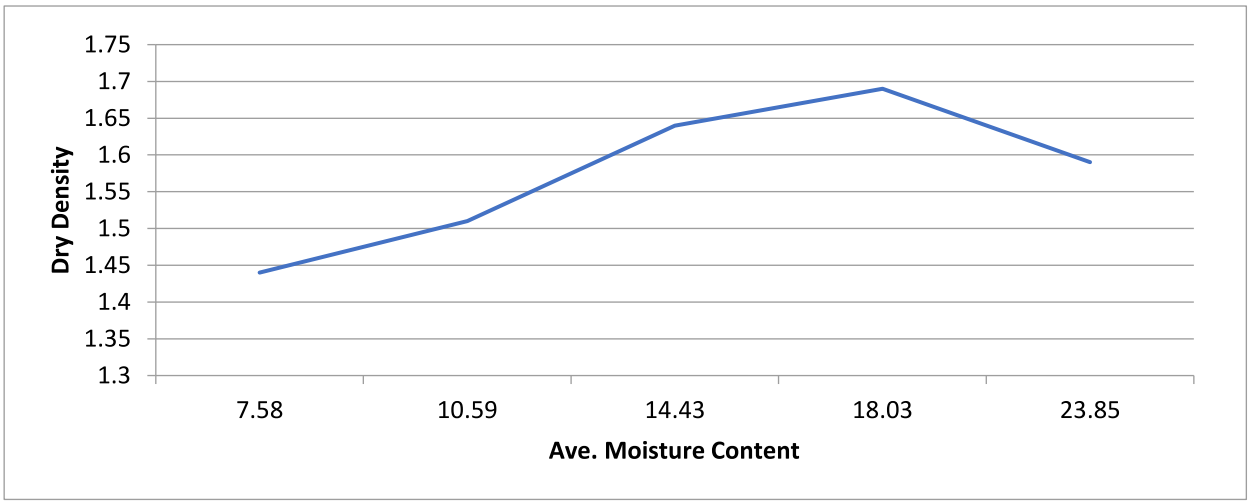

Figure 11: Compaction Graph of Dry Density against Ave. Moisture Content for sample A

Table 16: Compaction Test Table of Sample B

	8%		4%							
Weight of mould(kg)	1.986		1.986		1.986		1.986		1.986	
Weight of mould + soil (kg)	3.510		3.630		3.886		3.983		3.789	
Weight of compacted soil	1.524		1.644		1.900		2.000		1.806	
Bulk density	1.52		1.64		1.90		2.00		1.81	
Dry density	1..41	1.41	1.49	1.49	1.65	1.65	1.67	1.67	1.48	1.48
Tin number	33B	P3A9	PH(3	B_{PIT}	22A	G4	IRN	BH_{13}	G10	I
Tin weight	23.64	23.53	23.50	24.76	24.61	24.27	24.61	24.72	22.88	23.01
Tin + wet soil	66.60	66.02	59.70	60.94	66.02	60.21	55.23	54.83	60.27	58.27
Tin + dry soil	63.57	62.92	56.29	57.36	60.83	55.79	50.45	50.35	53.66	52.00
Weight of water	3.03	3.10	3.41	3.58	5.19	4.42	4.78	4.48	6.61	6.27
Weight of soil	39.93	39.39	32.79	32.60	36.22	29.52	25.84	25.63	30.78	28.99
Moist. cont. (%)	7.59	7.87	10.39	10.98	14.34	14.97	18.49	17.48	21.47	21.63
Ave. moist. Cont.		7.73		10.69		14.66		17.99		21.55

Table 17: Compaction Test Table of Sample C

	8%		**4%**							
Weight of mould(kg)	1.986		1.986		1.986		1.986		1.986	
Weight of mould + soil (kg)	3.630		3.780		3.986		4.083		3.889	
Weight of compacted soil	1.644		1.794		2.000		2.097		1.903	
Bulk density	1.64		1.79		2.00		2.09		1.90	
Dry density	1.51	1.51	1.62	1.62	1.74	1.74	1.77	1.77	1.56	1.56
Tin number	33B	P3A9	pH 3	B_{PIT}	22A	G4	IRN	BH_{13}	G10	I
Tin weight	23.64	23.53	23.50	24.76	24.61	24.27	24.61	24.72	22.88	23.01
Tin + wet soil	65.60	65.02	58.70	59.94	65.02	59.21	54.23	54.83	60.27	58.27
Tin + dry soil	62.47	61.72	55.49	56.56	59.93	54.59	49.45	50.35	53.66	52.00
Weight of water	3.13	3.30	3.21	3.38	5.09	4.62	4.78	4.48	6.61	6.27
Weight of soil	38.83	38.19	31.99	31.80	35.32	30.32	24.84	25.63	30.78	28.99
Moist. Cont. (%)	8.06	8.64	9.85	10.63	14.41	15.23	19.00	17.48	21.47	21.63
Ave. moist. Cont.		8.35		10.24		14.82		18.24		21.55

Table 18: Compaction Test Table of Sample D

	8%		**4%**							
Weight of mould(kg)	1.989		1.989		1.989		1.989		1.989	
Weight of mould + soil (kg)	3.738		3.860		4.046		3.910		3.750	
Weight of compacted soil	1.749		1.871		2.057		1.921		1.761	
Bulk density	1.75		1.87		2.06		1.92		1.76	
Dry density	1.62	I.62	1.69	1.69	1.79	1.79	1.63	1.63	1.44	1.44
Tin number	G4	G10	P3A9	22B	BH_{17}	BH_{13}	BHS	BH01	BH10	K2
Tin weight	26.27	22.91	23.53	24.34	24.89	24.70	24.82	23.79	24.38	23.91
Tin + wet soil	63.65	64.71	53.11	56.19	60.43	60.48	69.14	68.25	63.76	63.97
Tin + dry soil	60.95	61.63	50.17	53.11	55.87	56.00	62.31	61.61	56.50	56.78
Weight of water	2.70	3.08	2.94	3.08	4.56	4.48	6.83	6.64	7.26	7.19
Weight of soil	34.68	38.72	26.64	28.77	30.98	31.30	37.49	37.82	32.12	32.87
Moist. cont (%)	7.79	7.95	11.04	10.70	14.72	14.31	18.22	17.56	22.60	21.87
Ave. moist. cont		7.87		10.87		14.52		17.89		22.34

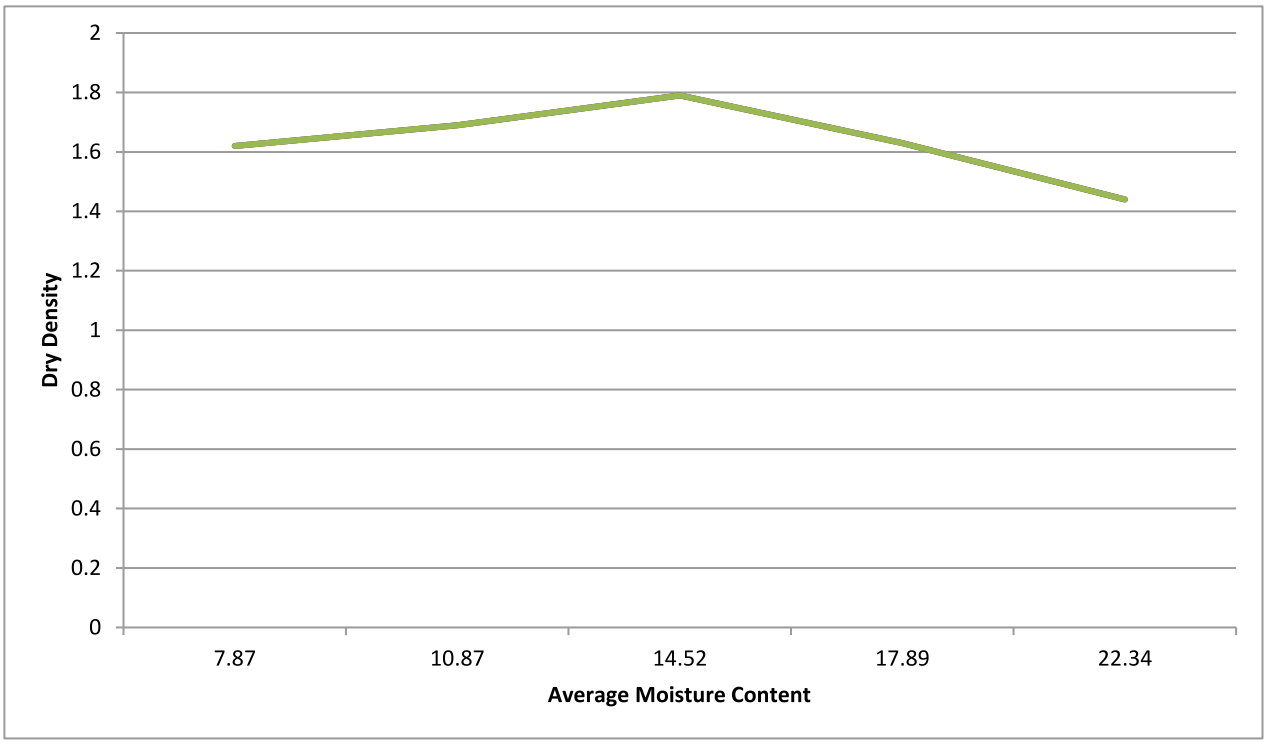

Figure 13: Graph of Dry Density against Average Moisture Content of Sample D

Table19: Result of Compaction Test

SAMPLES	OPTIMUM MOISTURE CONTENT
A	18.03
B	17.99
C	18.24
D	14.52

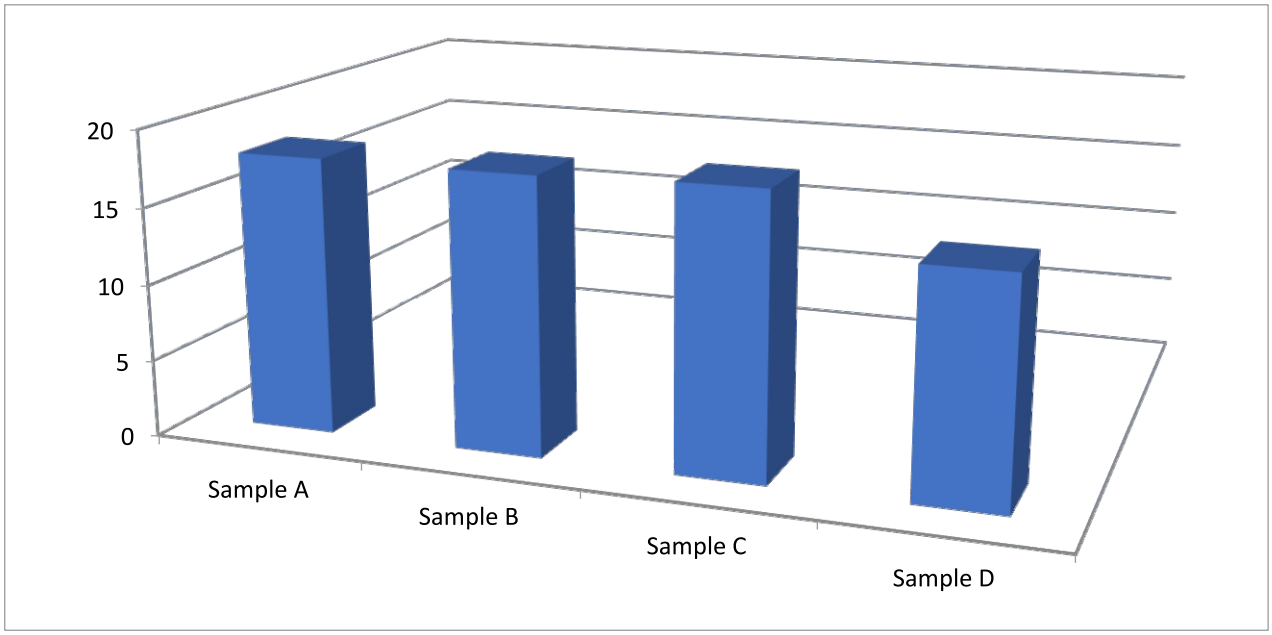

Figure 14: Bar Chart Representation of Compaction Test Result

Soil compaction is one of the ways to improve the ground; it is a process in which when the ground is pressed or compacted, the soil grains become exhaustively rearranged, increasing the shear strength, density, bearing capacity but reducing their void ratio, porosity, permeability and settlements as a result (Kaniraj, 1988, Prakash and Jain, 2002). The Compaction test is used to determine the optimum moisture content required for the soil to reach its peak dry density for a material that has been compacted with a given compactive effort before failure (Wray, 1986). From table 18, the optimum moisture content of samples A, B, C and D are 18.03, 17.99, 18.24 and 14.52. Since the essence of compaction test is to determine the optimum moisture content that will help in achieving maximum dry density of soil after compaction, each soil sample will be wetted in such manner not to exceed -2% and +2% allowable moisture increase so as not to affect compaction (Raj, 2012). When much more water is added to a soil under consideration, the incompressible nature of water makes it easier for the water to occupy the intergranular voids in the soil disallowing for maximum cohesion between soil particles when dry, thus affecting compaction. Say for soil sample A with optimum moisture content of 18.03, the maximum and minimum moisture content allowable for optimum compression and compaction will be between 17.6694 and 18.3906. In like manner, maximum compaction can be attained for soil samples B, C and D when the ranges of their optimum moisture are between 17.6302 and 18.3498; between 17.8752 and18.6048; and between 14.2296 and 14.8104 respectively.

SPECIFIC GRAVITY TEST RESULT

Table 20: Specific Gravity Test Result

Bottle Number	1	2	3
Weight of bottle + dry soil	36.31	36.03	37.82
Weight of empty bottle	22.35	25.73	23.88
Weight of dry soil	13.96	10.30	13.94
Weight of bottle + soil + water	81.06	80.47	82.07
Weight of water	50.41	48.48	49.88
Weight of water in full bottle	72.76	74.21	73.63
Weight of water displaced	44.75	44.44	44.25

For Sample A:

$$\text{Specific gravity G} = \frac{\text{weight of dry soil}}{\text{Weight of water} - \text{weight of water displaced}}$$

$$= \frac{13.96}{50.41 - 44.75} = 2.47$$

$$\text{Corrected specific gravity} = \frac{\text{Sp. gravity} \times \text{Relative density of water at room tempt}}{\text{Relative density of water 27°C}}$$

$$= \frac{2.50 \times 0.99704}{0.99651} = 2.501$$

Table 21: Actual and Corrected Specific Gravity and Strain at various Cell Pressures.

Description of quantity	Values			
Sample	A	B	C	D
Specific gravity G	2.47	2.55	2.46	2.55
Corrected G at 27ºC	2.501	2.551	2.421	2.531
Average G at 25ºC	2.50			
Strain at 100 cell pressure	0.000298			
Strain at 200 cell pressure	0.00223			
Strain at 300 cell pressure	0.00402			

Table 22: Standard specific Gravity of various Soils. (Source: Raj,2012)

SI NO	Soil Type	Specific Gravity
1	Gravel	2.65-2.68
2	Sand	2.65-2.68
3	Silty sand	2.66-2.70
4	Silt	2.66-2.70
5	Inorganic clays	2.68-2.80
6	Organic soils	Variable may fall below 2.00

Specific gravity is the ratio of the mass of soil solids to the mass of an equal volume of water, and it is related to mineralogy and chemical composition (Oyediran and Durojaiye, 2011). It also gives insight the suitability of any material for construction and backfilling, as greater value of specific gravity result in added strength to roads and backfilled foundations. Roy and Dass (2014) established that as the specific gravity increases, the shear strength parameters (cohesion and angle of shearing resistance) increases as well. Roy (2016) observed that increase in specific gravity lead to increase in the California Bearing Ratio i.e., thus, strength of the subgrade materials use for road construction, foundation making and backfilling. The specific gravities of soils A, B, C and D are 2.47, 2.55, 2.46 and 2.55 respectively with an average of 2.50. These specific gravities, from table 22, the high specific gravities define typical silt-loamy soils and clay-loamy soils (Bowles, 2007); such soils will have greater level of compaction and compressibility, with low void ratio and low permeability due to the large surface for particulate bonding (Raj, 2012). As backfill materials for mining are required to have low void ration for better compaction (Guyer, 2012).

TRIAXIAL TEST

Table 21: Results of Triaxial Tests

SAMPLE	Θ (Deg)	C(KPa)	Shear stress (Y) at100kPa	Shear stress (Y) at 200kPa	Shear stress (Y) at 300 kPa
A	18.11	97	191.23	279.46	370.69
B	22.23	120	144.35	168.7	193.05
C	27.51	67.5	163.37	259.24	355.11
D	24.40	138	227.99	317.98	407.97

To determine the strain of the various samples, the formula used is:

$$\text{Strain} = \frac{\text{R} - \text{dial} \times \text{Calibration ratio} \times (100 - \text{strain \%})}{(100 \times \text{Area}) \times 1000}$$

For sample A

At 100 cell pressure, the strain is 0.000298;

At 200 cell pressure, the strain is 0.00223;

At 300 cell pressure, the strain is 0.00402.

To determine the shear stress of the soil sample, the Mohr's cycle graph is plotted strain against cell pressure and the formula is:

Shear strength (Y) = C + ϭTanϴ …(i)

Where: C = cohesion, ϭ = stress and Tanϴ = friction Angle.

Raj (2012), Prakash and Jain (2002), and Kaniraj (1988) illuminated that the capability of a soil to support a loading from a structure, or to support its overburden, or to sustain a slope in equilibrium is governed by its shear strength, and it is a function of parameters, cohesion and the friction angle, and it is directly correlated to the maximum particle size, the coefficient of uniformity, grain size distribution, rate of strain, and direction of the strain, the density, the applied normal stress, and the gravel and fines content of the sample. Soil containing particles with high angularity tend to resist displacement and hence possess higher shearing strength compared to those with less angular particles (Ranjan and Rao, 1991). Akayuli et al. (2013) established that the angle of friction for sandy soil is high than its cohesion and vice versa for clayey soil. Shanyoug et al. (2009) in their study concluded that there is a general increase in cohesion with increase in clay content. It is consequently inferred that when clay particles are added to sandy materials, the clay particles tend to occupy and pad the void spaces in between the sand particles, thus inducing the sand with interlocking behaviour. Hence, clayey sand soils are expected to exhibit low cohesion whereas the cohesion increases with high clay content. From all these, samples A, B, C, and D – with their high angularity, high rate of strain, consequently, high shear strength, will all be suitable for backfilling. Of observation is that, since shear strength tends to increase with increase in the amount of clay in sandy soils, sample B will be the most suitable material for backfilling the mine sites in the study area.

5.0 CONCLUSION

In conclusion, based on the properties and characteristics of the four samples collected, the respective sizes of the material samples are fine-grained, with high specific gravity – thus high density which aid in a solid compaction and consolidation. The materials are almost all homogeneous as well. Therefore the entire samples are suitable and appropriate in forms for proper backfilling, which is despite the slightly varying sizes of the sand and silt grains. In addition, they have suitable moisture retaining capacity for holding particles together. They can be used in their natural state or remoulded with cement as backfill materials. From the undertaken tests, the compaction test revealed the optimum moisture content of the four samples: samples A, B, C and D were found to be 18.03%, 17.99%, 18.24% and 14.52% respectively. This is a clear indication that the soil samples are inorganic clayey-silty soil. The sieve analysis results indicate that 80% of cumulative percent passing through the resulting sieve size distribution of 2.00mm soil size are samples A, B and D. While for sample C the major soil distribution is 4.75mm. Specific gravity result for the sample A, B, C and D were 2.50, 2.55, 2.42 and 2.53 respectively. From the results of the tests carried out, it was found out that the soil samples A, B, and C are more suitable for backfilling due to their soil sizes and moisture content

5.1 Recommendation

For better enhancement of soil aggregate, proper soil mechanics of the soil must be carried out to the fullest to prevent chances of collapse in backfilling foundation of mine site.

Reference

Akayuli, C., Ofosu, B., Nyako, S.O. and Opuni, K.O., 2013, The influence of observed clay content on shear strength and compressibility of residual sandy soils., Int J Eng Res Appl., 3 (4), Jul-Aug, 2538-2542.

Alexandra M. Newman, Enrique Rubio, Rodrigo Caro, Andrés Weintraub, Kelly Eurek. (2010, May). A Review of Operations Research in Mine Planning.

Arizona, U. O. (2019). *Copper Mining and Processing: Life Cycle of a Mine.* Arizona: Arizona Board of Regents.

Bowles J. E. (2012) Engineering Properties of Soils and their Measurements, 4th edition, McGraw Hill Education (India) Private Limited, New Delhi.

Canine, C. (2019, March 8). *Wikipdia*. Retrieved November 07, 2019, from http://www.wikipedia.com

Ezekiel, Y. Y. (2008). The Geologic and the Climatic Conditions of Barkin Ladi LGA of Plateau State.

Ezekiel, Y. Y. (2004). *The Geology and Ground Water potentials of Vom-Kuru Area.* Scribd.

Fais. (2019). *Backfill Material specification- Basic things to consider when checking backfill materials.*

Huang P., Spearing A. J. S., Feng J., Jessu K. V., and Guo. S. (2018). Effects of solidbackfilling on overburden strata movement in shallow depth longwall coal mines in West China. *Journal of Geophysics and Engineering, vol. 15, no. 5*, 2194–2208.

Guyer, J. P. (2012). *An introduction into fill and backfilling.*

Kaniraj S.R. (1988): Design Aids in Soil Mechanics and Foundation Engineering, McGraw Hill Education (India) Private Limited, New Delhi.

Mongenstern, N. R. and Eigenbrod, K.D., (1974) Classification of argillaceous soils and rocks Journal of Geotechnical Engineering Division, Vol. 100, pp. 1137-1157

Potvin Y. and Thomas. E. (2005). Handbook on mine fill. *Australian Centre for Geomechan*

Prakash S. and Jain P.K. (2002) Engineering Soil Testing, Nem Chand & Bros, Roorkee

Queens Mine Design. (2011, April 05). *Queens Mine Design.* Retrieved November 09, 2019

Rankine R., Pacheco M., Sivakugan N. (2007). *Underground mining with backfills.* ResearchGate.

Raj P. P. (2012) Soil Mechanics and Foundation Engineering, Dorling Kindersley (India) Pvt. Ltd., New Delhi.

Ranjan G. and Rao A.S.R. (1991): Basic and Applied Soil Mechanics, New Age International (P) Ltd., Publishers, New Delhi.

Roy, S. and Dass, G. (2014) Statistical models for the prediction of shear strength parameters at Sirsa, India., I. Journal of Civil and Structural Engineering., 4(4), 483-498.

Roy, S., (2016) Assessment of soaked California Bearing Ratio value using geotechnical properties of soils., Resources and Environment., 6(4), 80-87.

Williams, D. (2016). *Gold Ore Processing (Second Edition).*

Wireman, M. (2001). Why are we still struggling with Acid Rock Drainage, *Groundwater monitoring and remediation*.

Wray, W.K. (1986) Measuring Engineering Properties of Soil, Prentice Hall, Englewood Cliffs, New Jersey

Wu D., Hou Y., Deng T., Chen Y. and Zhao X. (2017). Thermal, hydraulic and mechanical performances of cemented coal gangue-fly ash backfill. *International Journal of Mineral Processing, vol. 162*, 12–18.

Yagiz, S., (2001) Brief note on the influence of shape and percentage of gravel on the shear strength of sand and gravel mixture., Bull. Eng. Geol. Environ., 60(4), 321-323.

Zhang, J.X.; Zhang, Q.; Spearing, A.J.S.; Miao, X.X., Guo, S.; Sun, Q. (2017). Green coal mining technique integrating mining-dressing-gas draining-backfilling mining. *int. J.Min, Sci.Technol.* , 17-27.

Zhou, N.; Zhang, J.; Yan, H.; Li, M. (2017). *Deformation Behavior of Hard Roofs in Solid Backfill Coal Mining Using Physical Models.* Minerals MPDI.

Zhou N., Zhang Q., Ju F. and Liu. S. (2013). Pre-treatment research in solid backfill material in fully mechanized backfilling coal mining Technology. *Disaster Advances, vol. 6,* 118–125.

Salati, *et al* (2021) Nigerian Mining Journal, (19) 74 - 82

Appraising the Optimization of Load-Haul Operations in Open Cast Mining at Dangote Coal Mines, Effeche-Akpali, Benue State, Nigeria

Salati, L. K., Musa, J. O. and Bida, A. D.
Department of Mineral and Petroleum Resources Engineering, Kaduna Polytechnic, Kaduna, Nigeria

Abstract

This study is aimed at appraising the optimization of load-haul operations at Dangote Coal Mine Limited, Effeche-Akpali Site in Benue State. Data collection in this study was done through the review of related literature, personal interviews, field studies and personal observations. Data collected on the fleet performance assessment in the company included budgeted time, average incident time, maintenance time, number of hours per shift and number of shift hours per month. Results from the study indicated that the total cycle time/shift for Komat'su haul dump truck (HD) HD 785 and rigid dump truck (RD) used in the company is as follows: RD-22, 10.33 minutes, RD-05, 11.03 minutes, RD-19, 9.19, RD-27, 10.59 and RD-28, 10.57 minutes respectively. The corresponding annual production per truck was also found to be 317,604 tonnes, 337,075 tonnes, 294,940 tonnes, 327,180 tonnes and 311,858 tonnes respectively. The increase in cycle time of the dump trucks is found to be caused by unscheduled delays of waiting time in haulage unit processes. Hence, increasing the number of excavators during loading would reduce the waiting time of dump trucks, thereby improving cycle time efficiency and overall increase in productivity with a view to meeting production target of the company.
Keywords: Optimization, load-haul operations, fleet performance, productivity, cycle time.

1. Introduction

The productivity of any surface mining operation depends on the efficiency and success of its load-haul method. Application of modern and innovative mining equipment and their optimization would, no doubt, lead to a reduction in the unit cost of loading and hauling. Therefore, while increased machine size and improved automation of mining equipment and systems have been intensified, load-haul process has witnessed only a few innovations in recent years (Aguayo*et al.,* 2021). Haulage of materials is one of the most important aspects of the operations carried out in opencast mining after loading. Materials handling is mostly done through loading and transportation of blasted materials to the point of processing with the aid of haulage equipment (Adams and Bansah, 2016). This activity requires large equipment whose cost per hour is high; therefore, high productivity is required with the correct allocation of trucks and wheel loaders or shovels (Coronado, 2014). An adequate decision support system must, therefore, be made to increase productivity and reduce operating costs. However, emerging issues associated with dead times such as queuing trucks for loading, trucks waiting to be loaded and other forms of delays have created a huge obstacle for correct timing. This has often created inefficient fuel consumption and the emission of carbon and energy. Haulage delays and break downs are often traced to inadequacies in fleet operation but they can be eliminated through improved truck-loader match and allocation, effective scheduled shift operation and adequately designed haul roads thereby leading to improved productivity (Nel *et al.,* 2011). Achelpohl (2018) has also proposed planned and prompt maintenance of load-haul equipment by the technical support department to handle any eventual downtime. However, these emerging problems in materials haulage require improvement of cycle times in opencast mining operation.

Pasch and Uludag (2018) define the load-haul cycle time as the total time to complete a cycle whose critical stages comprise spotting at

loading, loading time, hauling-full time, travel empty time and queuing time. Optimizing the load-haul opencast operation thus requires effective management of these steps to improve loader-truck productivity (Soofastaei *et al*., 2015) as shown in Figure 1.

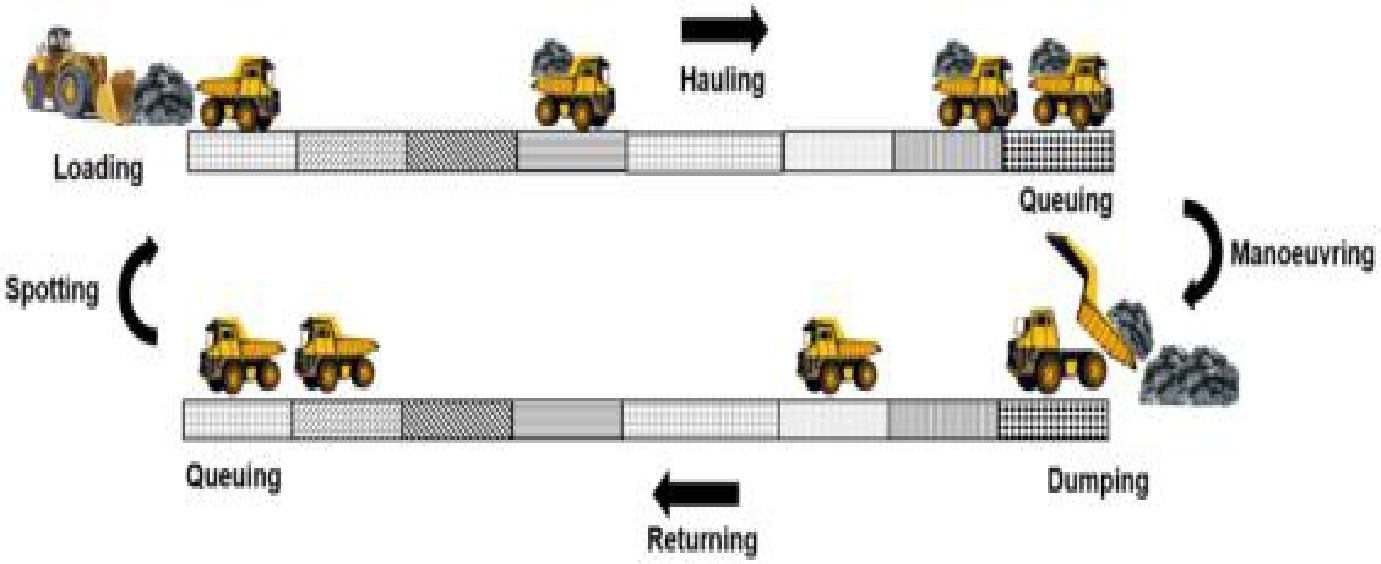

Fig. 1 Schematic of Truck Cycle in Surface Mines (Source: Soofastaei *et al*., 2015)

Fisonga and Mutambo (2017) agree with the above definition of cycle time but argue that the best way to determine the cycle time of a loader is by monitoring aspects of the equipment operations over several periods: excavation time, swinging to the dump truck, dumping time and swinging back to the extraction face. According to them, bucket cleaning is also made a priority especially during rainy seasons or when excavating wet materials and materials preparation, while machinery accommodation time is also given consideration. Figure 2 shows a method of improving fleet management in surface mining.

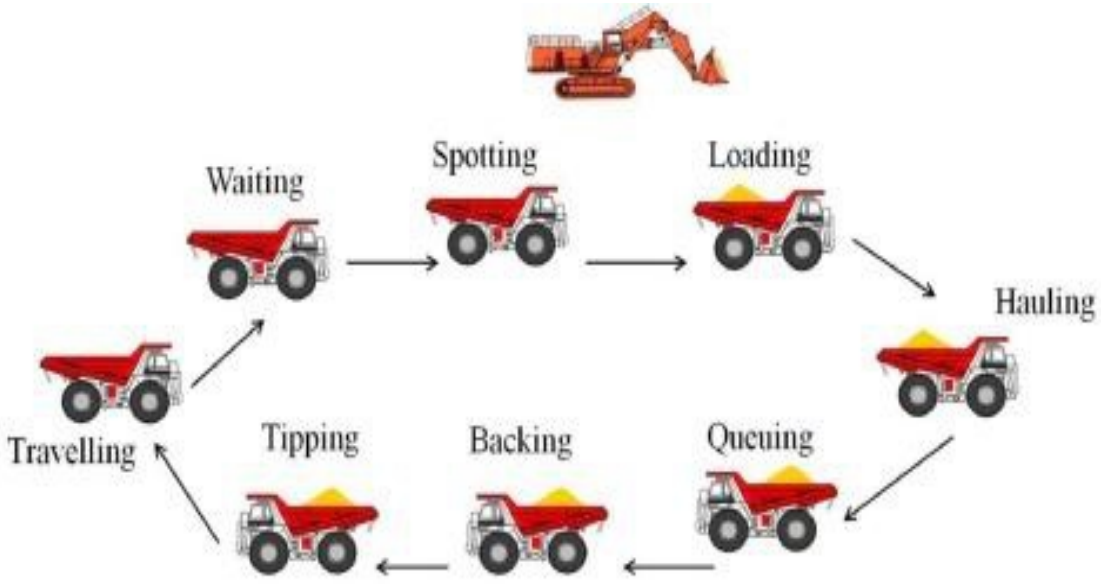

Fig. 2 Improving Fleet Management in Surface Mining (Source: Soofastaei *et al*., 2015)

Although Ercelebi and Bascetin (2009) harp on careful production estimation to optimize shovel-truck systems in surface mining, Fisonga and Mutambo (2017) have determined some basic dump truck productivity and cycle time estimations through various calculations below:

Estimated Volumetric Capacity of the Truck Bed

$$V_{bed} = V_{real} \times N_b \quad \text{... Equ. 1}$$

where V_{bed} is estimated volumetric capacity of the truck bed, V_{real} is estimated volumetric capacity of the backhoe bucket and N_b is assumed number of buckets.

Estimated Bulk Tonnage in the Truck Bed

$$M_w = C_{real} \times N_b \quad \text{... Equ. 2}$$

where M_w is estimated bulk tonnage in the truck bed, C_{real} is estimated bucket tonnage and N_b is assumed number of buckets.

Loading Time

$$T_{loading} = \frac{(N_b - 1) \times T_1}{60} \quad \text{... Equ. 3}$$

where T_l is loading duration per bucket and Nb is assumed number of buckets.

Transportation Time

$$T_{rc} = \frac{60 \times_{Le}}{Vrc} \quad \text{... Equ. 4}$$

where L_e is distance of transportation from the extraction site to the dumping point and V_{rc} is traveling velocity.

Dumping Time

$$t_d = 0.65min \quad \text{... Equ. 5}$$

Returning Time

$$T_{rv} = \frac{60 \times l_e}{Vrv} \quad \text{... Equ. 6}$$

Sampling Time

$$t_m = 0 \min \quad \text{... Equ. 7}$$

Cleaning Time for the Truck Bed

$$tl = 6 - 7min \quad \text{... Equ. 8}$$

Cycle Time for the Articulated Dump Truck

$$T_c = T_{loading} + T_d + T_{rv} + T_m + T_l + T_{mcd}$$

where T_{mc} is manoeuvring time for the Load and t_{md} is manoeuvring time for the dumping.

$$N_t = \frac{Tshift - (Toc + Tm + Ta + Tp)}{Tc} \quad \text{... Equ. 9}$$

Although Ercelebi and Bascetin (2009) harp on careful production estimation to optimize shovel-truck systems in surface mining, Fisonga and Mutambo (2017) have determined some basic dump truck productivity and cycle time estimations through various calculations below:

Estimated Volumetric Capacity of the Truck Bed

where T_{shift} is duration of the shift, T_{oc} is time to shift changing, T_m is resting time for lunch and snacks, T_a is resting half-time between night and day during the night this ranges between (0.66 to 0.75 h) and for a day it is 0.5 h and T_p is time lost by other causes.

Productivity of a Truck per Shift

Q_{dump} is N_t x V_{bed} x K_{mec}..... Equ. 10

where N_t is number of trips per truck in a day, K_{mec} is mechanical availability and V_{bed} is estimated volumetric capacity of the truck bed.

All the above formulae are demonstrations of the proof that fleet optimization in load-haul operations can achieve operational efficiencies and eventual cost reductions as adduced by

Nel*et al.* (2011). Therefore, given the highlighted variables for improving the productivity of opencast mining operations, this study attempts to appraise load-haul optimization at Dangote Coal Mine Limited, Efeche-Akpali site, Benue State. The objective is to determine the effectiveness of load-haul equipment towards improved productivity in spite of occasional breakdowns, delays and other operational bottlenecks.

2 Materials and Methods Used

Dangote coal mine is located in Effeche/Akpali community, Okpokwu local government area of Benue State, North-central Nigeria. The study area is on Latitude 7°03'27.60" N and Longitude 8°12'21.60" E. The mining area is 64.5 hectares and can be accessed through Idoba - Otukpa road along Enugu - Otukpo express – way. The 6 km access road was constructed by Dangote coal mine from Idoba to Effeche mining area in 2021. Figure 3 shows the map of Benue showing Okpokwu local government area, while figure 4 shows the Dangote coal mine offices situated within Effeche-Akpali community in Okpokwu.

Fig. 3 Map of Benue State showing the Study Area

Fig. 4 Dangote Coal Mine Offices in the Study Area

An appraisal of load-haul operations in coal mining in the study area was done using the raw data collected from the field and personal observations, coupled with empirical comparisons in the literature. In this study, spot and load time, travel haul time, delay period, turn and dump time, wait time and total cycle time of the wheel loader-truck were carefully determined by estimation. The various trucks used in the mine were identified and their capacities noted, while their haulage routes and distances were studied to determine the root causes of delays and break downs during haulage. An approach based on the principle of employing more loaders at the loading point was adopted with a view to determining the highest times consumed by a unit process in load-haul operation.

2.1 Data Collection

Data on budgeted time, the incident and maintenance time, the stand by hour, the number of shifts per month and the number of hours per shift were collected for analysis. The following indicators were subjected to various forms of assessment through the collection of both raw data, field studies and personal observation: mechanical reliability of equipment, physical availability of equipment, machine utilization factor and fleet efficiency in the company. Calculations based on raw data collected from the mine for each of the parameters on a weekly basis were used in arriving at the values for the respective indicators.

The indicators can be mechanically expressed as follows:

Physical availability (%) is

$$\frac{\text{Running hour} + \text{standby hour}}{\text{budget hours}} \times 100 \quad \ldots \text{Equ. } 11$$

Use of availability (%) is

$$\frac{\text{Running hour}}{\text{Running hour} + \text{Standby hour}} \times 100 \quad \ldots \text{Equ. } 12$$

Utilization factor % is

$$\frac{\text{Actual running hour}}{\text{Total hours}} \times 100 \quad \ldots \text{Equ13}$$

Efficiency factor % is

$$\text{Mechanical availability} \times \text{utilization factor} \times 100 \quad \ldots \text{Equ } 14$$

3 Results and Discussion

Results from Tables 1 to 5 showing the performance assessment of the fleet used at Dangote Coal Mine Limited, Effeche-Akpali Site in Benue State indicate that the fleet performance is fairly good. This implies that the working hours of the fleet are well utilized and they are performing well based on the utilization and efficiency factor calculated. The assessment was carried out over a period of six weeks and from the results, the mechanical and physical reliability of the fleet in the study area is high, while their utilization and efficiency are found to be equally high.

From the fleet assessment, it was indicated that the mechanical reliability of the fleet was high except for a few incidences of delays during repair/incident hours. The physical availability shows that fleet equipment is physically available which is an indication of higher production capable of meeting the company's proposed target. This high productivity is not only contributed by the mechanical and physical availability only but also by the record of hours the operators used in making use of the available machine. Although the fleet equipment are not 100% efficient, it is observed that about 92% can be said to be productive, while only about 8% appears to be lost due to repairs, thereby making it possible for the fleet to be adjudged to be working efficiently throughout the study period.

The utilization factor of the fleet on the other hand is fairly good, which contributes to the good production rate recorded since the matching of the correct equipment size has helped in making the fleet work faster thereby boosting the morale of the operators.

As shown in Table 6, the total cycle times/shifts for Komat'su HD 785 dump trucks' load-haul operations in the mine have been calculated to be as follows: RD-22, 10.33 minutes, RD-05, 11.03 minutes, RD-19, 9.19, RD-27, 10.59 and RD-28, 10.57 minutes respectively. Their corresponding average cycle times/shifts were also calculated to be 2.58 minutes, 3.15 minutes, 2.29 minutes, 3.04 minutes and 3.04 minutes respectively. The overall total cycle time for the load-haul operation is thus determined to be **52.51** minutes, while the overall average cycle time is **14.01** minutes. The result, therefore, in the opinions of Varghese and Xavier (2018), implies that the cycle time recorded by the load-haul equipment in the company is effective and has a positive impact on the overall production. From Table 7, working with one excavator to load a dump truck takes 2 minutes and 16 seconds, while an additional excavator would save the load-haul operation about 1 minute and 8 seconds. With one more excavator to the fleet, the operation would be saved approximately 23 seconds. Thus, there was an observable exponential reduction in the time spent on loading dump trucks. As the number of excavators is increased, the time spent on filling the trucks decreases. This, therefore, implies that increasing the number of excavators in the fleet during loading would not only reduce the waiting time of dump trucks but would subsequently improve the cycle time efficiency thereby leading to an increase in the overall productivity of the mine. This analysis is based on the calculation below:

With 1 excavator working;

$$\mathrm{T}_{\mathrm{loading}}\ is\ \frac{(4-1)*45.5}{60} = 2\ mins\ 16\ secs$$

With 2 excavators working;

$$\mathrm{T}_{\mathrm{loading}}\ \mathrm{is}\ \frac{(4-1)*45.5/2}{60} = 1\ mins\ 8\ sec$$

With 3 excavators working;

$$\mathrm{T}_{\mathrm{loading}}\ \mathrm{is}\ \frac{(4-1)*45.5/3}{60} = 45.5\ secs$$

Figures 3 and 4 respectively show a load-haul operation in the study area where an excavator loads a waiting truck, while an idle truck is parked as it is out of use in the mine.

From Figure 5, the annual production per truck in the mine was also found to be 317,604 tonnes, 337,075 tonnes, 294,940 tonnes, 327,180 tonnes and 311,858 tonnes respectively. Thus, the total annual production attained by the company was estimated to be 1,588,657 tonnes, thereby exceeding the company's production target of 1,500,000

tonnes per annum. With more excavators and dump trucks added to the production fleet of the company, the cycle time would be further reduced and higher production figures would be attained. This is further indicated in Figures 6 and 7 showing the load-haul operation and only one idle dump truck parked at the mining site of the company respectively. The stockpiled excavated coal already loaded from the pit as shown in Figure 8 is also an indication of a function of effective load-haul and cycle time operations taking place in the company.

Table 1 Fleet Performance Assessment per Day

No of Fleet	Budgeted hour (hrs)	Running Hour (hrs)	Stand by Hour (hrs)	Incident hour (hrs)
Dumpers	24	18	3	1.56
Wheel loaders	24	18	3	2.03
Excavators	24	18	3	1.45

Table 2 Fleet Performance Assessment per Shift

No of Fleet	Budgeted hour(hrs)	Running Hour (hrs)	Standby Hour (hrs)	Incident hour (hrs)
Dumpers	12	9	2+1	0.45
Wheel loaders	12	9	2+1	1.00
Excavators	12	9	2+1	1.12

Table 3 Fleet Performance Assessment per Week

No of Fleet	Budgeted hour(hrs)	Running Hour (hrs)	Standby Hour (hrs)	Incident hour (hrs)
Dumpers	84	63	21	4.50
Wheel loaders	84	63	21	6.13
Excavators	84	63	21	5.43

Table 4 Fleet Performance Assessment per Month

No of Fleet	Budgeted hour(hrs)	Running Hour (hrs)	Standby Hour (hrs)	Incident hour (hrs)
Dumpers	336	252	84	18
Wheel loaders	336	252	84	24.54
Excavators	336	252	84	22.52

Table 5 Fleet Performance Assessment per Year

No of Fleet	Budgeted hour (hrs)	Running Hour (hrs)	Standby Hour (hrs)	Incident hour (hrs)
Dumpers	4032	3024	100.8	216
Wheel loaders	4032	3024	100.8	294.48
Excavators	4032	3024	100.8	270.24

Table 6 Cycle Times of Load-Haul Operation

Dump Truck	No of passes	Load Time (Mins)	Haul Time (Mins)	Dump Time (Secs)	Return Time (Mins)	Waiting Time (Mins/secs)	Maneuver Time (Secs)	Cycle Time/ Shift (Mins)
RD 22	**4**	4.23	4.04	0.26	3.06	0.34	0.21	
HD 785	**4**	1.59	3.02	0.27	2.52	0.23	0.26	
	4	2.52	2.40	0.24	2.32	0.26	0.28	
	4	4.00	3.29	0.29	2.51	1.23	0.35	
	Total	**13.14**	13.15	1.06	10.41	**2.46**	1.1	**10.33**
	Average	**3.17**	3.19	0.27	2.60	**0.42**	0.28	**2.58**
RD 05 HD 785	**4**	2.50	2.37	0.27	2.24	0.53	0.32	
	4	3.49	3.02	0.14	2.43	2.44	0.43	
	4	2.43	3.00	0.24	2.09	3.07	0.38	
	4	3.07	3.53	0.38	3.09	0.53	0.27	
	Total	**12.29**	11.92	1.03	9.83	**7.37**	1.4	**11.03**
	Average	**3.04**	2.98	0.26	2.46	**1.54**	0.35	**3.15**
RD 19	**4**	4.01	3.24	0.32	2.57	0.41	0.25	
HD 785	**4**	1.57	2.37	0.38	2.28	0.50	0.44	
	4	2.35	3.47	0.25	3.01	0.25	0.29	
	4	2.31	3.27	0.39	2.37	0.36	0.27	
	Total	**11.04**	12.35	1.34	10.23	**2.32**	1.25	**9.19**
	Average	**2.51**	3.09	0.34	2.56	**0.38**	0.31	**2.29**
RD 27	**4**	3.31	3.21	0.25	3.02	0.43	0.28	
HD 785	**4**	2.28	3.17	0.31	2.58	0.35	1.20	
	4	2.55	3.24	0.29	2.47	0.56	0.30	
	4	2.43	4.01	0.40	3.01	1.10	0.26	
	Total	**11.37**	13.63	1.25	11.08	**3.24**	2.04	**10.59**
	Average	**2.50**	3.41	0.31	2.77	**1.06**	0.51	**3.04**
RD 28	**4**	2.44	3.55	0.25	2.54	0.35	0.20	
HD 785	**4**	3.56	3.06	0.26	2.27	0.43	0.32	
	4	3.24	3.27	0.30	2.01	0.26	0.43	
	4	3.01	3.38	0.33	3.02	0.28	0.27	
	Total	**13.05**	13.26	1.14	9.84	**3.12**	1.22	**10.57**
	Average	**3.16**	3.32	0.29	2.46	**1.03**	0.31	**3.04**
Overall	**Total**	**15.18**						**52.51**
Overall	**Average**	**3.02**				**1.04**		**14.01**

Table 7 $T_{loading}$VS increase in working excavators

	$T_{l\ (Secs)}$	N_b	$T_{Loading}$
1 Excavator	45.5	4	2 mins 16 secs
2 Excavators	45.5	4	1 min 8 sec
3 Excavators	45.5	4	45.5 secs
4 Excavators	45.5	4	34 secs
5 Excavators	45.5	4	27 secs

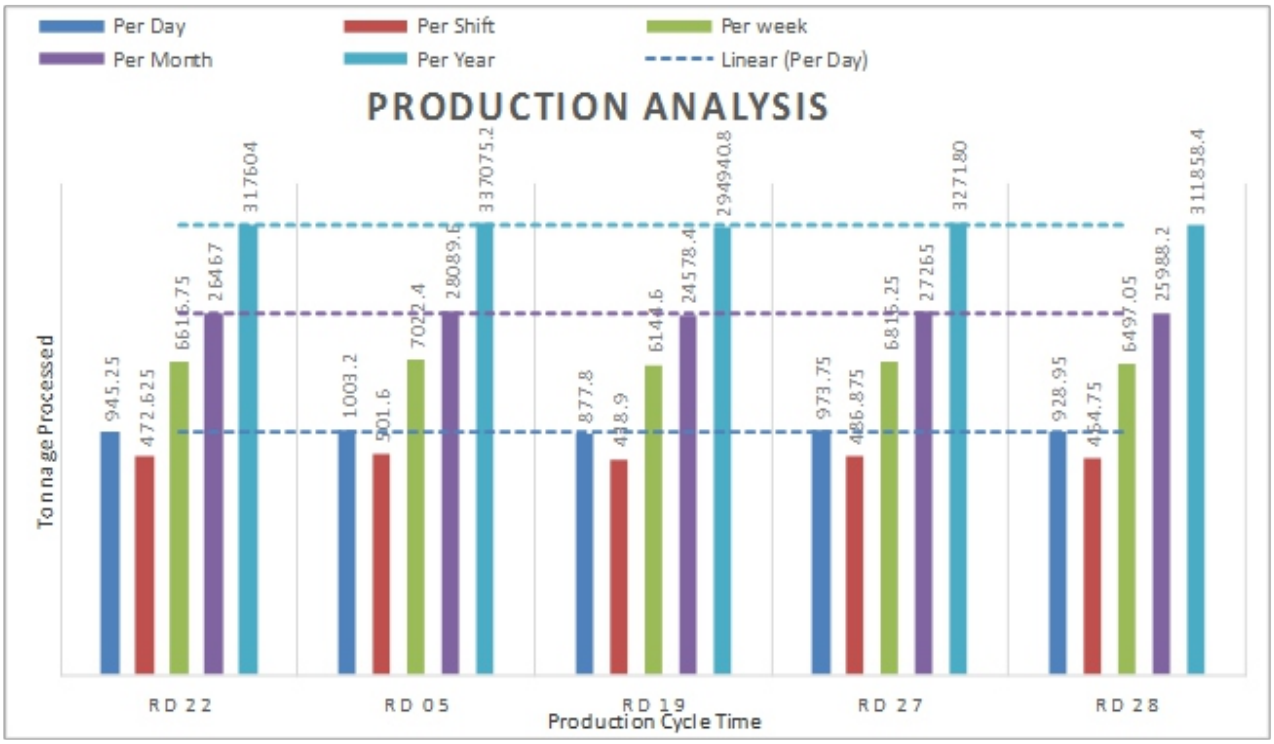

Fig. 5 Production Analysis for 5 Dump Trucks

Fig. 6 Load-Haul Operation in the Study Area

Fig. 7 Idle Dump Truck in the Study Area

Fig. 8 Excavated and Stockpiled Coal from the Mine

4 Conclusion

An appraisal of the optimization of load-haul operations has been carried out at Dangote Coal Mine Limited, Effeche-Akpali Site, Benue State. From the results of the study, it can be concluded that the cycle time of load-haul operations in the company is effective for coal mining operations. The good time management practices and load-haul equipment of high capacity employed by the company have been found to have contributed immensely to the annual production of 1,588,657 tonnes. Therefore, the fleets employed can be said to be performing optimally, while the company's production target has been attained with more promising achievements and sustenance of the present production level.

Acknowledgements

The authors acknowledge the contribution and assistance provided by the management of Dangote Coal Mines at Efeche-Akpali, Benue State, especially the mining engineer on the site, Mr. Tajudeen Olatunji. All the authors whose works have been used as references are equally acknowledged and appreciated.

References

Achelpohl, E.R. (2018). The Effect of Overloading on Reliability of Wheel Loader Structural Components. *Unpublished PhD Thesis,* Missouri University of Science and Technology, 196pp.

Adams, K.K. & Bansah, K.J. (2016). Review of Operational Delays in Shovel-Truck System of Surface Mining Operations. *4th UMaT Biennial International Mining and Mineral Conference,* 60-65.

Aguayo, I.A.O., Nehring, M. & Ullah, G. M.W. (2021). Optimising Productivity and Safety of the Open Pit Loading and Haulage System with a Surge Loader. *Mining 2021,* 1, 167–179. https://doi.org/10.3390/ mining1020011.

Coronado, P. P. V. (2014). Optimization of the Haulage Cycle Model for Open Pit Mining Using a Discrete-event Simulator and a Context-based Alert. *Unpublished MSc thesis,* The University of Arizona, 157pp.

Ercelebi, S.G. & Bascetin, A. (2009). Optimization of Shovel-Truck System for Surface Mining. *The Journal of The Southern African Institute of Mining and Metallurgy*, 109, 433-439.

Fisonga, M. & Mutambo, V. (2017). Optimization of the Fleet per Shovel Productivity in Surface Mining: Case Study of Chilanga Cement, Lusaka Zambia. Cogent Engineering, 4(1), 16pp.

Nel, S., Kizil, M.S. Knights, P. (2011). Improving Truck-Shovel Matching. *35th APCOM Symposium/Wollongong*, New South Wales, 24-30 September, 381-391.

Pasch, O. & Uludag, S. (2018). Optimization of the Load-and-Haul Operation at an Opencast Colliery. *The Journal of the Southern African*, Institute of Mining and Metallurgy, 118, 449-456.

Soofastaei, A., Aminossadati, S.M., Kizil, M.S. & Knights, P. (2015). Simulation of Payload Variance Effects on Truck Bunching to Minimise Energy Consumption and Greenhouse Gas Emissions. *Coal Operators' Conference*, University of Wollongong, 11 –13 February, 337-346.

Varghese, A. & Xavier, A.S. (2018). Literature Review on Hauling Equipment Productivity using Cycle Time Calculation. International Research Journal of Engineering and Technology, 5(11), 467- 471.